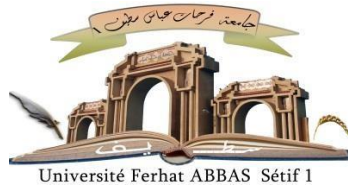


الجمهورية الجزائرية الديمقراطية الشعبية  
République Algérienne Démocratique et Populaire  
Ministère de L'Enseignement Supérieur et de la Recherche Scientifique



**UNIVERSITÉ FERHAT ABBAS - SÉTIF1**

**FACULTÉ DE TECHNOLOGIE**

**THÈSE**

**Présentée au Département de Génie des Procédés**

**Pour l'obtention du diplôme de**

**DOCTORAT SCIENCE**

**Domaine : Sciences et Technologie**

**Option: Génie des Polymères**

**Par**

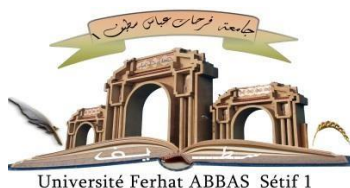
**BEDJAOUI Khaled**

**Effet du Polystyrène recyclé sur le Comportement  
du mélange à base de Styrène-Co-acrylonitrile**

**Soutenue le -/-/ 2021 devant le Jury:**

<b>BENANIBA Mohamed Tahar</b>	<b>Professeur</b>	<b>Univ. Ferhat Abbas Sétif 1</b>	<b>Président</b>
<b>KRACHE Rachida</b>	<b>Professeur</b>	<b>Univ. Ferhat Abbas Sétif 1</b>	<b>Directeur de thèse</b>
<b>ANGEL Marcos Fernandez</b>	<b>Vice-Director</b>	<b>Instituto de Ciencia y Tecnología de Polímeros (CSIC)</b>	<b>Co-Directeur</b>
<b>HELATI Abdelhak</b>	<b>Professeur</b>	<b>Univ. Mohamed El Bachir El Ibrahimi Bordj Bou Arreridj</b>	<b>Examineur</b>
<b>REFFAS Abdel Baki</b>	<b>Professeur</b>	<b>Univ. Msila</b>	<b>Examineur</b>
<b>ZOUKRAMI Fouzia</b>	<b>Professeur</b>	<b>Univ. Ferhat Abbas Sétif 1</b>	<b>Examineur</b>

الجمهورية الجزائرية الديمقراطية الشعبية  
DEMOCRATIC AND POPULAR REPUBLIC OF ALGERIA  
MINISTRY OF HIGHER EDUCATION AND SCIENTIFIC RESEARCH



**UNIVERSITY FERHAT ABBAS - SETIF1**

**FACULTY OF TECHNOLOGY**

## **THESIS**

**Submitted to the Process Engineering Department**

**for the degree of:**

**DOCTORATE IN SCIENCES**

**Field : Sciences and Technology**

**Option : Polymer Engineering**

**By**

**BEDJAOUI Khaled**

**The Effect of recycled Polystyrene On the behavior  
of the blend with Styrene-co-acrylonitrile (SAN).**

**Defended the -/-/2021 in front of the Committee Members:**

<b>BENANIBA Mohamed Tahar</b>	<b>Profesor</b>	<b>Univ. Ferhat Abbas Sétif 1</b>	<b>President</b>
<b>KRACHE Rachida</b>	<b>Profesor.</b>	<b>Univ. Ferhat Abbas Sétif 1</b>	<b>Advisor</b>
<b>ANGEL Marcos Fernadez</b>	<b>Vice-Director</b>	<b>Instituto de Ciencia y Tecnología de Polímeros (CSIC)</b>	<b>Co-Advisor</b>
<b>HELATI Abdelhak</b>	<b>Profesor</b>	<b>Univ. BBA</b>	<b>Examiner</b>
<b>REFFAS Abdel Baki</b>	<b>Profesor</b>	<b>Univ. Msila</b>	<b>Examiner</b>
<b>ZOUKRAMI Fouzia</b>	<b>Professor</b>	<b>Univ. Ferhat Abbas Sétif 1</b>	<b>Examiner</b>

## ACKNOWLEDGEMENTS

In the name of Allah, the Most Beneficent and the Most Merciful. All praises to Allah the Almighty for giving me the strengths, guidance and patience for completing this thesis. With His blessing, this dissertation is finally accomplished.

First of all I would like to express my genuine gratitude to my supervisor Pr RACHIDA Krache for her support and encouragement during period of my studies. Your practical view and guidance on my research work was of the utmost importance. Thank you very much for the unending help throughout the course of my research.

I would like to express my deepest gratitude to Dr. Angel Antonio Marcos Fernandez for his supervision and his support. Really, I am so thankful to him for providing me an unique opportunity to characterize my samples under his tutelage, as well as his assistance and insightful discussion, timely advice and encouragement during the time that I spent it in his laboratory (Elastomeros) at the Instituto de Ciencia y Tecnologia de Polimeros (CSIC) in Madrid.

Also special thanks to Dr. Juan Lopez Valentin, Alberto Fernandez and Rebeca Hererro for his help in learning different polymer characterization techniques such as TGA, DSC, DMTA and answering my technical questions regarding these equipment.

also wish to express my appreciation to the technical members of laboratory (Elastomeros) especially Dr. Alberto Fernandez, Dr. Rebeca Hererro for their assistance, long hours, infinite patience, humor, for helping me with equipments training.,

I would like to express gratitude to my committee member, foremost the president of the committee members Prof. Benaniba Mohamed Tahar, Prof. Hellati Abdelhak, Reffas Abdel Baki and Zoukrami Fouzia for their valuable time, constructive criticisms and suggestions. Thank you for the opportunity to revise my thesis, I really appreciate your careful review.

I also wish to express my appreciation to the technical members of our department Mr. Khitass Moncef, Abdelhakim Benmekideche and. Ibtissem for their help and friendship.

Finally, I would like to extend special thanks to my family (parents, sisters and brother) for their, encouragement and unconditional love. I am very lucky to have such wonderful family members. I dedicate this thesis to my family and all the teachers who have taught me since my childhood. I will never forget this time in my life and, most importantly, the people I met and who helped me to create, develop and complete this thesis.

**I dedicate this thesis to the memory of my Father, who sadly passed away during its preparation.**

## TABLE OF CONTENTS

Acknowledgements and Dedication .....	i
Table of Contents .....	ii
List of Figures .....	x
List of Tables.....	xii
List of Abbreviations and Symbols .....	xiii

### **Chapter I: Literature Review**

I.1 Introduction.....	1
I.1 Problem Statements.....	2
I.2 Objectives .....	3
I.3 Scope of Study .....	3
I.4 Outline Thesis Structure .....	4
References .....	5

### **Chapter II: State of the Art**

II.1. Introduction .....	7
II.2 Polymer blends .....	8
II.3 Thermodynamic of Polymer Blends.....	8
II.4 Methods of Polymer Blending.....	10
II.4.1 Solution Blending .....	11
II.4.2 Melt Blending .....	11
II.5 Miscibility of Polymer Blends .....	12
II.6 Factors affecting miscibility of polymer blends .....	13
II.6.1 Proportion of component polymers .....	14
II.6.2 Molecular mass.....	14
II.6.3 Polarity.....	14
II.6.4 Specific interactions .....	14
II.6.6 Crystallinity .....	14
II.7 Blend Morphology .....	14
II.8 Compatibilization interest of polymer blends.....	16
II.9 Interphase and interfacial phenomena in polymer blends .....	16
II.10 Compatibilization of polymer blends .....	19
II.11 Compatibilizers in polymer blends .....	19
II.11.1 How a compatibilizer functions.....	19
II.11.2 Reactive compatibilizer .....	21
II.11.3 Non- reactive compatibilizer .....	21
II.12 Conclusion.....	23
References .....	25

### **Chapter III: Materials and Methodology**

III.1. Introduction .....	30
III.2. Raw Materials.....	30
III.2.1 Polystyrene (PS) .....	30
III.2.2 Styrene-co-acrylonitrile (SAN) .....	31
III.2.3 Compatibilizer (SEBS).....	32
III.3. Blends preparation procedure.....	35
III.3.1 Blends Formulations.....	35
III.3.2 Preparation of blends .....	35
III.3.3 Melt blending process .....	36
III.4 Compression molding process.....	37
III.5 Characterization of PS, SAN and PS/SAN/Compatibilizer .....	37
III.5.1 Mechanical Testing .....	37
III.5.1.1 Tensile Test .....	37
III.5.1.2 Izod Impact Test.....	39
III.5.2 Rheological characterization (RPA).....	39
III.5.3 Differential Scanning Calorimetry (DSC).....	40
III.5.4 Dynamic Mechanical Analysis (DMTA) .....	42
III.5.5 Thermogravimetric Analysis (TGA) .....	43
III.5.6 Scanning electron microscopy (SEM).....	45
References .....	47

### **Chapter IV: Results and discussion**

IV. Characterization of PS/SAN blends without and with addition of compatibilizer.	
IV.1. Mechanical Properties .....	47
IV.1.1 Tensile Properties of PS/SAN compatibilized and noncompatibilized.....	47
IV.1.2 Impact Properties of PS/SAN compatibilized and noncompatibilized .....	50
IV.2. Thermal Properties Analysis .....	51
IV.2.1 Differential Scanning Calorimetry (DSC) .....	52
IV.2.2 Thermogravimetric Analysis (TGA).....	53
IV.3. Dynamic Mechanical Analysis (DMTA) .....	54
IV.4. Microstructure analysis (SEM) .....	56
IV.5. Conclusion .....	59
IV.2 Characterizations and Properties of rPS/SAN blends without and with addition of compatibilizer.	
IV.2.1. Rheological Properties .....	60
IV.2.2. Mechanical Properties.....	64
IV.2.2.1 Impact strength of rPS/SAN without and with SEBS .....	64
IV.2.2.2 Tensile Properties of PS/SAN without and with SEBS .....	66
IV.2.3 Differential Scanning Calorimetry (DSC) .....	70
IV.2.4 Scanning electron microscopy (SEM) .....	72
IV.2.5 Conclusion .....	75

References .....76

**Chapter V: General Conclusions and Recommendations**

V.1 General Conclusions..... 78  
V.2 Recommendations ..... 80  
Annexes .....81

## LIST OF FIGURES

<b>Figure II.1</b>	Interrelations in polymer blend nomenclature.	9
<b>Figure II.2</b>	Distributive and dispersive mixing.	12
<b>Figure II.3</b>	The correlation between glass transition temperature $T_g$ , composition and the morphology of the blend; (a) miscible blend, (b) partially miscible blend, and (c) immiscible	13
<b>Figure II.4</b>	Illustration of the different types of morphologies of immiscible blends: a) Nodular (dispersed); b) co-continuous; c) fibrillar; d) lamellar	15
<b>Figure II.5</b>	(a) Configuration of a perfect block copolymer at the interface between two phases of polymers A and B. (b) promotion of an interphase between the phases A and B in the presence of a compatibilizer	17
<b>Figure II.6</b>	Schematic of block copolymer at the interface of an immiscible polymer blend.	20
<b>Figure II.7</b>	Schematic of droplet breakup and coalescence in compatibilized and non-compatibilized blends.	20
<b>Figure II.8</b>	Schematic for reactive compatibilization. X and Y represent complementary functional groups that react at the interface in melt processing to form block copolymer.	21
<b>Figure II.9</b>	Schematic representation of copolymers at the interface of a mixture heterogeneous polymer.	23
<b>Figure III.1</b>	Structure of Polystyrene (PS)	30
<b>Figure III.2</b>	Structure of Styrene acrylonitrile (SAN).	31
<b>Figure III.3</b>	Structure of SEBS	32
<b>Figure III.4</b>	Research Flow chart of the experimental work	34
<b>Figure III.5</b>	Internal mixer ; (a) Mixing chamber ; (b) Counter –rotating (Rotors) blades of the internal mixer	36
<b>Figure III.6</b>	Typical tensile specimen, with a reduced gage section and enlarged shoulders	37
<b>Figure III.7</b>	Stress-strain - curves of ductile vs brittle materials	39
<b>Figure III.8</b>	Impact testing, (a) Izod testing	40

<b>Figure III.9</b>	The typical DSC thermogram of polymers	42
<b>Figure III.10</b>	Schematic diagram of a DSC apparatus	42
<b>Figure III.11</b>	DMTA thermogram of modulus values change with temperature and transitions in materials	43
<b>Figure III.12</b>	Block Diagram of a Thermobalance	44
<b>Figure III.13</b>	Typical TGA and DTG curves	44
<b>Figure IV.1</b>	Tensile strength of blend PS/SAN without and with compatibilizer.	48
<b>Figure IV.2</b>	Tensile modulus and Elengation at break of PS/SAN blends prepared without and with SEBS compatibilizer	49
<b>Figure IV.3</b>	Elengation at break of PS/SAN blends prepared without and with SEBS compatibilizer.	49
<b>Figure IV.4</b>	Impact strength of blend PS/SAN without and with compatibilizer.	50
<b>Figure IV.5</b>	DSC scans of PS/SAN blends melt blended without compatibilizer SEBS.	52
<b>Figure IV.6</b>	DSC scans of PS/SAN blends melt blended with SEBS compatibilizer.	52
<b>Figure IV.7</b>	The Variations of Loss Modulus for uncompatibilized and compatibilized PS/SAN blends.	53
<b>Figure IV.8</b>	The Variations of Loss Modulus for compatibilized PS/SAN blends.	54
<b>Figure IV.9</b>	TG thermograms of PS, SAN and their blends prepared without and with SEBS compatibilizer.	55
<b>Figure IV.10</b>	DTG thermograms of PS, SAN and their blends prepared without and with SEBS compatibilizer.	55
<b>Figure IV.11</b>	SEM micrographs of cryofractured surfaces of PS30 blend with and without SEBS compatibilizer.	57
<b>Figure IV.12</b>	SEM micrographs of cryofractured surfaces of PS70 blend with and without SEBS compatibilizer.	58
<b>Figure IV.13</b>	Schematic representation of morphology of SEBS compatibilized PS/SAN blend.	59
<b>Figure IV.14</b>	Effect of Complex viscosity ( $\eta^*$ ) of rPS, SAN and their blends without and with compatibilizer SEBS.	60



<b>Figure IV.15</b>	The Frequency-sweep plot of the storage modulus ( $G'$ ) for neat rPS, SAN and uncompatibilized/ compatibilized rPS/SAN/SEBS blends.	61
<b>Figure IV.16</b>	The Frequency-sweep plot of the loss modulus ( $G''$ ) for neat rPS, SAN and uncompatibilized/ compatibilized rPS/SAN/SEBS blends.	62
<b>Figure IV.17</b>	The storage modulus ( $G'$ ) and loss modulus ( $G''$ ) of rPS/SAN blends as a function of frequency for all the analysed compositions.	63
<b>Figure IV.18</b>	Effect of compatibiliser compositions on the impact strength of rPS/SAN blends.	64
<b>Figure IV.19</b>	Effect of SEBS compositions on the tensile strength of rPS/SAN compositions	66
<b>Figure IV.20</b>	Evolution of the elastic modulus of rPS/SAN noncompatibilized and compatibilized blends.	67
<b>Figure IV.21</b>	Evolution of the elongation at break of rPS/SAN noncompatibilized and compatibilized blends.	68
<b>Figure IV.22</b>	Stress <i>versus</i> strain plots of rPS, rPS/SAN blend and compatibilized ones as function of rPS content.	69
<b>Figure IV.23</b>	DSC scans of rPS/SAN blends without compatibilizer SEBS.	70
<b>Figure IV.24</b>	DSC scans of rPS/SAN blends with compatibilizer SEBS.	71
<b>Figure IV.25</b>	SEM micrographs of cryo-fractured surfaces of rPS/SAN with SEBS : <b>(a)</b> rPS/SAN 30/70, <b>(b)</b> rPS/SAN/SEBS 30/70/5, <b>(c)</b> rPS/SAN/SEBS 30/70/10.	72
<b>Figure IV.26</b>	SEM micrographs of cryo-fractured surfaces of rPS/SAN with SEBS <b>(d)</b> rPS/SAN 70/30, <b>(e)</b> rPS/SAN/SEBS 70/30/5, <b>(f)</b> rPS/SAN/SEBS 70/30/10.	73

## LIST OF TABLES

<b>Table III.1</b>	Material Properties of Polystyrene PS (GPPS-1540)	31
<b>Table III.2</b>	Material Properties of Poly (styrene-co-acrylonitrile) SAN (Luran 368R)	32
<b>Table III.3</b>	Properties of virgin Kraton G 1651 SEBS	33
<b>Table III.4(a)</b>	Blends formulation for polystyrene PS, recycled polystyrene and SAN blending process without compatibiliser	35
<b>Table III.4(b)</b>	Blends formulation for polystyrene PS, recycled polystyrene and SAN blending process with compatibiliser	35
<b>Table III.5</b>	Brabender® (GmbH & Co. KG) Characteristics	36
<b>Table IV.1</b>	Mechanical properties of PS, SAN and their uncompatibilized and compatibilized blends with SEBS	51
<b>Table IV.2</b>	Glass transition temperatures as measured from DMTA and DSC analyses for PS and SAN phases into uncompatibilized and compatibilized PS/SAN blends.	53
<b>Table IV.3</b>	Thermal stability parameters as determined from TG and DTG thermograms for PS, SAN and their blends with and without compatibilizer	56
<b>Table IV.4</b>	Average size of holes in SEM morphology of the blend analysed with ImageJ software.	57
<b>Table IV.5</b>	Crossing-point, $G' = G''$ , for rPS and their blends.	64
<b>Table IV.6</b>	The mechanical properties of recycled PS, rPS/SAN, and rPS/SAN/SEBS blend.	65
<b>Table IV.7</b>	Glass Transition Temperatures ( $T_g$ ) of rPS, SAN, and their alloys.	71

## LIST OF ABBREVIATIONS AND SYMBOLS

ABS	Acrylonitrile-Butadiene-Styrene
DCP	Dicumyl peroxide
PMMA	polymethyl methacrylate
PA6	Polyamide 6
FT-IR	Fourier transform infrared
SAN	Styrene acrylonitrile
PS	Polystyrene
rPS	Recycled polystyrene
PPO	Polyphenylene oxide
PP	Polypropylene
EPDM	Ethylene-propylene-diene monomer
SEM	Scanning electron microscopy
HIPS	High impact Polystyrene
TGA	Thermogravimetric analysis
DTG	Derivative of the Thermogravimetric curve
DSC	Differential scanning calorimetry
Phr	Per hundred rubber = per hundred resin
UCST	Upper Critical Solution Temperature
LCST	Lower Critical Solution Temperature
THF	Tetrahydrofuran
PB	Polybutadiene
SEBS-g-MAH	Styrene ethylene butylene styrene-grafted-maleic anhydride
MFI	Melt flow index

SEBS	Styrene-ethylene butylene-styrene triblock copolymer
PPS	Poly (phenylene sulphide)
DMTA	Dynamic mechanical analyser

$D_n$	Number average droplet diameter (m)
$\omega$	Angular frequency (rad/s)
$\Delta G_{mix}$	Gibbs energy of mixing [J/kg]
$T_m$	Melting temperature ( $^{\circ}\text{C}$ )
$E'$	Storage modulus
$E''$	Loss modulus
GPa	Giga Pascal
MPa	Mega Pascal
$\text{g/cm}^3$	Gram per cubic centimetre
J/m	Joule per meter
$\text{kJ/m}^2$	Kilo Joule per square meter
$T_{max}$	Temperature maximum
Rpm	Revolutions per minute
$\mu\text{m}$	Micrometre
$T_{5\%}$	Temperature corresponding to 5 % of weight loss.
$T_{50\%}$	Temperature corresponding to 50 % of weight loss
$T_{onset}$	Extrapolated start temperature of degradation
$T_g$	Glass transition temperature ( $^{\circ}\text{C}$ ).
$\eta^*$	Complex viscosity (Pa.s)
$G'$	Storage modulus (Pa)
$G''$	Loss modulus (Pa)

# **Chapter I**

**LITERATURE**

**REVIEW**

## I.1 Background of the study

The world produces and consumes thousands of tons of polystyrene every day. The enormous variety of application of polystyrene turned it into one of the most common plastic in everyday life. The amount of waste generated continues to increase due to the increasing population and development. Among these waste are food, paper and plastic, with plastics representing 24% of overall wastes. Furthermore, due to lack of responsibility and inefficient waste management, plastic waste has become a major source of environmental pollution as plastic wastes can be found easily everywhere, destroying and polluting environment. As a result, a big amount of polystyrene products ended up in the landfill as waste, the products made from polystyrene do not break down and takes up a lot of space in landfill. Their collection and recycling rate is rather smaller than the production and the consumption rate of polystyrene around the world. [1-3].

Blending is a technique in which at least two polymers are added together to create a new material with enhanced properties or reduced cost. It offers the advantage of reduced research and development expense compared to the development of new monomers and polymers to yield a similar property profile [4]. The role of polymer blend technology is pervasive in the products of our everyday life. In the rapidly emerging technology, polymer blend can quickly respond to the developing needs, much faster than the time needed in creating new monomer or developing a new polymer. As a result, many researches have been done to explore the advantages of the polymer blends.

Several polystyrene (PS) blends with other polymers such as high density polyethylene (HDPE), polyamide 6 (PA6), and polycarbonate (PC) has been investigated [5- 7]. Polystyrene (PS) is a particularly attractive class of polymers due to their properties such as high degree of hardness, excellent electrical properties, low moisture absorption, and ease of fabrication. Because of its low cost [8], the benefits of these polymer properties have led to the wide range of usage especially in automobile interior parts, appliance housings, packagings, food containers, etc.

Most of the physical blends are highly immiscible and this includes PS/SAN blend. Hence, the constituents tend to form aggregates, resulting in separated phases that lead to heterogeneous blends with poor adhesion at the interface, and therefore poor mechanical

properties. It is also difficult to obtain a good dispersion in polymer blends. In order to overcome the problem of an immiscible blend, some modifications of the interfaces or compatibilization are then necessary to obtain useful polymeric products with desired properties.

## I.2 Problem statement

Blends of polystyrene (PS) and Styrene-co-acrylonitrile (SAN) are immiscible over the whole composition range and they have consequently poor mechanical properties. An amorphous blend such as PS/SAN is very sensitive to temperature above their  $T_g$  around  $100^\circ\text{C}$  and  $110^\circ\text{C}$  respectively, therefore, in order to improve the PS/SAN blend toughness, miscibility and achieve better properties, the compatibilization process is usually necessary [9,10]. With the addition of a third component on PS/SAN blends as compatibilizer, the resulting material become rubbery and soft. Ideally, two or more polymers may be blended together to achieve desirable combinations of characteristics and in our case are PS and SAN blends. However, the main obstacle is to create a compatible blend of PS/SAN with a good balance of mechanical, rheological and thermal properties.

Moreover, a comprehensive literature survey also revealed that no significant work has been reported on PS/SAN especially on improving the compatibility and toughness of the blends with SEBS as compatibilizer. Furthermore, one of the more conventional methods and effective way for compatibilization of two polymers is by introducing the third component as compatibilizer in the blend. Block or graft copolymers (with the same or similar structure to blend components) are recommended as they are suitable as compatibilizer [11]. In this present work the following new areas which are not being revealed and discussed in previous researches will be presented

- i. The use of SEBS as compatibilizer to improve the toughness and compatibility of blends in different contents;
- ii. The use of impact and tensile strength for the study of the mechanical behavior of PS/SAN and recycled polystyrene (rPS)/SAN blends;
- iii. To explore the effect of blend compositions by using DSC, DMTA and TGA as a tool to study the dynamic mechanical properties, thermal stability;
- iv. The use of rheometer (RPA) to study the rheological properties of PS/SAN, rPS/SAN non-compatibilized and compatibilized blends;
- v. Correlate changes in morphology behavior of the compatibilized blends with changes in thermal, rheological, static as well as dynamic mechanical behaviour.



### I.3 Research Objective

The objectives of this research work have been achieved by carrying-out the study into two stages. A first part is to study the effect of recycled polystyrene in PS/SAN blends without compatibilizer and to analyse the changes in their properties. The idea was to see how the recycled PS affects the mechanical, rheological and thermal properties of blends and to compare with their morphology behavior versus pure polystyrene. In short, to determine if it is worth or not the recycling of polystyrene.

The study on the effect of compatibilizer SEBS in the PS/SAN, rPS/SAN blends and to improve the toughness of blends will be conducted in the second stage.

Overall, the objectives of this study are:

- a) Improving the compatibility and toughness of PS/SAN and recycled PS/SAN blends
- b) To study the effect of compatibilizer on mechanical, thermal and rheological as well as dynamic mechanical properties of PS/SAN, rPS/SAN blends.
- c) To correlate changes in structure and morphology of the compatibilized blends with changes in thermal, rheological, as well as dynamic mechanical behavior.
- d) To examine the optimum composition of blend using different amount of compatibilizer.
- e) To compare the performance of recycled compatibilized PS/SAN blends with therecycled PS and original PS

### I.4 Scopes of research

This research involved the preparation of samples (noncompatibilized and compatibilized PS/SAN and PS/SAN/SEBS blends) including the following stages:

- i. Dry blending;
- ii. Melt blending of Samples.

A Brabender internal mixer was used to produce pellets for both PS/SAN, rPS/SAN blends followed by compression moulding process to prepare test specimens according to the ASTM testing standard. The content of PS was 0, 30, 50, 70, 100 wt%. The SEBS as compatibilizer was added into PS/SAN. The ratios of SEBS were varied from 0 to 15 phr.

The tests below were done for characterization of the samples In order to achieve the objectives:

- 1) Mechanical properties of PS/SAN blends with varying percentages of PS, and compatibilizers SEBS were determined, specifically,
  - a) Tensile Properties (including tensile strength, modulus and elongation at break);
  - b) Impact Properties.
- 2) Fourier Transform Infrared Spectroscopy (FTIR) was done to characterize the composition and functional group in compatibilized PS/SAN/SEBS blend.
- 3) Scanning Electron Microscopy (SEM) was carried out to examine the phase morphology of the noncompatibilized and compatibilized PS/SAN blends.
- 4) Differential scanning calorimetry (DSC) was used to investigate the compatibility of the sample by obtaining the glass transition temperature ( $T_g$ );
- 5) Thermogravimetric Analysis (TGA) was done to determine the thermal stability and thermal decomposition of the blends;
- 6) Rheological studies (RPA) were used to investigate the rheological parameters of polymer blends;
- 7) Thermal dynamic mechanical Properties (DMTA) (including storage modulus, loss modulus and  $\tan \delta$ ).

### **I.5 Outline of Thesis Structure**

This dissertation is divided into five chapters including the present one.

**Chapter 1** is an introduction of the study with the background, problems statement, objectives and scope of the thesis.

**Chapter 2** provides a literature review on polymer blending, particularly those that are closely related to this work.

**Chapter 3** describes step-by step the experimental procedures employed. A detailed description of the experimental methodology is presented, which includes, sample preparation methods such as the mechanical testing, thermal investigation, morphological analysis and rheological analysis of PS/SAN blends and detailed description of the instruments used.

**Chapter 4** reports the results and discusses the findings.

**Chapter 5** presents the general conclusion and a summary of the key results of this thesis and a list of recommendations for future works.

## REFERENCES

- [1] A. G. Buekens. & H. Huang, (1998) « Catalytic plastics cracking for recovery of gasoline-range hydrocarbons from municipal plastic wastes ». *Resources, Conservation and Recycling* **23** (3), 163–181. [doi.org/10.1016/S0921-3449\(98\)00025-1](https://doi.org/10.1016/S0921-3449(98)00025-1)
- [2] S. Ross. & D. Evans, (2003) « The environmental effect of reusing and recycling a plastic-based packaging system ». *Journal of Cleaner Production* **11**(5), 561–571. [doi.org/10.1016/S0959-6526\(02\)00089-6](https://doi.org/10.1016/S0959-6526(02)00089-6)
- [3] W. Kaminsky., M. Predel, & A. Sadiki, (2004) « Feedstock recycling of polymers by pyrolysis in a fluidised bed. *Polymer Degradation and Stability* **85** (3), 1045–1050. [doi.org/10.1016/j.polymdegradstab.2003.05.002](https://doi.org/10.1016/j.polymdegradstab.2003.05.002)
- [4] O. Abdolrasou. and I.G. Meldrum (1999). Characterization of polyethylene terephthalate and functionalized polypropylene blends by different methods. *Iranian Polymer Journal*. **8** (3):1026-1265. [doi.org/10.1016/j.polymdegradstab.1999.05.00014](https://doi.org/10.1016/j.polymdegradstab.1999.05.00014)
- [5] F. Sahnoune; J. M. Lopez Cuesta; A. Crespy (2003). « Improvement of the mechanical properties of an HDPE/PS blend by compatibilization and incorporation of CaCO<sub>3</sub> ». *Polym. Degrad. Stab.* **43**(3), 647–660. [Doi.org/10.1002/pen.10053](https://doi.org/10.1002/pen.10053).
- [6] Feng-Po Tseng; Chen-Rui Tseng; Feng-Chih Chang; Jiang-Jen Lin; I-Jein Cheng (2005). « Compatibilization of PS and PA6 Blends by Means of Poly(oxyalkylene)amine Modified Styrene-Maleic Anhydride Copolymer ». *Polym. Degrad. Stab.* **12**(6), 439–447. [doi:10.1007/s10965-004-1875-x](https://doi.org/10.1007/s10965-004-1875-x)
- [7] Luciana Sartore; Maurizio Penco; Stefania Della Sciucca; Raniero Mendichi; Luca Di Landro; Salvatore D'Antone (2006). « PPO–PC block-copolymers used as compatibilizers in PS/PC blends ». *Polym. Degrad. Stab.* **100**(6), 4654–4660. doi:10.1002/app.23208
- [8] C.B.B. Luna., Araújo, E. M., Siqueira, D. D., Morais, D. D. de S., Filho, E. A. dos S. & Fook, M. V. L (2020) « Incorporation of a recycled rubber compound from the shoe industry in polystyrene: Effect of SBS compatibilizer content ». *Journal of Elastomers & Plastics* **52**, 3–28. [doi.org/10.1177/0095244318819213](https://doi.org/10.1177/0095244318819213)
- [9] N. Aranburu and, I.J. Eguiazábal, (2015) « Improved mechanical properties of compatibilized polypropylene/polyamide-12 blends » *Int. J. Polym. Sci.*, **2015** 1–8. [doi.org/10.1155/2015/742540](https://doi.org/10.1155/2015/742540)
- [10] Jiang G, Wu H and Guo S 2010 Reinforcement of adhesion and development of morphology at polymer-polymer interface via reactive compatibilization: a review *Polym. Eng. Sci.* **50** (12) 2273–2286. [doi.org/10.1002/pen.21686](https://doi.org/10.1002/pen.21686)

- [11] K. Bedjaoui., R. Krache, A. Marcos-Fernández .; M. Guessoum. « The effect of compatibilizer SEBS on the mechanical, morphological and thermal properties of the polystyrene/poly (styrene-co-acrylonitrile) copolymer blends ». Mater. Res. Express 2019, 6, 105334.

**Chapter II**  
**STATE OF ART**

## **Chapter II. Polymer blends and Compatibilization Strategies**

### **II.1. Introduction**

The preparation of polymer blends is now the most suitable strategy from the point of view of price and time for obtaining new materials since it is less expensive and faster to mix polymers than to develop monomers or new methods of polymerization. Polymer blends also offer the opportunity to obtain a wide range of characteristics and properties by just changing the composition of the combined polymers. Also, the main objectives of the materials obtained through polymer blends are to meet several requirements that may be necessary for manufacturers.

Polymer blending has many advantages, including the following:

- Fabrication of new materials with desired properties ;
- Development of new materials in a cost effective manner ;
- Better processability of materials ;
- Developing materials with combined properties of two or more polymers ;
- Tuning of final properties by controlling the morphologies ;
- Method of recycling of plastic waste ;
- Enhancement of the product performance to meet the rising customer needs ;
- Adjustment of performance requirements of consumer at a lower price ;
- Optimization of composition to suit the requirement [1].

Ideally, two or more polymers can be blended to form a wide variety of morphologies, statistical or structured, in order to obtain products that potentially should provide desirable combinations of characteristics. But in practice, it is very difficult to have these potential combinations through simple mixtures, because of some fundamental and inherent problems and situations at the interface which make the achievement of mixtures less profitable. Frequently, both polymers are thermodynamically immiscible, which excludes generation of homogeneous products. This is not often a problem since it is generally wanted to have products in two phases, but for this it is imperative that the synergistic nature of the Products must be revealed. Thus, the control of thermodynamic laws that govern these systems is the key to the understanding of their behavior and properties [2].

## II.2 Polymer blend terminology

Polymer blends can be divided into different types considering the miscibility, immiscibility, partial miscibility and compatibility of the components [3]. In this context, it is appropriate to clarify some terminology used in the field of polymer blends. The nomenclature adopted shows the interdependence (Figure I) of common terms defined by Utraki [4-5].

**a) Miscible** : It is considered to be the level of mixing of polymeric constituents of a blend yielding a material which exhibits the properties expected from a single phase material. Polymer blends which are homogeneous down to the molecular level are associated with the negative value of free energy of mixing:  $\Delta G_{mix} \approx \Delta H_{mix} \leq 0$ .

**b) Immiscibility**: A blend is considered immiscible if it is separated into phases composed by the individual constituents. Phase separation is also established from thermodynamic relationships. An immiscible polymer blend can be defined as the blend that does not comply with the thermodynamic conditions of phase stability. Any polymer blend whose  $\Delta G_{mix} \approx \Delta H_{mix} > 0$

**c) Partial miscibility** : A blend is considered partially miscible if there exists phase separation but each polymer rich phase contains a sufficient amount of the other polymer to alter the properties of that phase.

**e) Compatible polymer blend** : Term to be avoided ! visibly homogeneous polymer mixture, A term indicating a commercially attractive polymer mixture with enhanced physical properties over the constituent polymers.

**f) Polymer alloy**: An immiscible polymer blend having a modified interface and/or morphology.

## II.3 Thermodynamic of Polymer Blends

Mixing of two polymers can produce either a homogeneous mixture at the molecular level or a heterogeneous separated phase blend [3].

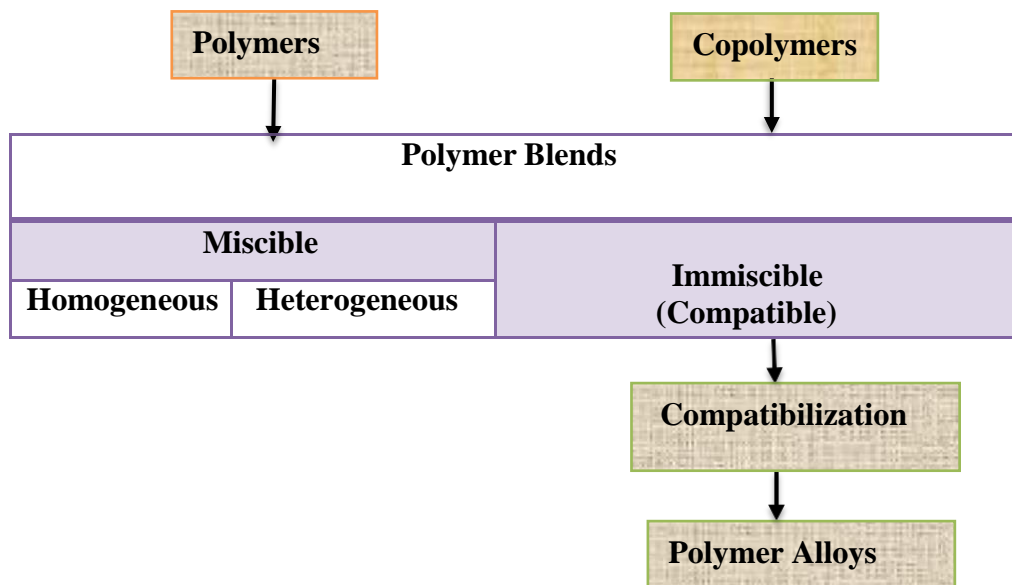


**Figure II.1** : Interrelations in polymer blend nomenclature.

At the equilibrium, a blend of two amorphous polymers can exist as one phase in which the segments of the two macromolecular components are mixed, or as two separate phases, each consisting essentially of a different polymer. The most important relationship governing mixtures of dissimilar components 1 and 2 is equation (II.1)

$$\Delta G_{mix} = \Delta H_{mix} - T\Delta S_{mix} \quad (\text{Eq.1})$$

Where  $\Delta H_{mix}$  is the enthalpy of mixing,

T is the absolute temperature, and  $\Delta S_{mix}$  is the entropy of mixing

Where  $\Delta H_{mix}$  is the enthalpy of interaction ; is the energy part linked to interactions.

$\Delta S_{mix}$  is combinatorial entropy ; this is related to conformation and disorder

$\Delta G_{mix}$  must also satisfy a second condition which ensures the miscibility and prevents phase separation:

The thermodynamic driving force for mixing is minimisation of  $\Delta G_{mix}$ . Thus if the free energy is positive, the system is immiscible. While for small molecules the entropy is high enough to ensure miscibility, for polymers the entropy is almost zero, causing enthalpy to be decisive in determining miscibility. For spontaneous mixing,  $\Delta G_{mix}$  must be negative, and so



$$\Delta H_{mix} - T\Delta S_{mix} < 0 \quad (\text{Eq.2})$$

For complete miscibility to occur, a negative free energy of mixing is necessary but not sufficient. Equation above shows that  $\Delta G_{mix}$  for a binary mixture can vary with composition in several ways [6]:

i) Complete immiscibility exists if  $\Delta G_{mix}$  is positive

ii) Complete miscibility exists only if

$$\Delta G_{mix} < 0 \quad (\text{Eq.3})$$

And for that, the second derivative of  $\Delta G_{mix}$  with respect to the volume fraction of either component must be greater than zero over the whole composition range.

$$\left( \frac{\partial^2(\Delta G_m)}{\partial \phi_i^2} \right)_{T,p} > 0 \quad (\text{Eq.4})$$

where:  $\phi_i$  – the volume fraction of component, T and p - temperature and pressure of the system.

Most of the binary systems have the Gibbs energy of mixing higher than 0 and they do not form homogenous mixtures.  $\Delta H_m$  is the main parameter influencing the miscibility of polymers (as  $\Delta H_m$  depends on the interactions occurring between components), while the contribution of  $\Delta S_m$  is smaller (as  $\Delta S_m$  depends on the number of rearrangements and decreases with increasing the molar mass) [6]. This is different from the solutions of low-molecular weight compounds where the entropy of mixing is the predominating factor. As  $\Delta S_m$  is relatively small in comparison with  $\Delta H_m$ , only the blends with  $\Delta H_m$  negative or very near zero are going to be miscible. The mixing is exothermic only if strong interaction occurs between components. Therefore, only the polymers with attractive interactions between molecules of the components or very similar on the molecular level can be miscible [7, 8].

#### II.4 Methods of Polymer Blending

The majority of polymer pairs are immiscible. The phase structure of polymer blends is not in equilibrium and depends on the process of their preparation. Two different methods are used for the preparation of the polymer blends: melt blending, and solution blending [9].

### *II.4.1 Solution Blending*

In this method, the polymers are dissolved in a common solvent. Blend is produced by evaporating the solvent and precipitating the resulting polymer mixture. The advantage of this technique is the quick mixing of the blend components without high demand of energy and hence no chance of crosslinking, degradation or chemical decomposition. The use of this method is limited due to the difficulty of finding a suitable co-solvent for the components of the blend and then to evaporate large quantities of organic solvent which are mostly environment unfriendly [10]. This technique is, therefore, used in industry only for preparation of paints, surface layers and thin membranes. Because of the limited use of this method, the method used in this study will be melt blending.

### *II.4.2 Melt Blending*

Melt mixing is the most widespread method of polymer blend preparation in practice. The blend components are mixed in the molten state in extruders or batch mixers [11]. High shear mixers can generate fine dispersions with droplet diameters smaller than 1 micrometer [12]. Once the ingredients have been fed in the correct proportions into the mixing device hopper, typically an extruder, the polymers and/or additives must be homogeneously blended together. This requires that the polymers be in the molten state. The mixing device melts the polymers, provides a means for mixing, and generates pressure for subsequent operations such as making film when in-line mixing and pelletizing when compounding. The main advantages of the method are well-defined components and universality of mixing devices—the same extruders or batch mixers can be used for a wide range of polymer blends. Drawbacks of the method are high energy consumption and possible unfavorable chemical changes of blend components. Mixing is described as either distributive or dispersive as it is illustrated in (Figure II.2).

In distributive mixing, the polymer is rearranged by deformation. Separation and rearrangement of flow and kneading are two examples of distributive mixing. In dispersive mixing, particles are broken up and dispersed within the polymer matrix.

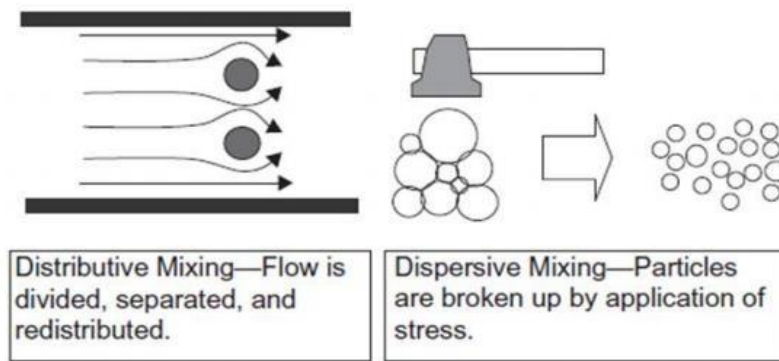


**Figure II.2:** Distributive and dispersive mixing.

Mixing in melt blending is very important in the formation of the final blend morphology. Melt mixing is a complex process involving melting of the solid pellets, distributive mixing (particle elongation), dispersive mixing and droplet coalescence [13]. In order to gain superior properties, both good dispersion and good distribution of the dispersed phase in the matrix are necessary. A good distributive mixing can be achieved by providing convoluted flow paths that split and reorient the flow repeatedly. A good dispersive mixing can be achieved by passing the mixture through small regions of intense deformation [11-14].

For example, although the PS, SAN, and PS/SAN blends systems presented in this study are known and have been reported to be theoretically immiscible [15], they could be rendered compatible by addition of a suitable compatibilizer, with the resultant blend achieving excellent properties. Thus, in this research, a blend is considered compatible if it exhibits a set of properties which are desirable and useful, regardless of whether the blend has complete or partial miscibility, or due to the application of a suitable compatibilization technique.

### II.5 Miscibility of Polymer Blends

In miscible blends, the chain segments of the two polymers are miscible on a molecular level. Such blends have only a single glass transition temperature ( $T_g$ ), which mainly depends on the composition (Fig II.3a). A well-known example of a blend which is miscible over a very wide temperature range and in all compositions is PS / PPO that combines the heat resistance, the inflammability and the toughness of PPO with the good processability and low cost of PS [16-21].

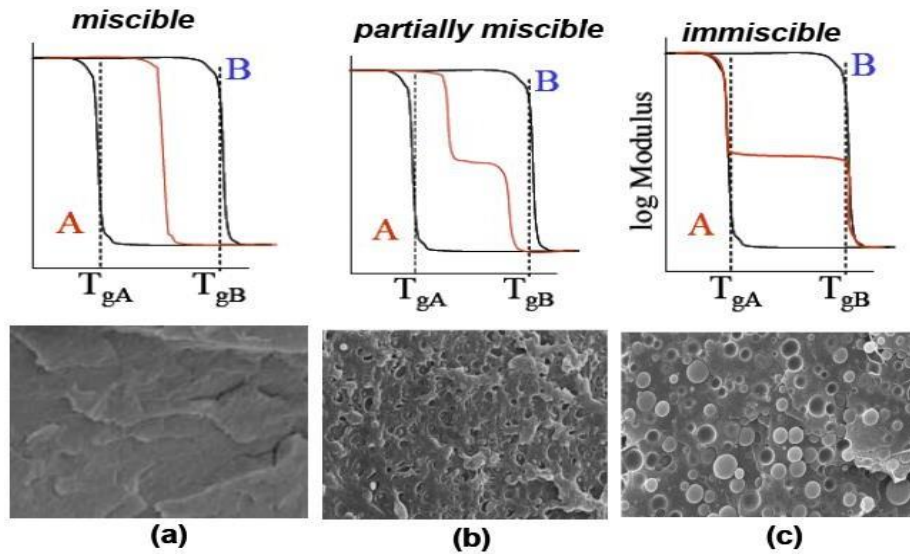


**Figure II.3** The correlation between glass transition temperature  $T_g$ , composition and the morphology of the blend; (a) miscible blend, (b) partially miscible blend, and (c) immiscible

As shown in Fig II.3a, this type of blend exhibits a single glass transition temperature ( $T_g$ ), which is between the  $T_g$ s of both blend components in a close relation to the blend composition [22]. A system that is either partially miscible such as PS and poly(styrene-co-bromostyrene) PBrS [24], or completely immiscible such as PS/PP and PS/PE [23], but offers attractive performances, is often designated as a compatible polymer blend. These blends usually have two glass transition temperatures, which may slightly deviate from the  $T_g$  of the blend components (Fig II.3b and Fig II.3c). The deviation of the glass transition temperatures from the  $T_g$  of the pure components might be different and depends on the partial miscibility of each component in the other. On a microscopic scale these polymer blends have a phase-separated structure (morphology), which could be of different nature (sphere, cylinder, or lamellar) depending on the composition of the blends. Usually the major component forms the matrix phase, wherein domains of the minor phase are dispersed. The size of the dispersed domain is related to the interfacial tension and viscosity ratio between the matrix and dispersed phase [25].

## II.6 Factors affecting miscibility of polymer blends

Some of the factors which affect the miscibility and immiscibility of the polymer blends are discussed over here.

### ***II.6.1) Blend ratio***

Two polymers appear immiscible when high amounts of both components. However, it is possible that a small amount of one polymer may be soluble in a large amount of the other polymer, as understood in conventional phase rules. This consideration is very important in natural compatibility [26].

### ***II.6.2) Polarity***

Polarity of constituent polymers plays decisive role in miscibility of polymer blends. Polymers with a similar structure or similar polarity are less likely to repel each other, and therefore more likely to form miscible blends [27, 28]. Differences in polarities usually produce immiscibility.

### ***II.6.3) Specific interaction***

Polymers that are drawn to each other by hydrogen bonding, acid-base, charge transfer, ion-dipole and donor-acceptor adducts. When these attractions occur they tend to produce miscibility [29,30].

### ***II.6.4) Molecular weight***

Normally, lower molecular weight permits greater randomization on mixing and therefore greater gain of entropy, which favors miscibility [31,32]. The polymers with similar molecular weights are more miscible, whereas polymers with different molecular weights may be immiscible, even if they both have the same composition.

### ***II.6.5) Crystallinity***

When a polymer crystallizes, it forms a two-phase system. Thus, in a polymer blend when a polymer crystallizes, this adds another phase to the system. If both polymers in a blend crystallize, they will usually form two separate crystalline phases; it is quite rare for the two polymers to cocrystallize in a single crystalline phase [33].

## **II.7 Blend Morphology**

A blend of polymers is mostly immiscible, whose properties are not only a function of blend composition but also depend crucially on the degree of dispersion, phase particle size, and phase interaction between the components of the blend. Controlling the morphology is therefore the control of polymer blend properties [34, 35]. Immiscible blends are characterized by poor mechanical properties coming from weak interfacial adhesion between the phases and/or stress concentrations at interface boundaries [36,37]. Several strategies have

been employed to overcome this and improve blend compatibility, such as chemical modifications, addition of block copolymers. Immiscible polymer blends exhibit different morphologies, such as nodular, lamellar or co-continuous structure [38]. (Fig.II 2).

**i) Nodular to fibrillar morphologies:**

When one of two polymers is strongly in minority, it is dispersed in the form of inclusions in the matrix consisting of the majority polymer. Depending on the parameters and properties of the polymers in the blend, the nodules may have a spherical, cylindrical or lamellar structure as shown in Fig II.4 (a, c and d).

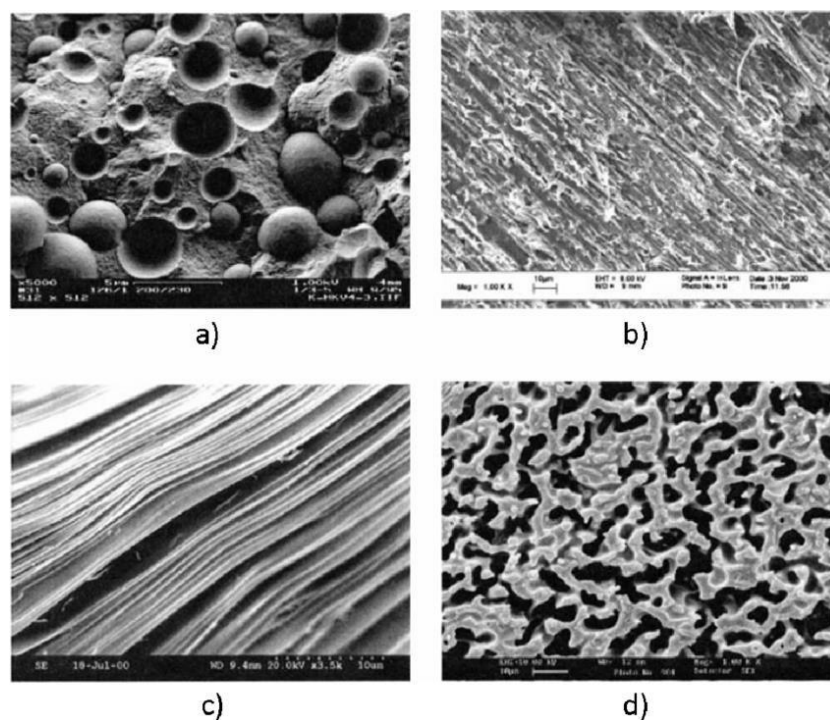


**Figure II.4** Illustration of the different types morphologies of immiscible blends.

a) Nodular (dispersed); b) co-continuous; c) fibrillar; d) lamellar [39].

**ii) Co-continuous morphologies:**

If we increase the volume fraction of the polymer minority, we obtain a co-continuous structure composed of two interpenetrating phases. The developing morphology in immiscible binary polymer blends can be classified into disperse/matrix or co-continuous structures (Fig II.4), where the maximum co-continuity of the blends means the concentration of phase inversion. However, most polymers are not compatible with each other, thus a suitable copolymer or a compatibilizer that contains functional groups to establish interactions with the phases is needed to achieve good miscibility



between the phases. This addition results in finer blend morphology as well as improved physical and mechanical properties.

The majority of polymers are immiscible and need to be compatibilized. Developing a homogeneous blend system to achieve useful properties soon became the promising

\* direction of research. It was discovered that some polymer pairs were completely miscible to give a homogeneous single phase. [40].

## II.8 Compatibilization of polymer blends

From a commercial point of view, the properties of manufactured items must be stable and reproducible. However, the change in morphology with the processing conditions and phase separation with aging are characteristics of heterogeneous systems that may deteriorate the privileged position of polymer blends on the market. To be safe from this disagreeable situation, the manufacturer must find polymers that can tolerate changes in processing and transportation conditions and, therefore, materials that behave like homopolymers on storage.

The first solution is to seek miscible systems with superior properties in terms of processing conditions and performance. But, practically, heterophasic systems are by far the most attractive; the dispersed phase often improves the impact resistance and always gives a strengthening effect. As a result, it is better to produce heterophasic systems which are stable and reproducible as the corresponding homopolymers. For this, the safest way is to stabilize these phases by compatibilization, which can be achieved by numerous ways which have been proved in obtaining successful polymer alloys. Stabilization of heterogeneous systems is done primarily by overcoming the interface problems [41].

## II.9 Interphase and interfacial phenomena in polymer blends

By definition, a multiphase system has two or more phases. The most frequent is the system composed of two phases; one is the continuous phase, or matrix, in which the other phase is dispersed. Interfaces always appear between phases regardless of the system under study (a mineral-reinforced composite material or a polymer blend), and the fact that a material has properties that necessarily reflect those of its constituents and the interface. It also appears that to better understand the final properties of a multiphase system,

it is essential to take into account the interfacial region. It is also important to recognize that the interfacial zone can be extended to the thickness of the layer where the properties are different from bulk properties of each constituent. Therefore, in the vicinity of interfaces, an area of special structure (which is different from the two polymers in contact, but still dependent on them), is formed with a thickness  $\Delta l$  ranging from a few nanometers to a few hundred nanometers [1]. This area provides phase continuity condition and any kind of transfer between the continuous and dispersed phases. It is defined by the term interphase. The interphase can be considered as a third phase with its own characteristics and region of interdiffusion of the two types of macromolecules. Its stabilization results in the performance reproducibility, better processing conditions and recyclability of materials. In general, the mobility of segments in the interphase is slow and its thickness depends on the thermodynamic interactions of the macromolecular segment size, and the composition. Consequently, the interphase layer is not a homogeneous entity but a complex of micro and macro heterogeneities.

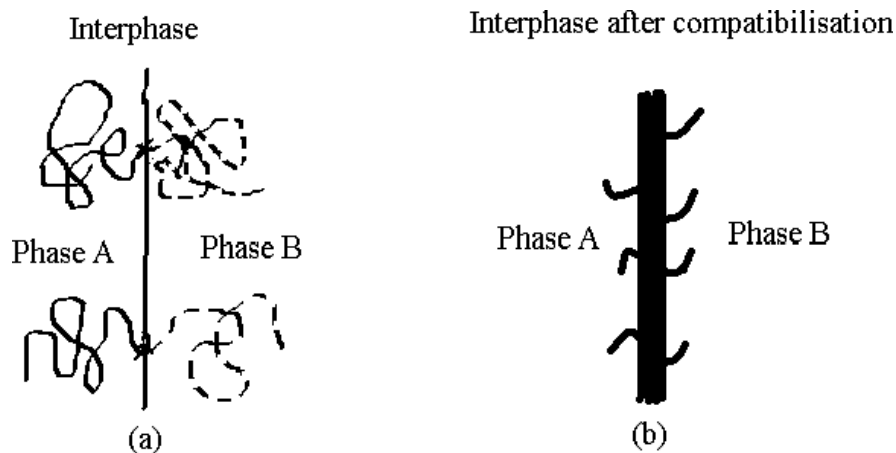


**Figure II.5:** (a) Configuration of a perfect block copolymer at the interface between two phases of polymers A and B. (b) promotion of an interphase between the phases A and B in the presence of a compatibilizer [42].

For all these reasons, we can conclude that in polymer technology, the concept of interface / interphase is the point of interest and its study is the key of the problems presented by heterophasic systems. Thus, discussing a product's performance means the discussion of the dispersion, morphology and adhesion between the different phases, and these are all related to the properties of the interfacial region. It was confirmed that the interphase thickness  $\Delta l$  varies from 2 to 60 nm [42].



The first value is typical of immiscible polymer pairs and antagonists while the second is valid for polymer alloys compatibilized through reactive ways. For these systems, it has been proved that  $\Delta l$  increases with the annealing time up to a constant value. This value depends heavily on system, temperature and concentration of reactive sites. This equilibrium value ranges from 10-50 nm, whereas the thickness of the interphase is only 6-8 nm when adding a block copolymer [42].

The interphase is characterized by two important parameters, including the coefficient of interfacial tension and adhesion area. The interfacial tension coefficient depends strongly on the structure of the polymers composing the mixture and this is inversely proportional to the thickness  $\Delta l$  of the interphase. Also, adhesion domain is based on the size and deformability of the interphase [41]. Typical cases that can generally be encountered when carrying out any combination are a high interfacial tension, or very low interfacial adhesion between the two phases. The interfacial tension contributes to the inherent difficulty to obtain a desired degree of dispersion, and thus unstable mixtures which can subsequently lead to separations or stratification process.

Furthermore, poor adhesion leads to very poor mechanical behavior as it may also prevent certain morphologies which are highly structured [43]. Thus it is imperative to consider the interphase as the key parameter and always make a change in its thickness and structure when the components of a blend are thermodynamically immiscible and this leads to the concept of multiphase system compatibilization. The operation of compatibilization can control the state of phase separation of a mixture in order to better respond to the problem of high interfacial tension which is manifested by the difficulty of mixing and also leads directly to poor interfacial adhesion. Thus, by replacing the clear interface by interfacial areas with blurred boundaries, which is a continuation property of the phases of the system, compatibilization helps in the achievement of synergy between the characteristics of the various constituents [42].

Furthermore, the existence of physical or chemical interactions along this area controls all performance of polymer blends and composites. Strong interactions provide good adhesion and a very effective stress transfer from the continuous phase to the dispersed phase. But in the absence of these interactions or if they are weak, the use of a compatibilizer is needed [44].

## II.10 Compatibilization of polymer blends

Compatibilization is a process of modification of the interfacial properties in an immiscible polymer blend that results in the formation of the interphases and stabilization of the morphology [45]. As it follows from thermodynamics, the blends of immiscible polymers obtained by simple mixing show a strong separation tendency, leading to a coarse structure and low interfacial adhesion. The final material then shows poor mechanical properties. On the other hand, the immiscibility or limited miscibility of polymers enables the formation of wide range structures, some of which, if stabilized, can impart excellent end-use properties to the final material [46-48]. The essential roles and functions of compatibilization are to:

- Reduce the interfacial tension and improve adhesion between phases which facilitates a fine dispersion ;
- Stabilization of morphology in order to avoid its evolution during the subsequent processes of transformation of the material;
- Increased adhesion between different phases in the solid state to promote in particular stress transfer between phases and therefore improve the mechanical properties of the blends [49,50].

Thus, the refinement and stabilization of the morphology and the increase in interfacial adhesion can often promote a material with industrial interest, for which the beneficial properties of both components are utilised and deficiencies are effectively hidden.

## II. 11 Compatibilizers in polymer blends

### II.11.1 How a compatibilizer functions

Compatibilizers are used to allow blending of immiscible polymers, creating a homogenous blend. Immiscible materials, form two phases when mixed together. A compatibilizer works like a surfactant, reducing the interfacial tension between two incompatible polymers and allowing the incompatible materials to blend. While the blend is still in two phases, the compatibilizer allows mixing and stability of the two phases to such an extent that the polymers behave as if they were partially miscible. The compatibilizer typically is a block copolymer. Each block interacts with one of the other polymers in the blend. The copolymers can assemble at the interface with one block in either material, providing a stitching across the interface (Figure II.6).

These macromolecular surfactants reduce surface tension (promoting droplet breakup) and provide steric stabilization to droplets (preventing coalescence), leading to finer dispersion (Figure II.7). [51]. Finally, block copolymer compatibilizers increase the energy of adhesion by entangling with homopolymers of both component materials.

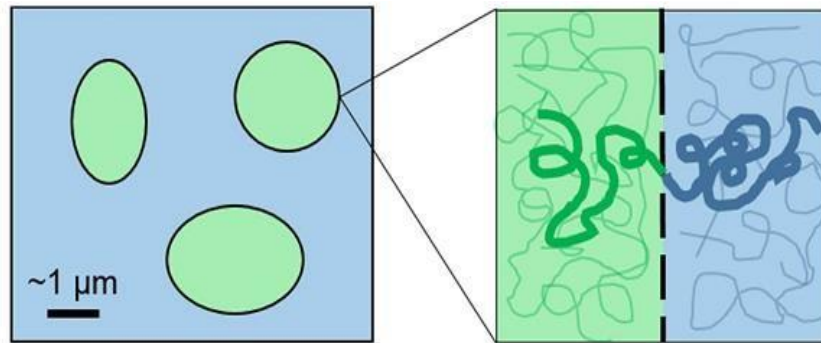


**Figure II.6** Schematic of block copolymer at the interface of an immiscible polymer blend.

During the melt mixing procedure the compatibilizer reduces the interfacial tension between the immiscible polymers, which results in a significant size reduction of the dispersed domains. Since the surface of the domain is covered by the compatibilizer

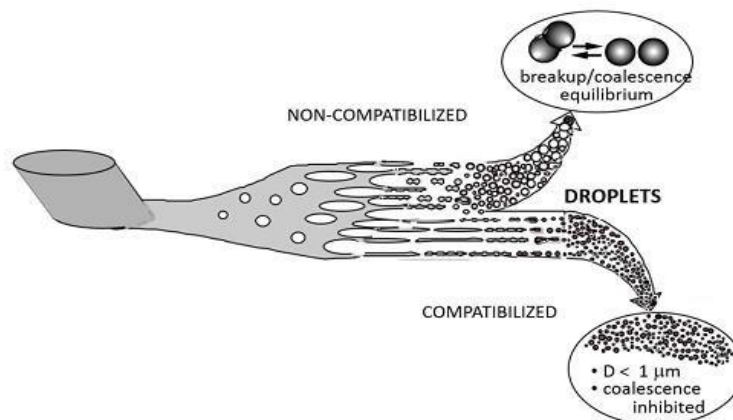


**Figure II.7** Schematic of droplet breakup and coalescence in compatibilized and non-compatibilized blends. [51].

the coalescence rate of the dispersed domain is tremendously reduced, which is helpful to keep the morphology of the material stable during the processing steps. [52-53] Thus the compatibilizers are able to generate and to stabilize a finer morphology.

The compatibilization strategies of polymer blends are different and their choice is intimately related to the structure of the mixed materials and the existence of the adequate equipment for achieving the desired blend. Two general methods used for compatibilization of immiscible systems. The first type is a **reactive compatibilizer** and the second type, which is the aim of this study, is a **non-reactive** third component, detailed in the following in this section.

### II.11.2 Reactive Compatibilization

Reactive compatibilization is used to create block or graft copolymers at the interface of blends during melt mixing. In this method, complimentary functional groups are attached to a small number of chains for each of the homopolymers. During melt mixing, these functional groups can come to the interface and react to form block copolymers, which are thereby localized at the interface instead of residing in micelles (Figure II.8). Interfacial localization and the relatively inexpensive process of adding functional groups (compared to making premade block copolymer) are the main advantages of this strategy [54]. The conditions for reactive processing require that there is:

- i) Sufficient dispersive and distributive mixing to ascertain required renewal of the interface;
- ii) Presence of a reactive functionality, capable to react across the interphase;
- iii) Sufficient reaction rate making it possible to produce sufficient quantity of the compatibilizing copolymer within the residence time of the processing unit;
- iv) Stability of the formed chemical structures; and
- v) Stability of the morphology.

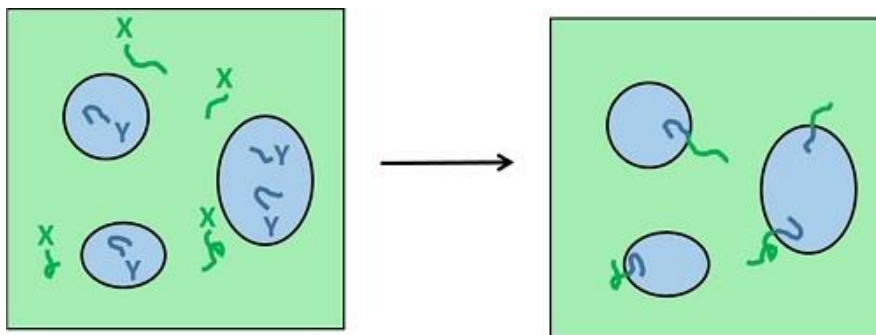


**Figure II.8** Schematic for reactive compatibilization. X and Y represent complementary functional groups that react at the interface in melt processing to form block copolymer.

During the reactive processing, during extrusion or injection molding, block or graft copolymers are usually formed. The chemical reaction leads to covalent or, less frequently, ionic bonds [53].

### *II.11.3 Non-reactive Compatibilization*

This has been the most common method of compatibilization, and consists on the addition of a third component in an immiscible system. In most cases, such an additive is either a block or a graft copolymer. Since the key requirement is miscibility, it is not necessary for the copolymer to have identical chain segments as those of the main polymers. It suffices that the copolymer has segments having specific interactions with the main polymeric components such as hydrogen bonding, dipole-dipole interaction, or dipole-ionic interaction [54]. Theoretical calculations suggest that efficiency of a compatibilizer increases with its molecular weight. However, thermodynamics requires that the added copolymer not only concentrates in the interphase (Figure II.6), but also dissolves in both phases, where it may form micelles. It is essential that the compatibilizer is designed to migrate to the interface, broadening the segmental concentration profile. Addition of a block or graft copolymer reduces the interfacial tension and alters the molecular structure at the interface.

One of the drawbacks of this method is the tendency of the added copolymers to form micelles. These reduce the efficiency of the compatibilizer, increase the blend viscosity and may lessen the mechanical performance. For these reasons, the copolymer must be designed in such a way as to:

- (i) Maximize miscibility of the appropriate part of its macromolecule with the specific polymeric component of the blend,
- (ii) Minimize its molecular weight just to about the entanglement molecular weight for each interacting block,

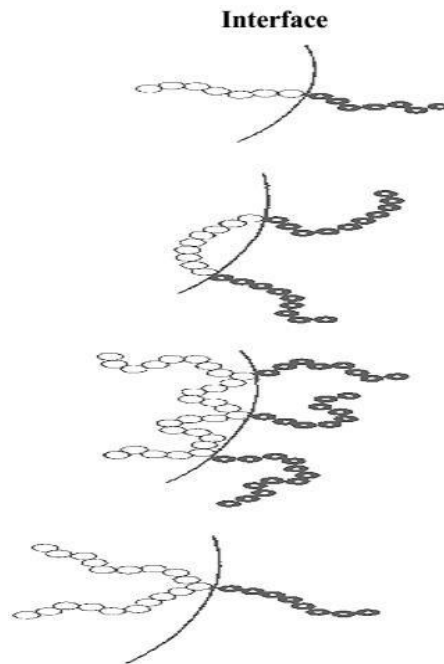


**Figure II.9** Schematic representation of copolymers at the interface of a mixture

(iii) Minimize copolymer concentration in the blend. Addition of 0.5 to 2 wt% of well-designed, tapered block copolymer has been found sufficient [54].

While reduction of the interfacial tension is relatively simple, the two other functions (stabilization of morphology and improvement of interfacial adhesion in the solid state) rarely are simultaneously achieved. Often, a combination of compatibilizers, or use of other strategies, e.g. crosslinking of one of the three phases (by chemical, thermal or irradiation treatment), may be more appropriate [55].

## II.12 Conclusion

With the intensification of the use of polymer blends in applications where the use of a homopolymer does not provide all the required properties, it is becoming increasingly important to further accentuate the research to overcome the problem of immiscibility which is the major limitation to many applications of these materials. Compatibilization techniques are different and they all target a common goal. However, the suitability of a method to a specific industrial development depends on many factors such as price, the final performance, recyclability and the possibility of biodegradability of the mixture.

The non-reactive compatibilization requires materials designed according to stringent specifications that make their syntheses excessively costly. Thus, the reactive compatibilization is more attractive in terms of price and equipment. However, control of the kinetics of the reactive system must be subjected to extreme conditions to ensure a better selectivity and prevent chemical degradation reactions which can produce undesirable effects on the final properties of the mixture.

For these reasons, science and technology of polymer blends and their compatibilization will continue to grow in the future. Efforts will continue to further refine compatibilization processes to continually improve the desired properties of these materials.

## References

- [1] L. A. Utracki, —Commercial Polymer Blends, (1998). Ed. Chapman and Hall, New York pp 21
- [2] D. R. Paul, (1978) « Chapter 12 - Interfacial Agents (“Compatibilizers”) for Polymer Blends », polymer blends. Academic pres. New York, p35-62, [doi.org/10.1016/B978-0-12-546802-2.50008-7](https://doi.org/10.1016/B978-0-12-546802-2.50008-7)
- [3] C.I.W. Calcagno, C.M. Mariani, S.R. Teixeira, R.S. Mauler (2008), «The role of the MMT on the morphology and mechanical properties of the PP/PET blends, Compos. Sci. Technol. **68** (10-11) 2193-2200. [doi.org/10.1016/j.compscitech.2008.03.012](https://doi.org/10.1016/j.compscitech.2008.03.012).
- [4] S.-L. Bai, G.-T. Wang, J.-M. Hiver, C. G’Sell, (2004) «Microstructures and mechanical properties of polypropylene/polyamide 6/polyethylene-octene elastomer blends», Polymer **45** (9), 3063-3071. [/doi.org/10.1016/j.polymer.2004.02.070](https://doi.org/10.1016/j.polymer.2004.02.070).
- [5] J.S. Higgins, M. Tambasco, J.E.G. Lipson, (2005) « Polymer blends; stretching what we can learn through the combination of experiment and theory », Prog. Polym. Sci. **30** (8-9), 832-843. [doi.org/10.1016/j.progpolymsci.2005.06.001](https://doi.org/10.1016/j.progpolymsci.2005.06.001).
- [6] Ming, X. Hankun, (1991) « Miscibility and morphology in block copolymer/homopolymer blends », Prog. Polym. Sci. **16** (6) 977-1026. [doi.org/10.1016/0079-6700\(91\)90002-3](https://doi.org/10.1016/0079-6700(91)90002-3).
- [7] C.R. Lopez-Barron, C.W. Macosko, (2014) « Rheology of compatibilized immiscible blends with droplet-matrix and cocontinuous morphologies during coarsening », J. Rheol. **58** (6) 1935-1953. [doi.org/10.1122/1.4897409](https://doi.org/10.1122/1.4897409).
- [8] J. Li, P.L. Ma, B.D. Favis, (2002) « The role of the blend interface type on morphology in cocontinuous polymer blends », Macromolecules **35** (6) 2005-2016. [doi.org/10.1021/ma010104+](https://doi.org/10.1021/ma010104+)
- [9] P. Mederic, J. Ville, J. Huitric, (2011) « Effect of processing procedures and conditions on structural, morphological, and rheological properties of polyethylene/polyamide/nanoclay blends», Polym. Eng. Sci. **51** (5) 969-978. [doi.org/10.1002/pen.21825](https://doi.org/10.1002/pen.21825).
- [10] M. Minale, P. Moldenaers, J. Mewis, (1997) « Effect of shear history on the morphology of immiscible polymer blends », Macromolecules **30** (18) 5470-5475. [doi.org/10.1021/ma9617330](https://doi.org/10.1021/ma9617330)
- [11] D.P. Dharaiya, S.C. Jana, (2005) « Nanoclay-induced morphology development in chaotic mixing of immiscible polymers », J. Polym. Sci. Part B Polym. Phys. **43** (24) 3638-3651. [doi.org/10.1002/polb.20657](https://doi.org/10.1002/polb.20657).
- [12] P. Van Puyvelde, S. Velankar, P. Moldenaers, (2001) « Rheology and morphology of compatibilized polymer blends », Curr. Opin. Colloid & Interface Sci. **6** (5-6) 457-463. [doi.org/10.1016/S1359-0294\(01\)00113-3](https://doi.org/10.1016/S1359-0294(01)00113-3).



- [13] S. Cho, J.S. Hong, S.J. Lee, K.H. Ahn, J.A. Covas, J.M. Maia, (2011) « Morphology and rheology of polypropylene/polystyrene/clay nanocomposites in batch and continuous melt mixing processes, *Macromol. Mater. Eng.* **296** (3-4) 341-348. [doi.org/10.1002/mame.201000194](https://doi.org/10.1002/mame.201000194).
- [14] C.W. Macosko, H.K. Jeon, T.R. Hoyer, (2005) « Reactions at polymer-polymer interfaces for blend compatibilization », *Prog. Polym. Sci.* **30** (8-9) (2005) 939-947. [doi.org/10.1016/j.progpolymsci.2005.06.003](https://doi.org/10.1016/j.progpolymsci.2005.06.003)
- [15] K. Bedjaoui. R. Krache . A. Marcos-Fernández. M. Guessoum. (2019) « The effect of compatibilizer SEBS on the mechanical, morphological and thermal properties of the polystyrene/poly(styrene-co-acrylonitrile) copolymer blends ». *Mater. Res. Express*, **6**, 105334.
- [16] J. Stoelting ., F. Karasz. E., MacKnight, W. J., *Polym. Eng. Sci.*, **19**, 10, 133.
- [17] D. Lefebvre. B. Jasse. L. Monnerie. (1981) « Fourier transform infra-red study of uniaxially oriented poly(2,6-dimethyl 1,4-phenylene oxide)-atactic polystyrene blends» *Polymer*, **22** (12), 1616.1620. [doi.org/10.1016/0032-3861\(81\)90374-8](https://doi.org/10.1016/0032-3861(81)90374-8).
- [18] W. Prest. M., Porter, R. S., *J. Polym. Sci., Polym. Phys. Ed*, (1972), **10**, 163
- [19] A. R. Shultz, B. M. Gendron., *J. Appl. Polym. Sci.*, (1972), **16**, 461.
- [20] A. R. Shultz., Gendron B. M., *Polym. Preprint, Am. Chem. Soc., Div. Polym. Chem.*, (1973), **14**, 571.
- [21] Y. Agari., M. Shimada., Veda A. *Polymer* (1997), **38**, 2649. [doi.org/10.1016/S0032-3861\(97\)85598-X](https://doi.org/10.1016/S0032-3861(97)85598-X)
- [22] J. Brandrup., E.H. Immergut, E.A. Grulke. *Polymer handbook*; Wiley: New York, 1999; Vol. 4.
- [23] F. Bruder., R. Brenn., B. Stuhn, B. (1989) « Interdiffusion in the partially miscible polymer blend of deuterated polystyrene and poly(styrene-co-bromostyrene) ». *Macromolecules*, **22**, 4434-4437.
- [24] J. Pospil, Z. Horak. Z. Kruli (1999) « Degradation and aging of polymer blends I. Thermomechanical and thermal degradation ». *Polymer Degradation and Stability*, **65**, 405-414. [doi.org/10.1016/S0141-3910\(99\)00029-4](https://doi.org/10.1016/S0141-3910(99)00029-4)
- [25] L. Reimer. (1998) *Scanning Electron Microscopy Physics of Image Formation and Microanalysis*, ch. 1, p. 2, Springer Press, Berlin.
- [26] L. A. Utracki. *Polymer blends handbook*, Verlag: Springer, (2002).
- [27] S.N. Angove. *Rubber J.*, **149**, 37 (1967)
- [28] M. Xanthos and S. S. Dagli, (1991) « Compatibilization of polymer blends by reactive processing », *Polym. Eng. Sci.*, **31**, (13), 929–935. [doi.org/10.1002/pen.760311302](https://doi.org/10.1002/pen.760311302)
- [29] N. G. Gaylord, (1989) « Compatibilizing agents: structure and function in polyblends,» *J. Macromol. Sci. Part - Chem.* **26**, (8). 1211–1229. [doi.org/10.1080/00222338908052043](https://doi.org/10.1080/00222338908052043)
- [30] R. L. Markham. *Advance Polymerization Tech.*, **10**, 231 (1991).

- [31] M. Jiang, Xiu. Huang, T. Yu., Polym. 24, 125 (1983).
- [32] W. J. Work, K. Horie, M. Hess, and R. F. T. Stepto, (2007) « Definition of terms related to polymer blends, composites, and multiphase polymeric materials » (IUPAC Recommendations 2004), Pure Appl. Chem. **76**, (11), pp., 200.
- [33] C. C. Chen and J. L. White, (1993) « Compatibilizing agents in polymer blends: Interfacial tension, phase morphology, and mechanical properties », Polym. Eng. Sci. **33**(14), 923–930. [doi.org/10.1002/pen.760331409](https://doi.org/10.1002/pen.760331409).
- [34] L.H. Sperling (2006) « Introduction To Physical Polymer Science » A John Wiley & Sons, New Jersey.
- [35] K. Yang, S.H. Lee and J.M. OH. (1999) « Effects of viscosity ratio and compatibilizers on the morphology and mechanical properties of polycarbonate/acrylonitrilebutadiene-styrene blends », Polym. Eng. Sci., **39** (9), 1667-1677. [doi.org/10.1002/pen.11561](https://doi.org/10.1002/pen.11561).
- [36] Paul DR, Barlow JW (1979) A Brief Review of Polymer Blend Technology. In: Cooper SL, Estes GM (eds) multiphase polymers. Advances in Chemistry, Washington, 176. 315-335. [doi.org/10.1021/ba-1979-0176.ch017](https://doi.org/10.1021/ba-1979-0176.ch017)
- [37] DR. Paul, JW. Barlow (1980) Polymer Blends (or Alloys). J. Macromol. Sci., Rev. Macromol. Chem. Phys. 18:109-168. [doi.org/10.1080/00222358008080917](https://doi.org/10.1080/00222358008080917).
- [38] U. Nishikawa and S. Iizuka and M. Takahashi. (2013) « X-ray CT observation of a “mosaic-tiling” structure and a “worm-like” structure in the ternary polymer blends », Polymer., **54** (23), 6267- 6270. [doi.org/10.1016/j.polymer.2013.09.028](https://doi.org/10.1016/j.polymer.2013.09.028).
- [39] P. Pötschke and D.R Paul. (2003) « Formation of co-continuous structures in melt-mixed immiscible polymer blends », J. Macromol. Sci , Part C: Polym. Rev., **43** (1) 87-141. [doi.org/10.1081/MC-120018022](https://doi.org/10.1081/MC-120018022)
- [40] S. Thomas, R. Shanks, (2014). « Nanostructured polymer blends »; Elsevier Science and Technology Books, Inc.: Oxford, United Kingdom.
- [41] L. A. Utracki, (1989) « Polymer Alloys and Blends, Thermodynamics and Rheology », Ed. Hanser Publishers, Munich.
- [42] A. Hellati (2011) « Etude des Propriétés Rheologiques, Mécaniques, Thermiques et Spectrales des mélanges PET/iPP/ SEBS-g-MAH renforcés par la montmorillonite » thèse de doctorat, Institut de Génie des Procédés, Université de Setif1 (Algerie).
- [43] D.R. Paul, C.E. Locke, C.E. Vinson., Polym. Eng. Sci., 13, 202 (1973).
- [44] M. Xanthos, Polym. Eng. Sci., Vol. 28, pp 1392 (1988).

- [45] Z. Horak, I. Fortelný, J. Kolařík, D. Hlavat , and A. Sikora, (2005) « Polymer blends,» in Encyclopedia of Polymer Science and Technology, John Wiley & Sons, Inc., Ed. Hoboken, NJ, USA: John Wiley & Sons, Inc. 1–59.
- [46] S. Hudson, A. Jamieson. Morphology and Properties of Blends Containing Block Copolymers In Polymer Blends. Wiley-Inter science. New York. 2000.
- [47] B. Majumdar, D. Paul. (2000) « Reactive Compatibilization In Polymer Blends. Wiley-Inter science. New York.
- [48] S. P. Lyu. (2003) « Block Copolymers Suppressing Droplet Coalescence through Stopping Film Rupture » *Macromol.* **36** (26) 10052. [/doi.org/10.1021/ma025868j](https://doi.org/10.1021/ma025868j)
- [49] U. Sundararaj. C. W. Macosko, R. J. Rolando. (1992) « Morphology development in polymer blends ». *Polym. Eng. Sci.* **32**(24), 1814–1823. [doi.org/10.1002/pen.760322404](https://doi.org/10.1002/pen.760322404)
- [50] C. E. Scott., C. W. Macosko C. W., *Polymer* (1994), 35, 5422.
- [51] A. Nakayama, T. Inoue , A. Hirao , P. Guegan , P. Khandpur , Macosko C. W. *Polym. Prepr.* (1993), 34, 840,
- [52] W. E. Baker, C. E.Scott, G. H. Hu. *Reactive polymer blending*, Munich: Hanser, (2003).
- [53] C. W. Macosko, P. Guegan, A. K. Khandpur, A. Nakayama, P. Marechal, T. Inoue. *Macromol.* Vol 29 (1996) 5590.
- [54] A. I. Isayev, C.K. Hong. *Polym Eng Sci.* Vol 43 (2003) 91.
- [55] Utracki, L.A. (2002). *Compatibilization of Polymer Blends*, The Canadian Journal of Chemical Engineering, Vol. 80.

# **Chapter III**

## **Materials and experimental techniques**

### Chapter III. Materials and experimental techniques

#### III. Introduction

In the present chapter, the experimental work is summarised in Figure III.4, involving drying of all the raw materials followed by mechanical mixing to form polymer blends: uncompatibilised PS/SAN, rPS/SAN and compatibilised PS/SAN with SEBS. The chapter also includes general information about the laboratory equipment and techniques utilized to process and to evaluate the properties of the materials.

#### III.1. Raw Materials

##### III.1.1 Polystyrene (PS)

Polystyrene has a very simple repeating structure as shown in the Figure III.1 below. It is an atactic polymer thus is regarded as amorphous. This commercially available thermoplastic has been around for quite sometime and the PS used in this work has the trade name GPPS 1540, supplied by Total petrochemical, Belgium. The specific tacticity of the benzene ring is sufficiently random to inhibit crystallization [1].

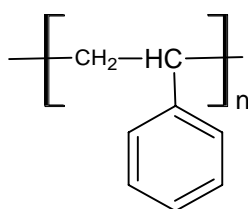


**Figure III.1** Structure of Polystyrene (PS) [2].

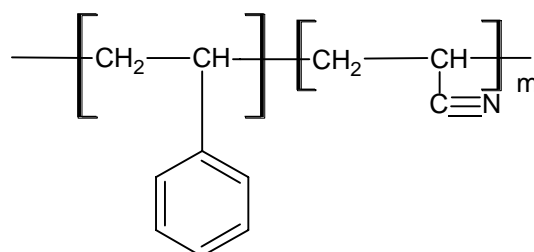
Polystyrene is a hard, crystal clear, amorphous solid at room temperature that exhibits high stiffness, good dimensional stability, moderately high heat deflection temperature and excellent electrical insulating properties [3]. It retains its stiffness to about 20-25°C below glass transition temperature (T<sub>g</sub>). However, polystyrene will become softer as it getting closer to its T<sub>g</sub> which is around 100°C. Above T<sub>g</sub>, polystyrene behaves under stress as a viscous fluid. When the temperature is further raised, it will become rubbery and highly extensible. Polystyrene is easily processed by all usual thermoplastic processes to produce common products such as wall tiles, electrical parts, lenses, bottle caps, transparent display boxes, etc. Properties of the polystyrene used in this work are listed below in table III.1

**Table III.1** Material Properties of Polystyrene PS (GPPS-1540) [3].

	Unit	Value	Test Method
Melt Flow index at (200°C/5kg)	g/10min	11	ISO 1133
Unnotched Charpy impact strength	KJ/m <sup>2</sup>	8	ISO 179
Tensile strength at break	MPa	42	ISO 527
Elongation at break	%	2	ISO 527
Tensile modulus	MPa	3000	ISO 527
Flexural modulus	MPa	2900	ISO 178

### III.1.2 Styrene Acrylonitrile (SAN) copolymer.

Styrene acrylonitrile (SAN) is a copolymer of styrene with acrylonitrile. The usual content of acrylonitrile in the SAN composition is between 20 and 30 %. It is basically used in general purpose polystyrene applications when additional chemical resistance and slightly higher temperature resistance are needed. SAN used in this work has the trade name Luran 368R and was supplied by Total petrochemical, Belgium.

**Figure III.2** Structure of Styrene acrylonitrile (SAN) [4].

SAN is similar in use to polystyrene, is a rigid transparent plastic produced by the copolymerization of styrene and acrylonitrile. It is a combination of clarity and rigidity of polystyrene with hardness, strength and solvent resistance of polyacrylonitrile. Styrene-based materials offer excellent qualities including durability, high performance, versatility of design, simplicity of production and economy. The copolymer has a glass transition temperature greater than 100 °C owing to the acrylonitrile units in the chain, thus making the material resistant to boiling water. It is structurally related to ABS plastic,

where polybutadiene is copolymerised with SAN to give a much tougher material [5]. Their materials properties are listed in Table III.2.

**Table III.2** Material Properties of Poly (styrene-co-acrylonitrile) SAN (Luran 368R)

	Unit	Value	Test Method
Melt Flow index at (220°C/10 kg)	g/10min	10.8	ISO 1133
Izod notched impact strength	KJ/m <sup>2</sup>	2	ISO 179
Tensile strength at break	MPa	75	ISO 527
Elongation at break	%	3	ISO 527
Tensile modulus	GPa	2 - 3.5	ISO 527
Flexural Strength	MPa	175	ISO 178

### III.1.3 Poly (Styrene-b-Ethylene- -Butadiene-b-Styrene) SEBS

SEBS used in this work was Kraton G 1651, supplied by Kraton Polymer (USA). It has a molecular weight of 20,000 g/mol and a styrene content of 28 wt%.. It is a copolymer called tri- block copolymer made of three segments. The first is a long chain of polystyrene, the middle is a long chain of poly(ethylene-butadiene), and the last segment is another long chain of polystyrene. Chemical formula for SEBS is:

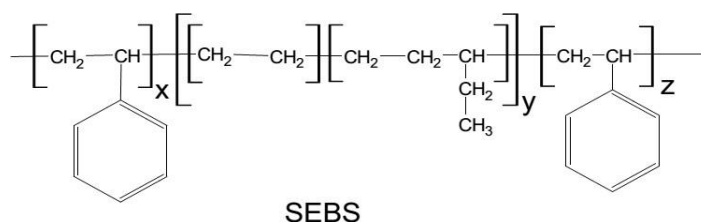


**Figure III.3** Structure of SEBS.

Polystyrene is a tough hard plastic, and this gives SEBS its durability. Polybutadiene is a rubbery material, and this gives SEBS its rubber-like properties. Since SEBS contains rubber and plastic, it acts like both materials.

**Table III.3** Properties of virgin Kraton G 1651 SEBS.

	<b>Unit</b>	<b>Value</b>
Melt flow index (200°C/5kg)	g/10 min	1,5
Density	g/cm <sup>3</sup>	0,91
Tensile strength at break	MPa	7,2
Elongation at break	%	550
Tensile modulus	MPa	5



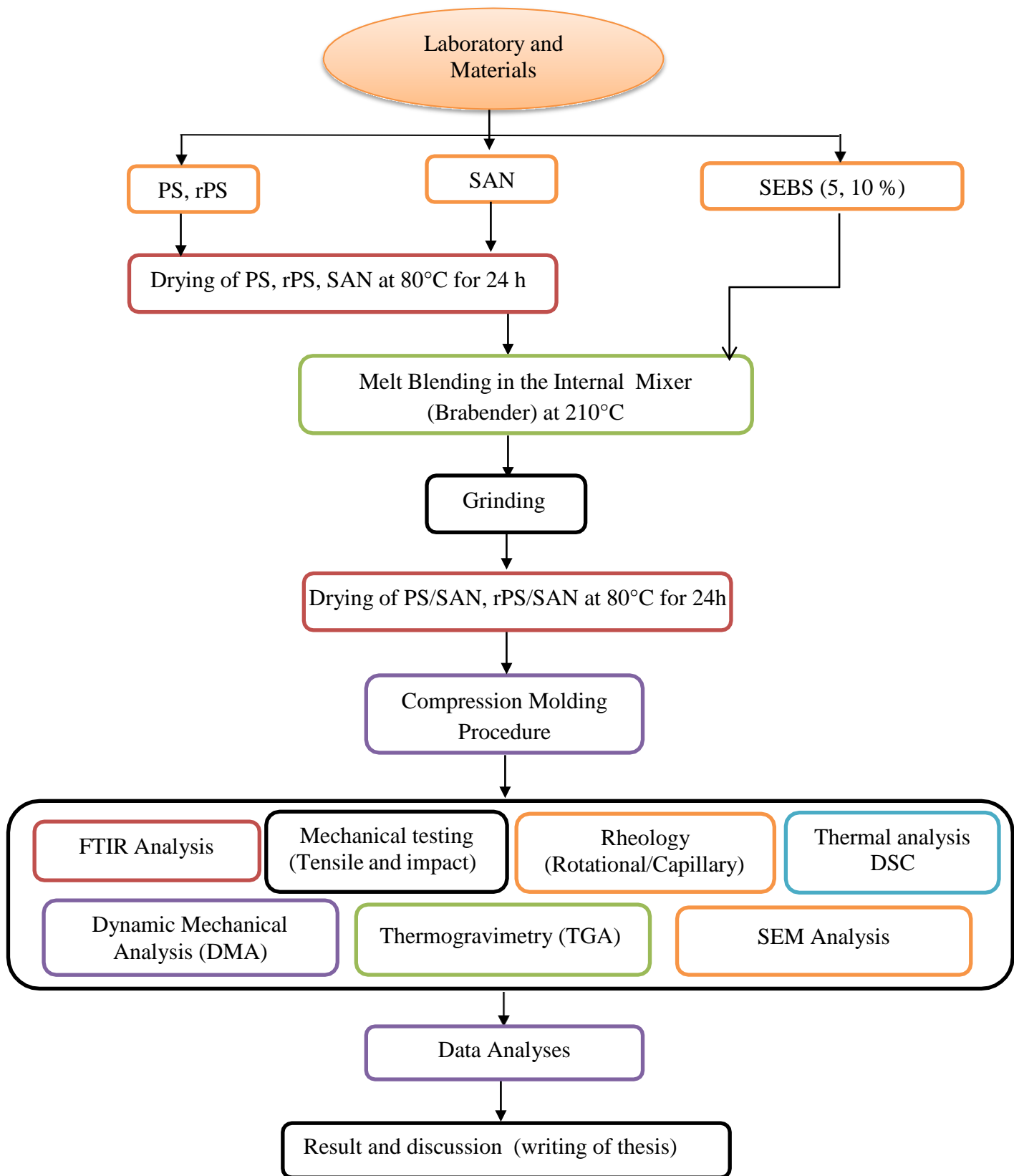


**Figure III.4:** Research Flow chart of the experimental work.

**III.2. Blends preparation procedure**

**III.2.1 Blends Formulation**

The basis of formulation was based on the percentage weight ratio between PS, SAN and PS/SAN blends uncompatibilized and compatibilized with SEBS as compatibilizer. The weight ratios of blends are shown in Table III.4 (a)-(b).

**Table III.4 (a):** Blends formulation for polystyrene PS, recycled polystyrene and SAN blending process without compatibiliser.

Designation	PS, rPS (wt% <sup>o</sup> )	SAN (wt%)
<b>PS</b>	100	-
<b>PS30</b>	30	70
<b>PS50</b>	50	50
<b>PS70</b>	70	30
<b>SAN</b>	-	100

**Table III.4 (b):** Blends formulation for compatibilized polystyrene (PS), recycled polystyrene and SAN blending process with SEBS as compatibiliser.

N <sup>o</sup>	PS, rPS (wt%)	SAN (wt%)	SEBS (wt%)
<b>PS30C5</b>	30	70	5
<b>PS50C5</b>	50	50	5
<b>PS70C5</b>	70	30	5
<b>PS30C10</b>	30	70	10
<b>PS50C10</b>	50	50	10
<b>PS70C10</b>	70	30	10

**III.2.2 Preparation of blends**

The PS, SAN and SEBS polymer were obtained in the form of pellets. Prior to processing, all composition of PS, rPS and SAN blend were dried at 80°C, respectively, overnight in a vacuum oven. Uncompatibilized and compatibilized PS/SAN and rPS/SAN blends of various compositions were prepared. The uncompatibilized mixtures contained 0, 30, 50, 70 and 100 wt% of SAN and are denoted respectively as PS, PS30, PS50, PS70, and SAN.

The compatibilized blends consist of the same contents of PS, rPS and SAN with 5 and 10 wt% SEBS and are denoted according to the same designation but with C5 or C10 termination, respectively.

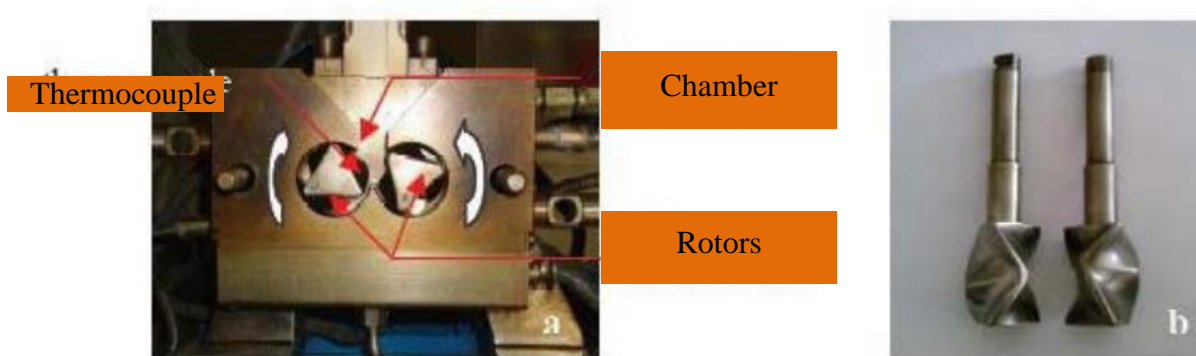


**Figure III.5:** Internal mixer ; (a) Mixing chamber ; (b) Counter –rotating blades (Rotors)of the internal mixer [6].

**Table III.5 :** Brabender® (GmbH & Co. KG) characteristics

Chamber volume	55 Cm <sup>3</sup>
Sample mass	40-70 g
Maximum torque	200 N.m
Maximum temperature	500 °C

### III.2.3 Melt blending

PS/SAN and rPS/SAN blends were studied with the aim of investigating and enhancing the miscibility and the compatibility of the blends. The first part of the study consists of the blending of PS with SAN without and with the addition of SEBS (styrene-ethylene-butadiene-styrene) as compatibilizer. The compositions were selected from preliminary literature review. According to the review, the optimum blend ratios for PS/SAN and rPS/SAN blends were determined as (30/70), (50/50) and (70/30). The second part of the work is dedicated to study the effect of recycled PS on the properties of blend rPS/SAN and compatibilized blend.

PS and SAN blends were prepared according to Table III.4 (a) and (b). All the raw materials were blended using a Brabender® (GmbH & Co. KG, Duisburg, Germany) internal mixer, allowing the monitoring of the torque versus temperature curves for each formulation. The mixing was carried out at 210°C during 10 min and at a rotor speed of 50 rpm. At the start, PS, rPS and SAN were allowed to soften for 2 min then SEBS was added thereafter. At the end of the mixing process, the molten mixtures were removed from the chamber, cooled and then pelletized. Samples for the mechanical and viscoelastic characterizations were compression- molded at 200°C for 5 min in a preheated hydraulic press.

### III.3. Compression molding process

The PS/SAN and rPS/SAN blends melt mixed samples of different compositions (Table III.2) were cut into small pieces and then compression molded into 2 mm thick sheets and thin films at the temperature of 200°C for 5 min using a CARVER™ hydraulic press (Hampton, New Hampshire, USA) at a pressure of 75 Pa.

### III.4 Characterization techniques

To investigate the effect of recycled PS and compatibilizing agents on the improvement of microstructure and PS/SAN properties, the prepared formulations were analyzed using a variety of different techniques to determine specific properties. Each one of the following techniques is described in more detail in the following sections;

- ✚ Mechanical Testing (including tensile and impact strength).
- ✚ Rheological Properties (RPA) ;
- ✚ Differential scanning calorimetry (DSC) for the thermal properties; Dynamic
- ✚ Mechanical Analysis (DMTA);
- ✚ Thermogravimetric analysis (TGA) for the thermal stability; Scanning
- ✚ electron microscopy (SEM) for morphologies.

#### III.4.1 Mechanical testing

##### III.4.1.1 Tensile Test

Tensile tests are performed for several reasons. The results of tensile tests are used in selecting materials for engineering applications and frequently are included in material specifications to ensure quality. They are often measured during development of new materials and processes, so that different materials and processes can be compared, and often used to predict the behavior of a material under forms of loading other than uniaxial tension.

The tensile behavior of the samples was evaluated using a Universal Testing Instron 4301 (USA) machine.

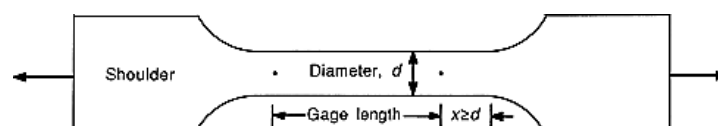


**Figure III.6** Typical tensile specimen, with a reduced gage section and enlarged shoulders [7].

At least seven specimens for each formulation were tested at a cross-head speed of 10 mm min<sup>-1</sup>. Tensile strength, elongation at break and Young's modulus were determined, and the average values were calculated and reported. A typical tensile specimen is shown in **Figure III.4**. A tensile test involves mounting the specimen in a machine and subjecting it to tension. The tensile stress ( $\zeta$ ) and the strain ( $\epsilon$ ) are defined in equation (1) and (2), respectively.

$$\sigma = \frac{F}{A_0} \quad (\text{eq. II.1})$$

$$\epsilon = \frac{\Delta L}{L_0} \quad (\text{eq. II.2})$$

Where F is the tensile force and  $A_0$  is the initial cross-sectional area of the gage section.  $L_0$  is the initial gage length and  $\Delta L$  the change in gage length ( $L-L_0$ ). When a solid material is subjected to small stresses, the bonds between the atoms are stretched. When the stress is removed, the bonds relax and the material returns to its original shape. This reversible deformation is called elastic deformation. At higher stresses, planes of atoms slide over one another. This deformation, which is not recovered when the stress is removed, is termed plastic deformation. For most materials, the initial portion of the curve is linear. The slope of this linear region is called the elastic modulus or Young's modulus (E) as shown in equation (3).

$$E = \frac{\sigma}{\epsilon} \quad (\text{eq. II.3})$$

The stress-strain curves of tensile tests are shown in Figure III.7. The tensile strength (ultimate strength) is defined as the highest value of engineering stress. The tensile test gives the data as a stress vs strain graph. The highest point of this stress versus strain curve is the tensile strength of the material being tested. Tensile strength unit is N/mm<sup>2</sup> or MPa.

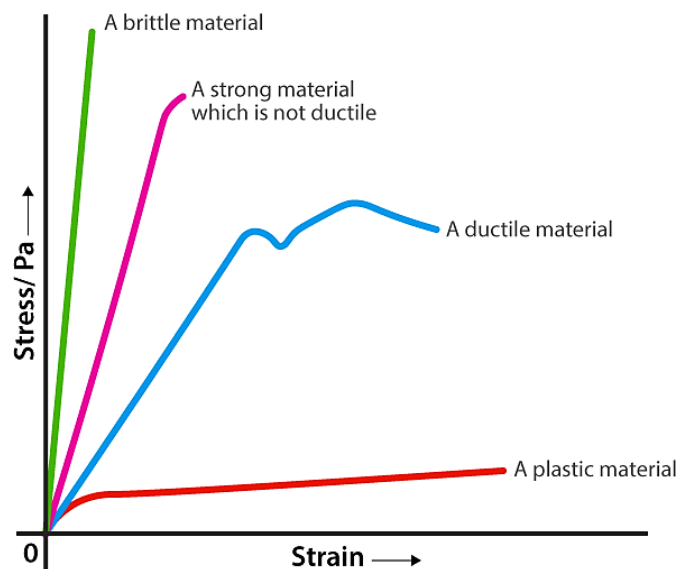


**Figure III.7** Stress-strain - curves of ductile vs brittle materials [7].

### III.4.1.2 Impact Test

Notched Izod impact test was performed at room temperature using a resil impactor (Ceast 6548). Five replicates of each composition were tested and the average values were recorded to check the good reproducibility of the experiment.

Toughness is a measure of the amount of energy a material can absorb before fracturing. Impact test conditions are chosen to represent those most severe relative to the potential for fracture of (1) deformation at a relatively low temperature, (2) a high strain rate, and (3) a triaxial stress state which may be introduced by the presence of a notch. Standardized test, the Izod, are commonly used to measure impact energy. It is illustrated in Figure III.8 [8].

## III.4.2 Rheological Properties

### III.4.2.1 Dynamic rheological analysis

For the dynamic rheological analysis, a brabender type plastograph was used. The processability of the different components has been evaluated by measuring the torque required to mix the molten components in a heated chamber, under fixed conditions, i.e., temperature, time and rotor speed.

Polymer viscoelasticity is usually described in terms of response of fluid to a sinusoidal shearing, where the shear strain is given by :

$$\gamma(t) = \gamma_0 \sin(\omega t) \quad (\text{eq II.4})$$

where  $\omega$  is the frequency of the oscillatory strain,  $\delta$  is the phase angle or mechanical loss angle and  $\gamma_0$  is the strain amplitude. If the strain amplitude is sufficiently small, the shear stress is also sinusoidal and is given by

$$\eta(t) = G \cdot \eta_0 \cdot \sin(\omega t + \delta) \quad (\text{eq. II.5})$$

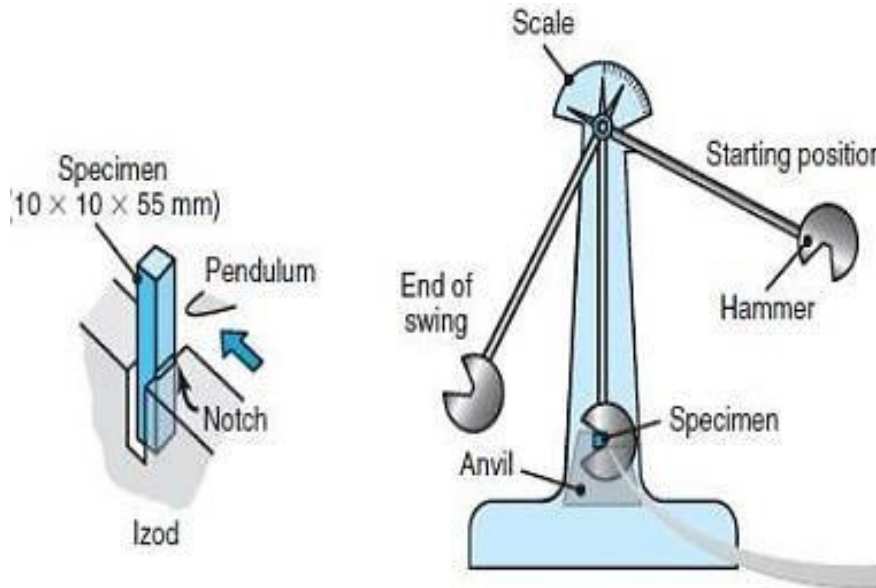


**Figure III.8** Impact testing, (a) Izod testing, [8].

where  $\eta_0$  is the stress amplitude.  $\eta_0$  at a given frequency is proportional to  $\gamma_0$ , if the strain is sufficiently small. This type of behaviour is called linear viscoelasticity. The linear viscoelasticity could be described using trigonometric identity as follows:

$$\eta(t) = \gamma_0 [G' \sin(\omega t) + G'' \sin(\omega t)] \quad (\text{eq. II.6})$$

where  $G'(\omega)$  is the storage modulus and  $G''(\omega)$  is the loss modulus, which are functions of frequency. Both are linear viscoelastic material functions.

Another term of importance is the ratio of loss to storage modulus defined as

$$\text{Tan } \delta = G''(\omega) / G' \quad (\text{eq. II.7})$$

It is also possible to define a dynamic complex viscosity in terms of  $G'$  and  $G''$  as follows:

Dynamic viscosity :

$$\eta'(\omega) = G''(\omega) / \omega \quad (\text{eq. II.8})$$

Imaginary part of the complex viscosity :

$$\eta''(\omega) = G'(\omega) / \omega \quad (\text{eq. II.9})$$

Complex viscosity function :

$$\eta^*(i\omega) = \eta'(\omega) - i\eta''(\omega) \quad (\text{eq.II.10})$$

In the same manner as above, a complex modulus can be defined as below :

Complex viscosity function :

$$G^*(i\omega) = G'(\omega) + i G''(\omega) \quad (\text{eq.II.11})$$

The storage modulus  $G'(\omega)$  and imaginary part of the complex viscosity  $\eta''(\omega)$ , are to be considered as the elastic contributions to the complex functions. They are both measures of energy storage. Similarly, the loss modulus  $G''(\omega)$  and the dynamic viscosity  $\eta'(\omega)$  are the viscous contributions or measures of energy dissipation.

Samples for rheological and morphological analyses were obtained by compression molding. Discs with a 25 mm diameter and 1 mm thickness were molded at 190°C under 18 MPa for 10 minutes. The viscoelastic behavior of the PS/SAN was studied using a RPA rubber process analyzer (RPA2000, Alpha Technologies, USA). Around 4 g of material were placed in the cavity of RPA with a biconical moving die. The Frequency sweep was performed from 0.01 to 100 Hz to measure storage modulus ( $G'$ ), loss modulus ( $G''$ ) and complex viscosity ( $\eta^*$ ) as a function of frequency, at 190°C and keeping the strain constant at 5.02 %.

### III.4.3 Thermal properties

#### III.4.3.1 Differential scanning calorimetry (DSC)

There are two set of samples that were prepared for DSC analysis besides that of the virgin PS and SAN ; uncompatibilised PS/SAN blends, and compatibilised PS/SAN blends with SEBS. These samples were investigated under nitrogen using a Perkin Elmer DSC8500 device. The samples were heated from 25°C to 200°C at a rate of 20°C/min to eliminate previous thermal history and were held at this temperature for 2 min before starting the cooling. Cooling was carried out from 200°C to -70°C at 20°C/ min followed by heating from -70°C to 150°C at 20°C/min. All thermal properties were obtained from the second heating scan curves. The curves were analyzed as follows: the glass transition temperature ( $T_g$ ) was taken as the average of the intersection points of the extrapolated lines before and after transition, respectively, with tangent at the point of return at the rising curve.



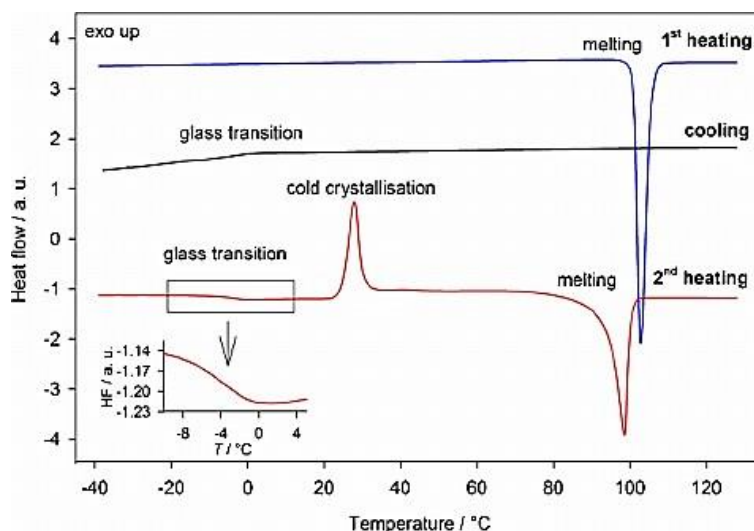


**Figure III.9** The typical DSC thermogram of polymers [9]

Throughout the DSC work, samples were encapsulated in aluminum pans and placed in the holder. An empty aluminum pan of the same weight as that used with the sample, was used as reference. Each holder has its own temperature sensor.

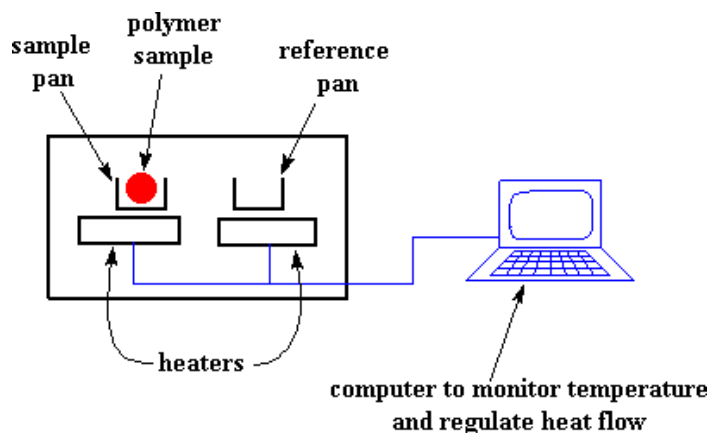


**Figure III.10** Schematic diagram of a DSC apparatus [9].

### III.4.3.2 Dynamic Mechanical Analysis (DMA)

Dynamic mechanical analysis (DMA) was carried out in a TA Q800 Instrument. The scans were carried out from  $-100^{\circ}\text{C}$  to  $150^{\circ}\text{C}$  at a constant heating rate of  $4^{\circ}\text{C}/\text{min}$  and at a frequency of 1 Hz. The device applied a continuous sinusoidal oscillatory deformation on the sample and measured the force required to produce a specific oscillation amplitude. The moduli were derived from the value of this force and its phase difference with respect to the

deformation. These are the elastic (storage) modulus,  $E'$ , and viscous (loss) modulus,  $E''$ , terms of the complex dynamic tensile modulus of a viscoelastic material and dynamic mechanical  $\tan \delta$ .

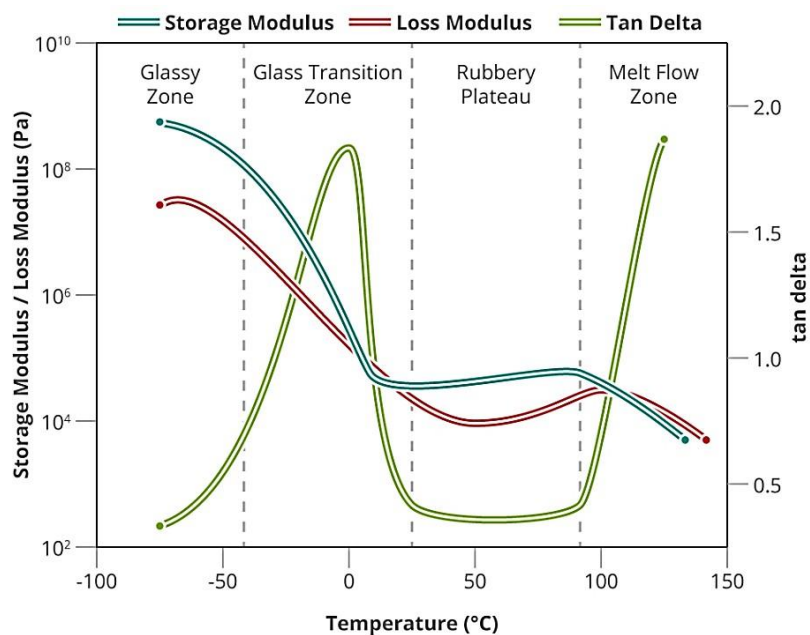


**Figure III.11** DMTA thermogram of modulus values change with temperature and transitions in materials [9].

As shown in Figure III.9, the  $T_g$  is seen as a large drop (a decade or more) in the storage modulus when viewed on a logarithmic scale. The frequency of the applied oscillations was 1 Hz and the deformation amplitude was set to 5  $\mu\text{m}$  ( $\sim 0.05\%$  strain).

#### III.4.3.3 Thermogravimetric analysis (TGA)

TGA is an analytical technique used to determine a material's thermal and/or oxidative stability and its fraction of volatile components by monitoring the weight change that occurs as a specimen is heated. Figure III.7, shows a diagram of a thermobalance. The measurement is normally carried out in air or in an inert atmosphere, such as Helium (He), Argon (Ar) or Nitrogen (N<sub>2</sub>), and the weight is recorded as a function of increasing temperature. The measurement was performed using a TA Q500 analyzer TA Instrument (New Castle, Delaware, USA). Samples of 5-9 mg were heated from 25°C to 600 °C in Hi-Resolution mode with an initial heating rate of 10 °C·min<sup>-1</sup> under nitrogen atmosphere at the flow rate of 10 ml·min<sup>-1</sup>.

The thermogravimetric (TGA) and derivative (DTG) curves are generally plotted as mass versus temperature, as illustrated in Figure III.8. The TGA curve shows the plateau of constant weight (region A), the mass loss portion (region B), and another plateau of constant mass (region C) [10].

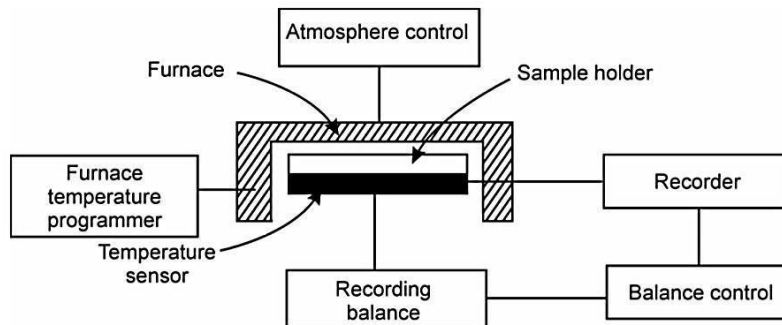


**Figure III.12** Block Diagram of a Thermobalance [10].

The onset temperature (onset) was determined from the thermogravimetric curves as being the temperature at which the weight loss begins. The temperatures corresponding to the weight loss of 5 % and 50 % were also determined from the thermogravimetric curves.

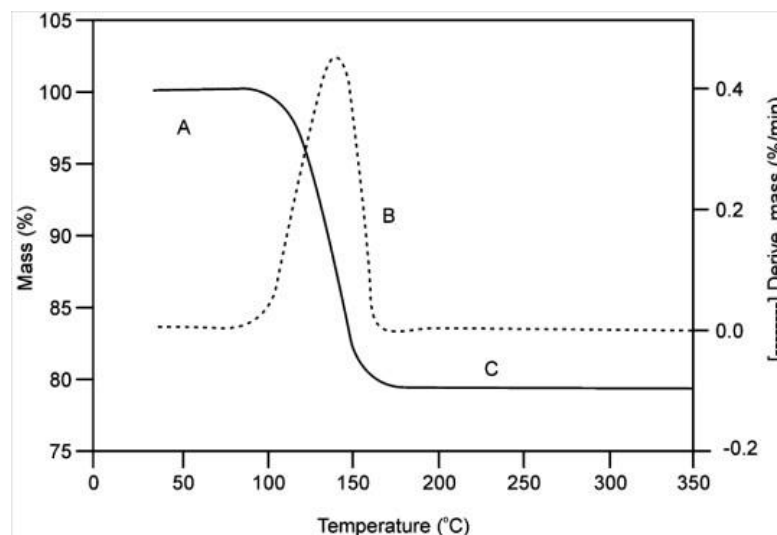


**Figure III.13** Typical TGA and DTG curves [10].

### II.4.3 Scanning electron microscopy (SEM)

The fractured surface was obtained by breaking the specimens under liquid nitrogen. The cryogenically fractured surfaces of PS/SAN blends specimens were observed, after gold coating, by scanning electron microscopy using a scanning electron microscope (SEM, Philips, XL30). These micrographs were analysed using image analysis software. The particle sizes of the particles were calculated from the diameter of the particles which were approximated to spheres. More than 50 particles were evaluated and these were taken for the calculation of the mean diameter and hence mean size of the particles. The dispersion and distribution behavior of the dispersed phase were also analysed from the particles diameter and percentage of each particles diameter. The calculation of the particles average number and volume diameter values was performed using the following equations (1) and (2) [11]:

$$R_n = \frac{\sum n_i * R_i}{\sum n_i} \quad (1)$$

$$R_w = \frac{\sum n_i * R_i^4}{\sum n_i * R_i^3} \quad (2)$$

Where  $n_i$  is the number of droplets “i” of diameter  $R_i$ .

## REFERENCES

- [1] M. Kutz., Handbook of Materials Selection; (2002), Wiley: NJ, p. 341. [Google Scholar].
- [2] T. Takebe, K. Yamasaki, K. Funaki, M. Malanga, Properties of Syndiotactic Polystyrene, Syndiotactic Polystyrene, John Wiley & Sons, Inc.2009, pp. 267- 289.
- [3] J.E. Gray, Polystyrene: Properties, Performance, and Applications, Nova Science Publishers2011.
- [4] Jump up-Charles A. Harper, ed. Modern Plastics Handbook, ISBN 0-07-026714 6, (2000).
- [5] S. Ahmed Salahudeen, R.H. Elleithy, O. AlOthman, S.M. AlZahrani, (2011) « Comparative study of internal batch mixer such as cam, banbury and roller: Numerical simulation and experimental verification », Chemical Engineering Science **66** (12) 2502 – 2511. [doi.org/10.1016/j.ces.2011.02.017](https://doi.org/10.1016/j.ces.2011.02.017)
- [6] J. R. Davis, (2004). Tensile testing, 2nd Ed. Materials Park, OH, USA.
- [7] Jr. Callister., D. William. (1991). Materials science and Engineering: An introduction. 7th Ed. John Wiley & Sons, Inc., New York, USA.
- [8] G. Höhne, W. F. Hemminger, H. J. Flammersheim, (2003). Differential Scanning Calorimetry. Springer Berlin Heidelberg, 1-298.
- [9] M. P. Sepe., (1997). Thermal analysis of polymers. SmithersRapra Publishing, Shrewsbury, SY4 4NR, United Kingdom.
- [10] PerkinElmer, (2012). Thermogravimetric analysis (TGA). A Beginner's Guide.
- [11] N. Yin, Y. Zhang, Y. Zhang, X. Zhang, et W. Zhou, (2007) « Preparation and properties of PC/SAN alloy modified with styrene-ethylene-butylene-styrene block copolymer », J. Appl. Polym. Sci.. 106 (1). 637-643. [doi.org/10.1002/app.26681](https://doi.org/10.1002/app.26681)

**CHAPTER V**

**RESULTS AND**

**DISCUSSION**



***Chapter IV: RESULTS AND DISCUSSION*****IV.1 Characterizations and Properties of PS/SAN blends without and with addition of compatibilizer.**

This chapter includes all the experimental results that are obtained from the mechanical and physical analysis of the materials. The experimental tests and the results of blends systems were used to investigate the effect of recycled PS on mechanical properties including tensile test and impact test, on physical properties including differential scanning calorimeter (DSC), on viscoelastic properties using dynamic mechanical thermal analysis (DMTA) and on thermal stability by thermogravimetric analysis (TGA). Finally the morphology of polymer blends was characterized using Scanning electron microscopy (SEM).

In this chapter, the results of two blend systems are reviewed.

- a) PS/SAN and PS/SAN/SEBS ;
- b) rPS/SAN and rPS/SAN/SEBS.

All results are discussed together with presentation of the data obtained from measurement of virgin PS and compared with that of the recycled PS.

**IV.1.2 Mechanical Properties****IV.1.2.1 Tensile properties of PS/SAN blends**

The assessment of the mechanical behavior of blends is considered as the more crucial parameter to conclude about the compatibilizing effect. Generally, immiscible blends show poor mechanical properties due to the weak interfacial adhesion between the components [1]. The results of tensile test including tensile strength, tensile modulus, and elongation at break and those of impact strength for PS/SAN blends are summarized in table IV.1. It can be seen that the mechanical properties of SAN are higher than those of PS.

Figures IV.1-3, shows the variation of PS/SAN blends tensile properties as a function of both blend ratio and compatibilizer content. As expected, PS and SAN are immiscible and did not show any improvement in the mechanical properties for the whole studied compositions.

This may be due to the weak interfacial adhesion between the PS and SAN phases [2], which induces a poor stress transfer between the two phases of the blends [3].

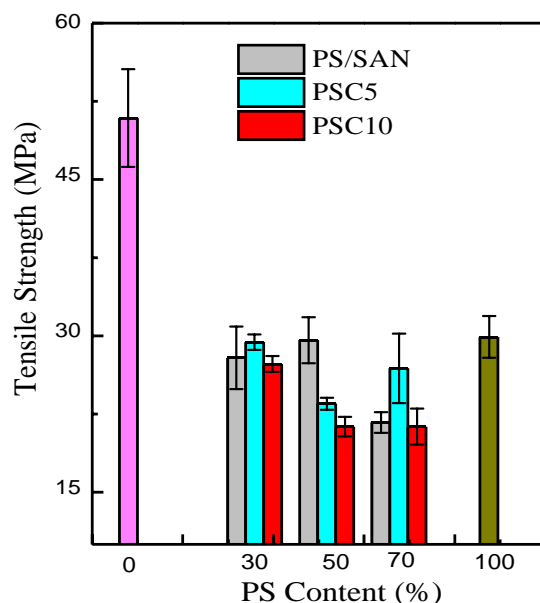


**Figure IV.1** : Tensile strength of blend PS/SAN without and with compatibilizer.

From figure IV.1 and Table IV.1, it can be seen that the tensile strength of uncompatibilized PS/SAN blends is higher than compatibilized ones. After the addition of 5 wt% of SEBS, the tensile strength of the PS/SAN blend exhibits a slight increase, especially, for the PS30, PS50 and PS70 mixtures. This result is attributed to the favorable intermolecular interactions between PS/SAN, which is originated from their structural similarity and expected compatibility between the PS and SAN matrix phases and the compatibilizer segments [4]. However, the addition of 10 wt% of compatibilizer produces a lower tensile strength compared to the sample with 5 wt% of SEBS. This could be explained by the eventual effect of SEBS micelles in the blend when added with higher concentration.

The evolution of the PS/SAN blends tensile modulus as a function of both the PS and SEBS contents is displayed in figure IV.2. The tensile modulus of the pure PS and SAN are 2920 MPa and 3140 MPa, respectively. The tensile modulus of uncompatibilized mixtures show higher values than that of the PS due to the contribution of the SAN phase and to the fact that the tensile modulus is closely related to the harder domain of the material [5].

After adding SEBS, the tensile modulus shows a sharp decrease and it is observed that the higher the SEBS content, the lower are the blends moduli. The tensile strength and tensile



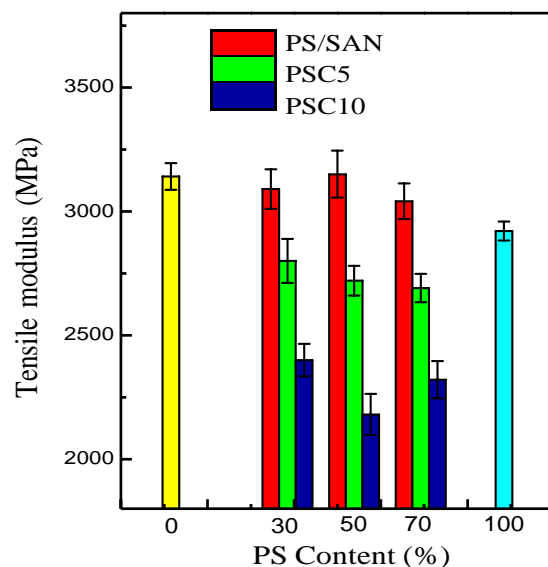


**Figure IV.2** tensile modulus of PS/SAN blends prepared without and with SEBS compatibilizer.

Modulus of the PS/ SAN blends are found to be negatively affected by the addition of SEBS due to the elastomeric nature of the later. Thus, the incorporation of soft molecules belonging to an elastomer compatibilizer, as it is the case of SEBS triblock copolymer, plays a major role in improving the blend ductility by inducing a transition from a brittle behavior of the incompatible mixture to a more ductile one. This is due to better interphase adhesion and the rubbery nature of the compatibilizer. As revealed in literature by la Mantia et al [6].

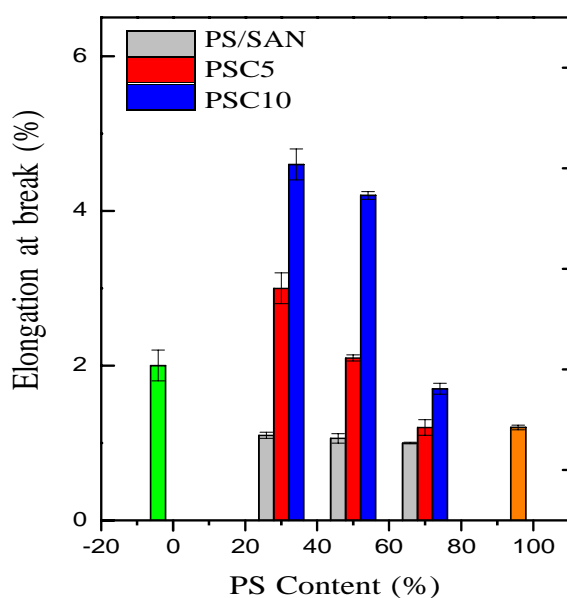


**Figure IV.3** Elongation at break of PS/SAN blends prepared without and with SEBS compatibilizer.

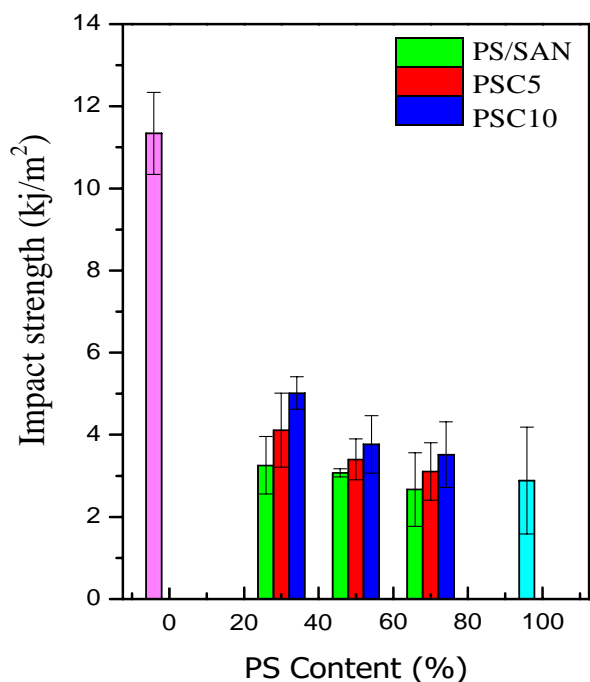


**Figure IV.4** Impact strength of blend PS/SAN without and with compatibilizer.

The SEBS is able of reducing the brittleness of at least one of the two phases and locates selectively at the interface. Figure IV.3 shows the variations of the elongation at break as a function of both the blend ratio and SEBS content. It can be observed that the elongation at break of uncompatibilized blends shows lower values compared to the pure components and it increases as the SAN contribution in the mixture increases. As SEBS is added, the blends ductility is favored and an enhancement of the elongation at break is registered, particularly for 10 wt% of the compatibilizer as shown in Table IV.1. These results confirm the effectiveness of SEBS as a compatibilizer for PS/SAN blends and fit well with those found by other researchers [7] who have reported that the elongation at break shows a positive deviation for the composition 25/75, thus indicating some favorable interactions between the components of the blend.

#### IV.1.2.2 Impact strength of PS/SAN blends

The notched Izod impact strength is used to evaluate the toughness of the samples. The variations of the impact strength for PS/SAN blends before and after the incorporation of SEBS are shown in figure IV.4. As for tensile properties, the impact strength of SAN is higher than that of PS and as expected, the uncompatibilized blends reveal lower impact strength values than those of the neat polymers, due to the mixtures immiscibility. After the

blend compatibilization, the impact strength increased for both 5 to 10 wt% of SEBS. The increase is more prominent for the composition PS30 containing 10 wt% of SEBS. The trend is the same, although in a lower extent than the trend found in elongation at break (Figure IV.3).

**Table IV.1.** The Mechanical properties of PS, SAN and their uncompatibilized and compatibilized blends with SEBS.

Samples	Tensile Strength (MPa)	Tensile Modulus (MPa)	Elongation at break (%)	Impact Strength (kJ/m <sup>2</sup> )
SAN	51 ± 4	3140 ± 50	2 ± 0.2	11 ± 1
PS <sub>30</sub>	28 ± 3	3010 ± 80	1.1 ± 0.04	3.2 ± 0.7
PS <sub>50</sub>	30 ± 4	3150 ± 90	1.06 ± 0.06	3.1 ± 0.1
PS <sub>70</sub>	22 ± 2	3040 ± 70	0.8 ± 0.01	2.6 ± 0.9
PS	30 ± 1	2920 ± 40	1.2 ± 0.03	2.9 ± 1.3
PS <sub>30</sub> C5	29.4 ± 0.7	2800 ± 90	3.0 ± 0.2	4.1 ± 0.9
PS <sub>50</sub> C5	23.5 ± 0.6	2720 ± 60	2.1 ± 0.04	3.4 ± 0.5
PS <sub>70</sub> C5	27 ± 6	2690 ± 90	1.2 ± 0.1	3.1 ± 0.7
PS <sub>30</sub> C10	27 ± 4	2400 ± 60	4.7 ± 0.9	5.2 ± 0.4
PS <sub>50</sub> C10	21 ± 0.8	2180 ± 80	4.2 ± 0.8	3.8 ± 0.7
PS <sub>70</sub> C10	21 ± 1	2320 ± 70	1.7 ± 0.5	3.5 ± 0.8

. This demonstrates that the adhesion between the PS dispersed phase and the SAN matrix phase has been notably increased and that the stress is actually more efficiently transferred from one phase to the other. Also, this confirms that SEBS triblock copolymer is very effective for overcoming the brittleness of the uncompatibilized PS/SAN blend and for inducing a more energy dissipative process which is reflected in a more ductile behavior of the blends, as also concluded from the tensile test.

### IV.1.3 Thermal behavior of the blends

To ascertain the immiscibility and study the thermal properties of PS/SAN blends, DSC and DMA analyses have been performed (figures IV.5-6 and IV.7-8 respectively) and the glass transition temperatures of PS and SAN in both uncompatibilized and compatibilized have been determined (Table IV.2). A miscible system blend exhibits a single T<sub>g</sub> characteristic of a unique phase system, whereas, a two phase-separated blend exhibits two glass transitions. As determined from DSC, neat PS and SAN exhibit T<sub>g</sub> values around 93°C and 111°C, respectively, while from the variations of the loss modulus or damping factor (Tanδ), higher values are obtained about 102 and 118°C for PS and SAN, respectively. This difference may be attributed to the different nature of the response of the sample toward DSC and DMA

analysis conditions [8].

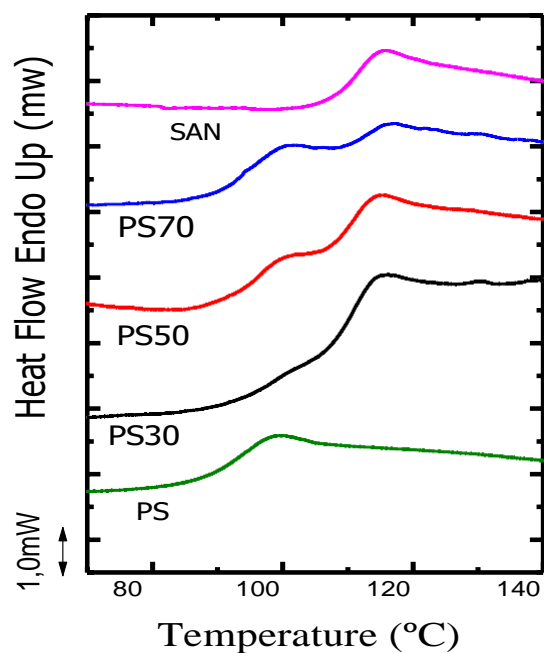


**Figure IV.5** DSC scans of PS/SAN blends melt blended without compatibilizer SEBS.

After melt blending without compatibilizer, the DSC thermograms showed that all the blends compositions PS30, PS50 and PS70 exhibited two distinct Tg values slightly different from those of the neat PS and SAN phases, but very close, thus suggesting the immiscible nature of the blend. Only for PS70 the Tg for PS is significantly higher than for pure PS, that could be due to the low content of the PS phase surrounded by the more rigid SAN phase that could hamper the mobility of the PS chains.. However

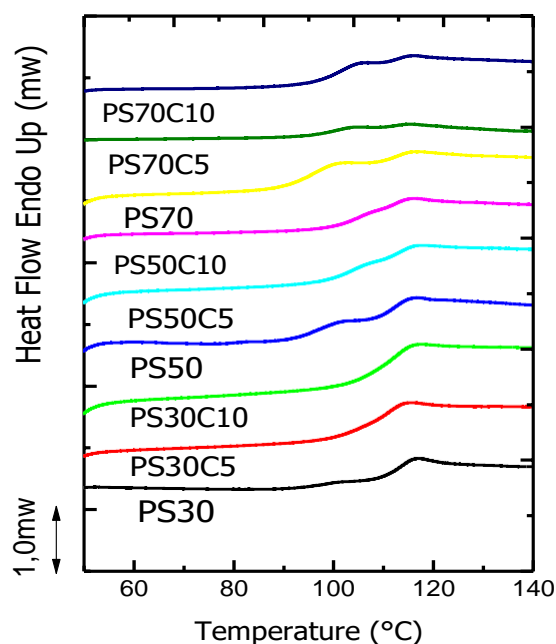


**Figure IV.6** DSC scans of PS/SAN blends melt blended with SEBS compatibilizer.

When the SEBS was added to blend with 5 and 10 wt %, a slight shift toward higher and lower temperature for PS and SAN respectively was found. The same trend is observed for the DMA analysis, which pointed out that the closeness of the PS and SAN T<sub>g</sub> values caused the merging of the glass transition peaks as an indication of a somewhat blend compatibility.

**Table IV.2.** Glass transition temperatures as measured from DMTA and DSC analyses for PS and SAN phases in uncompatibilized and compatibilized PS/SAN blends.

Composition	Mesured From DMA		Mesured From DSC	
	T <sub>g</sub> PS /°C	T <sub>g</sub> SAN /°C	T <sub>g</sub> (PS)	T <sub>g</sub> (SAN)
SAN	–	118	–	111
PS30	102.3	114.8	105	109
PS50	95.6	105.7	94.1	110.6
PS70	95	104.5	94.2	112.6
PS	102	–	93	
PS <sub>30</sub> C5		115.5		109.3
PS <sub>50</sub> C5	101.2	113.3	101.7	113.8
PS <sub>70</sub> C5	97	107.2	99.7	112
PS <sub>30</sub> C10		116		110.8
PS <sub>50</sub> C10	101.8	112.4	104.5	112.2
PS <sub>70</sub> C10	102.4	113	105.3	114.5

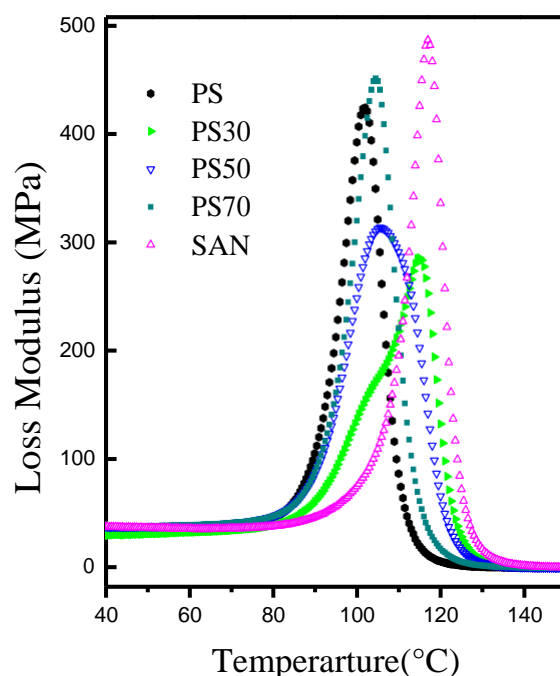


**Figure IV.7** Loss Modulus for uncompatibilized PS/SAN blends.

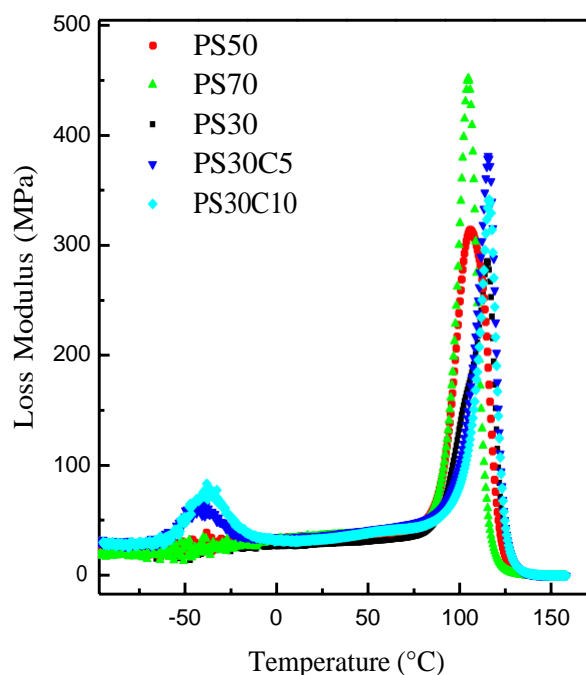


**Figure IV.8** Loss Modulus for compatibilized PS/SAN blends.

SEM photographs demonstrated the existence of a two phase morphology and therefore, the existence of a single T<sub>g</sub> can be only explained by the impossibility to detect the T<sub>g</sub> of the PS phase, due probably to the sum of the facts that the low content of PS makes the change in calorific capacity small (as seen for PS30) and that the improvement on the interfacial adhesion produced by the compatibilizer increases slightly the T<sub>g</sub> value for PS phase and probably makes it wider which makes it difficult to distinguish the transition.

#### IV.1.4 Thermal stability of PS/SAN blends

Thermogravimetry (TG) was performed to estimate the effects of the compatibilizer on the thermal stability and thermal decomposition behavior of PS/SAN blends.

The TG and DTG curves give, respectively, the weight variations with temperature and its derivative, versus time. Curves for PS, SAN and their uncompatibilized and compatibilized PS/SAN blends are shown in figure IV.9-10. The thermal decomposition values are listed in table IV.3.

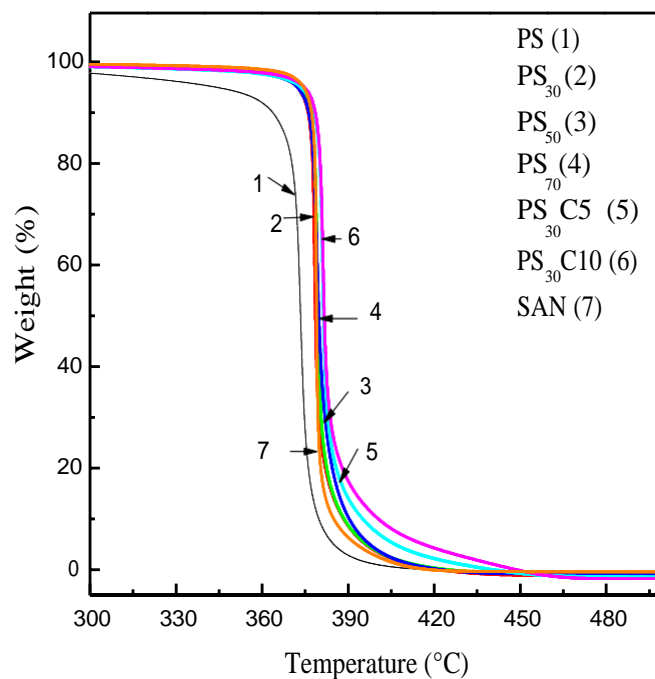


**Figure IV.9** TG thermograms of PS, SAN and their blends prepared without and with SEBS compatibilizer.

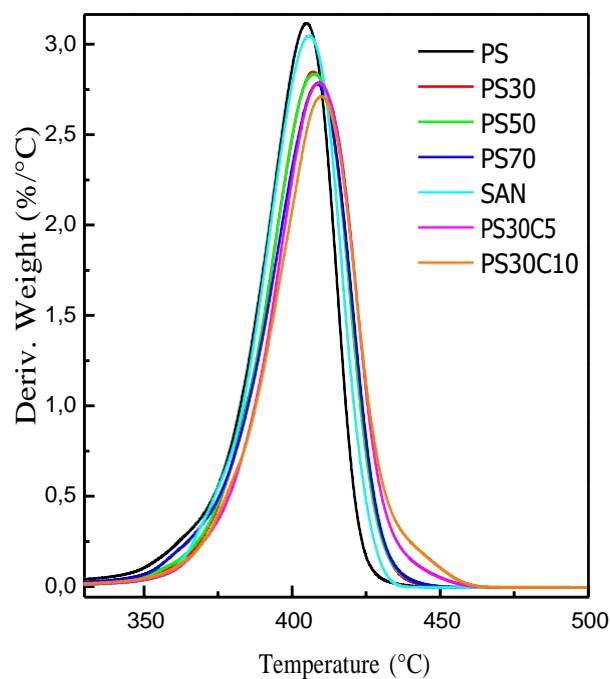


**Figure IV.10** DTG thermograms of PS, SAN and their blends prepared without and with SEBS compatibilizer.

**Table IV.3.** Thermal stability parameters as determined from TG and DTG thermograms for PS, SAN and their blends with and without compatibilizer.

Samples	$T_{\text{Onset}}$ (°C)	$T_{50\%}$ (°C)	$T_{\text{end}}$ (°C)	$T_{\text{max}}$ (°C)	Residue $_{475^{\circ}\text{C}}$ (%)
SAN	363	402	418	405	0.25
PS <sub>30</sub>	362	404	421	407	0.19
PS <sub>50</sub>	361	403	420	407	0.25
PS <sub>70</sub>	360	404	421	408	0.17
PS	353	400	416	405	0.01
PS <sub>30</sub> C5	363	409	423	409	0.2
PS <sub>50</sub> C5	364	407	425	411	0.25
PS <sub>70</sub> C5	359	410	424	411	0.11
PS <sub>30</sub> C10	362	407	423	409	0.36
PS <sub>50</sub> C10	364	407	424	410	0.17
PS <sub>70</sub> C10	361	407	424	410	0.46

It can be seen that pure PS presents a slightly lower thermal stability than SAN. They start to lose weight ( $T_{\text{onset}}$ ) at about 353 and 363°C and they end at  $T_{\text{end}}$  of 416 and 418°C and reveal a  $T_{50}$  where half of the sample has been decomposed at around 400 and 402°C, respectively. The neat PS/SAN blends exhibit a marginal increase in thermal stability as witnessed by the very slight increase observed on the values  $T_{\text{onset}}$ ,  $T_{\text{end}}$  and  $T_{50}$ . The incorporation of SEBS does not increase significantly the thermal stability other than a marginal increase of a few degrees. Thus, thermal stability is unchanged respect to the virgin polymers for both, the uncompatibilized blends and the compatibilized blends.

#### IV.1.5 Microstructure analysis

Morphology of polymer blends depends on several factors such as the composition, the mixing conditions and the interfacial tension between the mixed polymers. Figures IV.11 and IV.12

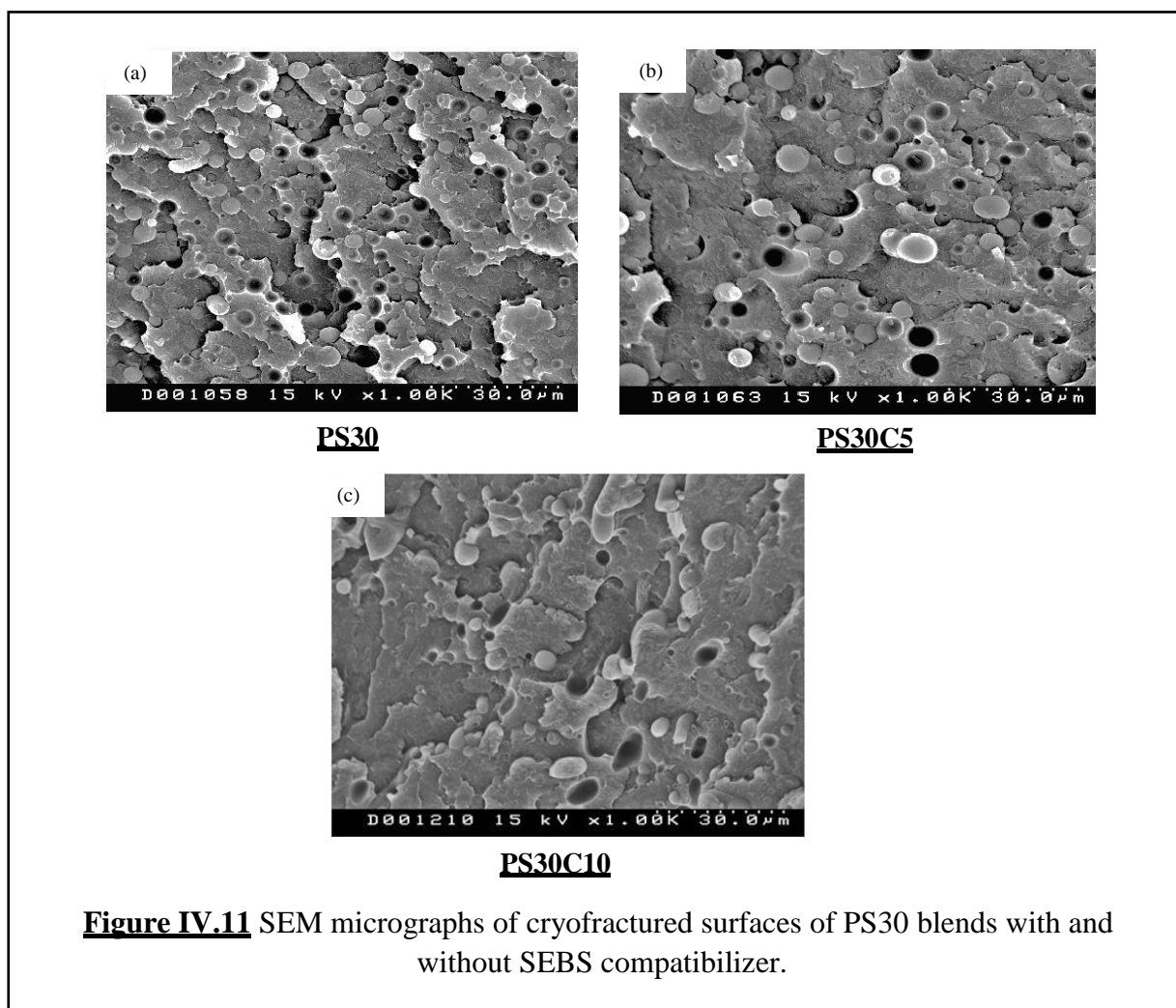
exhibit the microstructure of PS<sub>30</sub> and PS<sub>70</sub> blends prepared without and with 5 and 10 wt% of SEBS as compatibilizer. Also, **Tab IV.4** reports the values of  $R_n$  and  $R_w$  as determined for uncompatibilized and compatibilized PS<sub>30</sub> and PS<sub>70</sub> blends using Image J analyzer.



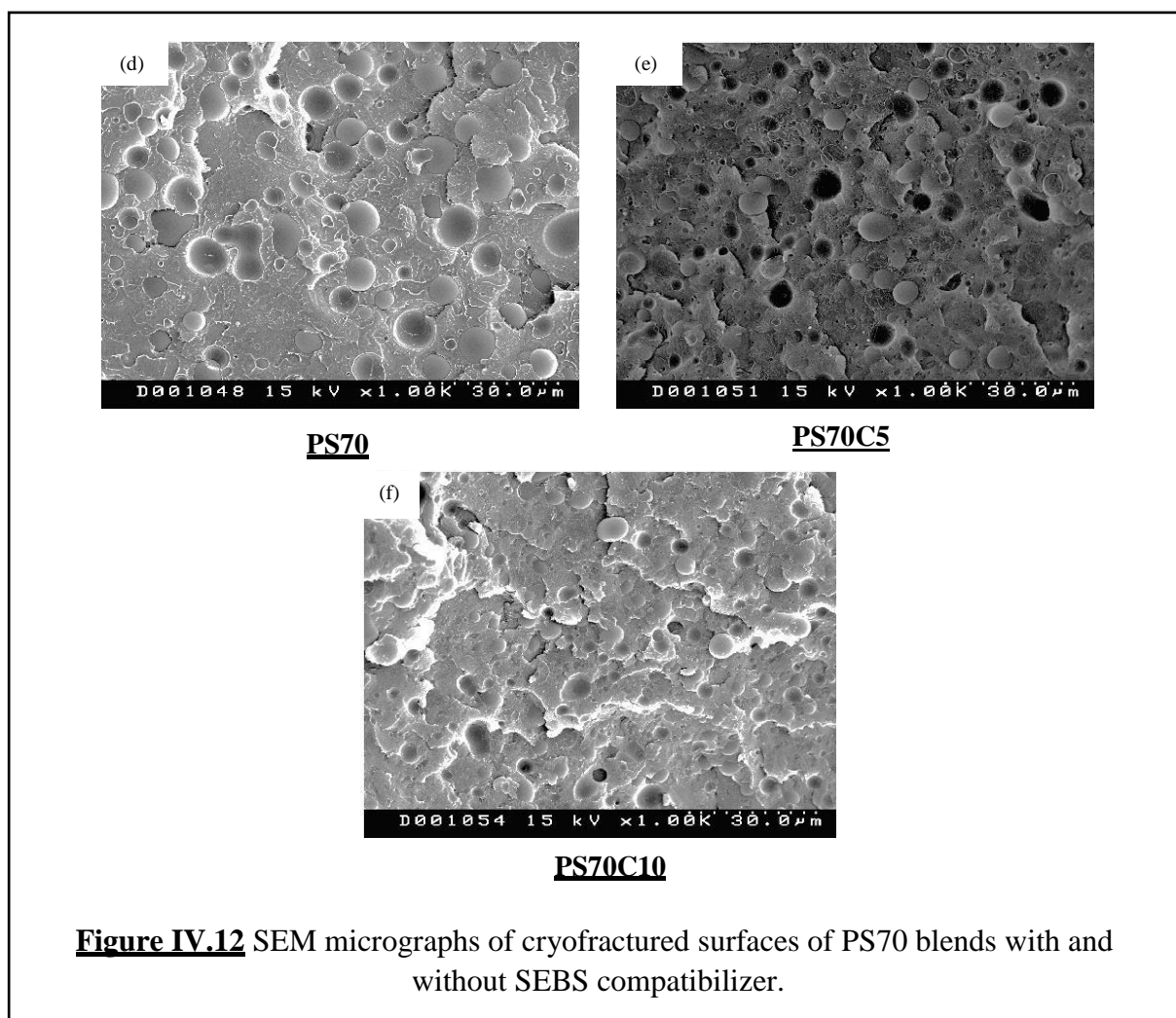
**Table IV.4** Average size of holes in SEM morphology of the blend analysed with ImageJ software.

Composition	$R_n$ ( $\mu\text{m}$ )	$R_w$ ( $\mu\text{m}$ )
PS <sub>30</sub>	3.70	10.69
PS <sub>30</sub> C5	5.52	13.86
PS <sub>30</sub> C10	2.37	10.57
PS <sub>70</sub>	7.58	13.14
PS <sub>70</sub> C5	4.50	9.71
PS <sub>70</sub> C10	3.43	8.57

The micrographs of figures IV.11 and IV.12 (a-f) showed a droplet/matrix two-phase morphology typical of immiscible polymer blends. The PS phase in PS30 blends was dispersed as spherical domains with a droplet size of 3.70  $\mu\text{m}$  which seems to be the result of the interplay between the mixture composition, the mixing conditions, the existing interfacial tension and finally the system rheology [9].



After adding 5 and 10 wt% of SEBS, the PS droplet size changed to attain 5.52 and 2.37  $\mu\text{m}$ , whereas  $R_w$  presented values of 13.86 and 10.57  $\mu\text{m}$ , respectively. It is expected that droplet decreased with compatibilizer, as it happened with PS30C10 and it is not known why it increased in PS30C5. The PS70 blends showed a considerable morphology refinement as the SEBS concentration increased, as expected. The SAN droplet size decreased from 7.58 for the uncompatibilized blend to 4.50 and 3.43  $\mu\text{m}$  for the blends compatibilized, respectively by 5 and 10 wt% of SEBS.



At the same time,  $R_w$  declined from 13.14 for the blend without SEBS to 9.71 and 8.57  $\mu\text{m}$  for the blends with 5 and 10 wt% of the compatibilizer. The evident reduction in the droplet size of PS and SAN with increasing the SEBS concentration resulted from the decrease in the interfacial tension which is expected to be caused by the localization of the SEBS molecules at the interface between the droplets and the matrix.

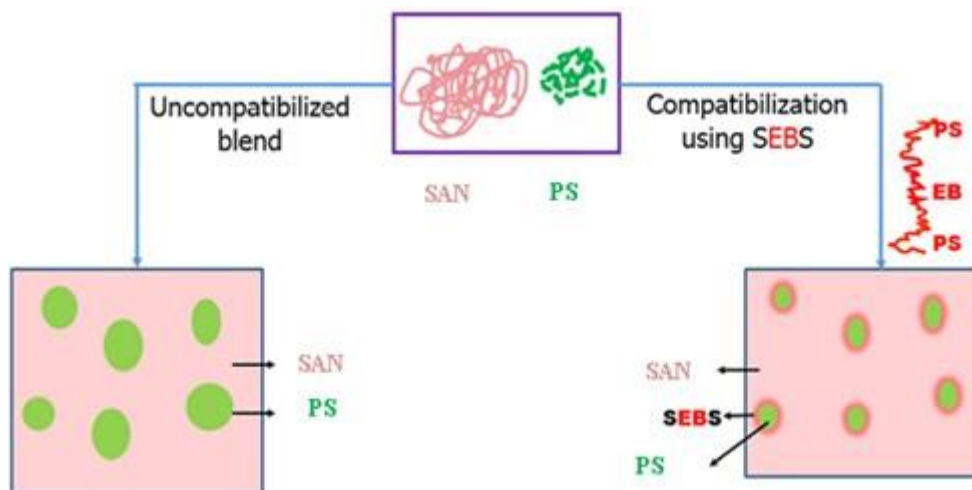


**Figure IV.13** Schematic representation of morphology of SEBS compatibilized rPS/SAN blend.

#### IV.1.6 Conclusion

In this work, the effect of SEBS compatibilizer on the properties of PS/SAN blends was studied. It was found that the addition of 5 wt% of SEBS has a beneficial effect on the morphology, mechanical and thermal properties of the blends. The PS/SAN blend without SEBS did not improve its mechanical properties due to the weak interfacial adhesion between PS and SAN phases. However, materials with improved mechanical properties have been obtained when the adhesion between the PS and SAN phases has been enhanced by the presence of SEBS. These results were confirmed by SEM observations which revealed that the incorporation of SEBS was effective in reducing the domain size of the PS or SAN dispersed phases. The DSC results revealed that the compatibility of blend is improved with addition of compatibilizer SEBS. A single T<sub>g</sub> was observed only for PS30 blend with 5 and 10 wt% of SEBS, thus confirming a better interfacial adhesion between the two phases. The TGA analysis indicated that the thermal stability of PS/SAN blends with and without compatibilizer was unchanged respect to the virgin polymers. The overall variations in all properties suggest that the SEBS copolymer could be used as an effective compatibilizer for the PS /SAN mixtures.

## IV.2 Characterizations and Properties of rPS/SAN blends without and with addition of compatibilizer.

### IV.2.1 Rheology behavior of the polymer blends

The results of the rheological measurements carried out on the blends are shown in Fig. IV.14 -16, where their complex viscosity ( $\eta^*$ ), storage moduli ( $G'$ ) and loss moduli ( $G''$ ) curves are plotted as a function of frequency (together with those of the pure components rPS, SAN) at 190 °C in the frequency range 0.01–100

Hz . Rheological properties provide information about the compatibilization effect, as well as the correlations between their rheological– morphological– mechanical properties [10].

Fig.IV.14 shows the changes in complex viscosity ( $\eta^*$ ) as a function of angular frequency ( $\omega$ ) of rPS, SAN, and their rPS/SAN blends without and with 5 and 10 wt% of SEBS. It can be observed that the complex viscosity of the SAN was higher than that of the recycled PS. The complex viscosity of the uncompatibilized blends decreased with the increase in the rPS content. At rPS30 the curve is close to rPS and at higher content rPS50 and rPS70 is lower than for pure rPS. Thus the blend of rPS and SAN gives a more fluid material than the pure components at high rPS content.

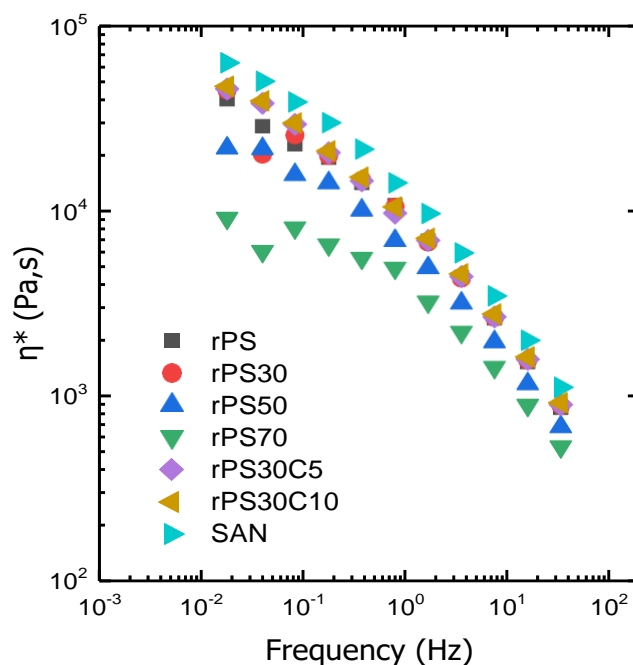


**Figure IV. 14** Complex viscosity ( $\eta^*$ ) of rPS, SAN and their blends without and with compatibilizer SEBS.

In addition Fig IV.14 also shows the effect of SEBS copolymers with different ratios 5 and 10 wt%, on the complex viscosity of rPS/SAN 30/70 blend. For this ratio, the addition of SEBS does not change the rheology of the material.

The complex viscosity of all formulations shows a downward trend with increasing the frequency, reflecting the shear thinning phenomenon and exhibiting the typical motion characteristics of pseudoplastic fluid [11]. This is because the molecular chain entanglement decreases with increasing the shear force, leading to a better fluidity of blends. However, compared with pure rPS/SAN blends, the complex viscosity of the blends increases a little bit after adding SEBS copolymers which is probably due to the physical compatibilization of SEBS and may be due to a low fluidity of SEBS when compared to rPS and SAN, or to the interactions performed during blending, Suggesting the changes have occurred in the interface of compatibilized blends [10]. Which may directly impact the mechanical properties. This assumption correlated with the results obtained with mechanical properties and SEM images in the following section.

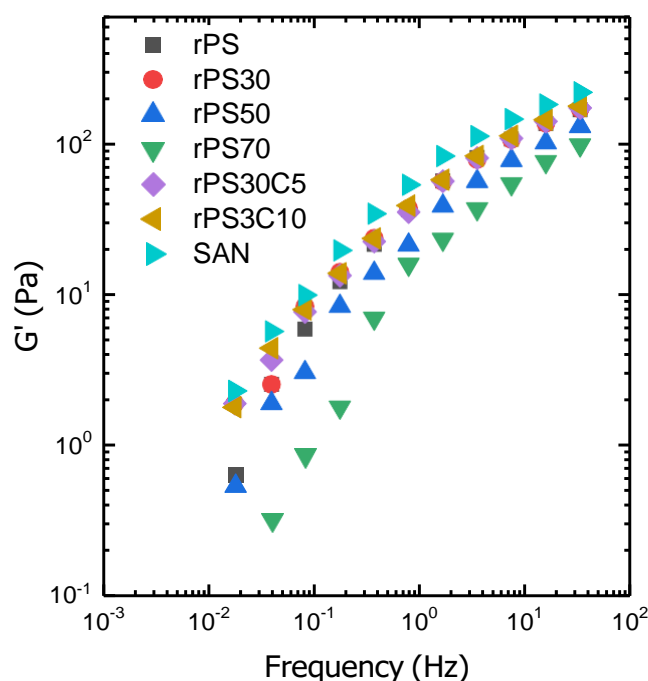


**Figure IV.15** Frequency-sweep plot of the storage modulus ( $G'$ ) for neat rPS, SAN and uncompatibilized/ compatibilized rPS/SAN/SEBS blends.

The curves of storage modulus ( $G'$ ) and loss modulus ( $G''$ ) of rPS/SAN blends as a function of the frequency are shown in Figures IV.15-16, respectively.  $G'$  and  $G''$  of all samples increase with the



increase in the frequency. In the low frequency region, the movement of molecular chain is synchronized with the change of external force, and the flexibility and elasticity of molecular chain are high, which result in a lower  $G'$  of the blends. Meanwhile, the smaller friction between the molecules causes the lower  $G''$ . In the high frequency region, the movement of molecular chain could not keep up with the change of external force, and the friction consumption between the molecular chains is also increased, which leads to the increase of  $G'$  and  $G''$  [11]. It can also be seen that the storage modulus ( $G'$ ) and loss modulus ( $G''$ ) of the rPS/SAN blend compatibilized with SEBS copolymers are higher than those of the uncompatibilized rPS/SAN blends, indicating an increased of the interaction between rPS and SAN on addition of SEBS compatibilizer. The rheological properties in the low frequency region can be considered to reflect the relaxation and motion of the whole polymer chains. Also the  $G'$  and  $G''$  of the blends reach the maximum value at 10 wt% of SEBS. Which is due to the chain entanglement between SEBS and the blends. In other hand this increase in  $G'$  and  $G''$  is associated with relaxation time of dispersed phase [12-13].

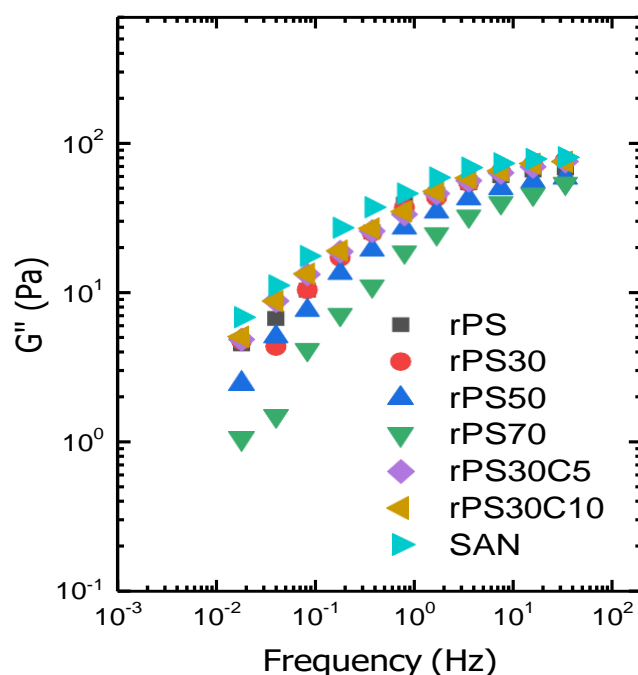


**Figure IV.16** Frequency-sweep plot of the loss modulus ( $G''$ ) for neat rPS, SAN and uncompatibilized/ compatibilized rPS/SAN/SEBS blends.

It is mentioned in literature [10] that the storage modulus of an immiscible blend is characterized by the presence of a relaxation shoulder, which arises due to deformation and relaxation of dispersed phase. This trend is verified for all blends analyzed. Compared to binary blends (rPS/SAN),  $G'$  of SEBS compatibilized blends is higher at low frequencies, indicating higher elasticity, possibly this increase is related with SEBS addition, these  $G'$  data

strengthen the fd agent, favoring Interactions between chemical groups <sup>[13]</sup>. Which presents high viscoelasticity, as well as with dispersed phase reduction particle size,

The relation curves of storage modulus ( $G'$ ) and loss modulus ( $G''$ ) rPS/SAN blends as function of the frequency at 190°C are showed in Figure IV.17. It is observed that, at lower frequencies below 1 Hz, the viscous response is higher than the elastic response for all samples analysed, until reaching a frequency, where the modules intersect  $G' = G''$  (where the dissipative feature is equal to the elastic

Feature at the same frequency). For values higher than 1 Hz, the elastic response ( $G'$ ) exceeds the viscous response ( $G''$ ).

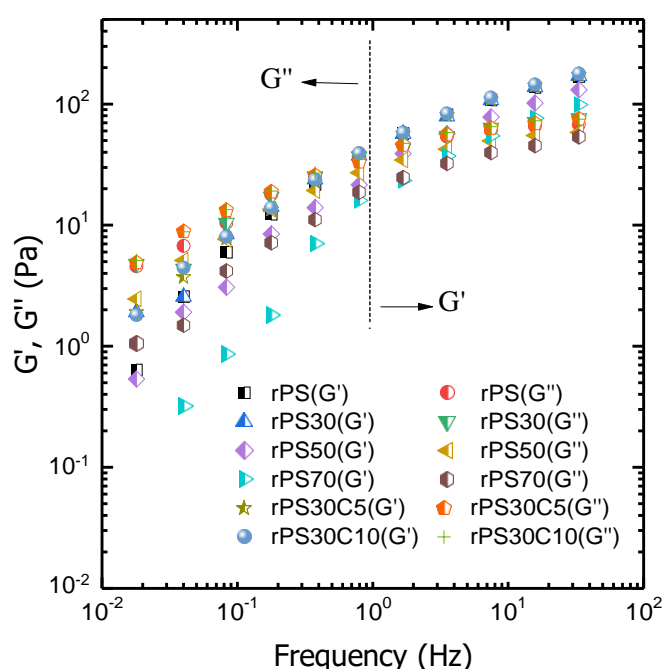


**Figure. IV.17** The storage modulus ( $G'$ ) and loss modulus ( $G''$ ) of rPS/SAN blends as function frequency for all compositions analysed.

Bousmina and Muller <sup>[14]</sup> reported similar behavior for other copolymers containing rubber. In these studies, the  $G' = G''$  cross-points were attributed to network type structures formed through the association of elastomeric particles. While this inversion of behavior is associated with hindrance in molecular mobility, since the molecular segments can not move and respond as rapidly as the applied frequency. Table IV.5 shows values for the point  $G' = G''$ , for all investigated compositions.

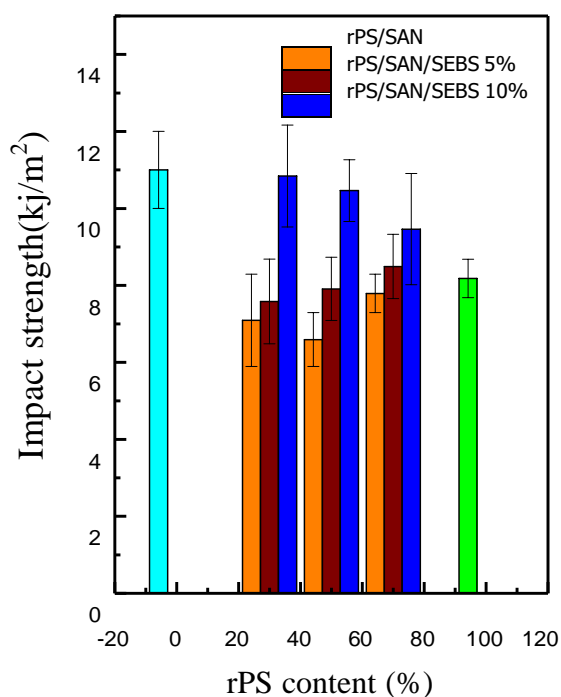
**Table IV.5** Crossing-point,  $G' = G''$ , for rPS and their blends.

Composition (MPa)	Frequency (Hz)	$G' = G''$
rPS	0.77	38.11
rPS30	0.80	37.03
rPS50	1.67	37.10
rPS70	3.52	35.56
rPS30C5	0.79	34.07
rPS30C10	0.79	36.48

## IV.2.2 Mechanical Properties

### IV.2.2.1 Impact strength of recycled rPS/SAN blends

The notched Izod impact strength is one of the most important properties for rigid polymers such as the rPS/SAN alloy because of their notch sensitivity. Figure IV.18, shows that SEBS is a good compatibilizer and improves very significantly the impact strength of the rPS/SAN with a SAN content 30–70 wt %. The impact strength of the rPS/SAN alloy can be greatly enhanced by the addition of 5 and 10 wt % SEBS. For example, the impact strength increases from  $7.1 \text{ kJ/m}^2$  of rPS<sub>30</sub> to  $10.8 \text{ kJ/m}^2$  when 10 wt % SEBS is added. The impact strengths of simple rPS/SAN blends without SEBS are lower than for pure rPS, decreasing with the increase of SAN content up to 70 wt %, indicating a negative synergistic effect between the rPS and the SAN because of their poor interfacial interaction in the rPS/SAN blends, as further shown in SEM images.

**Figure IV.18** Effect of compatibiliser compositions on impact strength of rPS/SANBlends.



It is known that the phase morphology and the interfacial adhesion between component polymers influence the mechanical properties of polymer blends. Two-phase morphology with lack of adhesion between the component polymers leads to premature failure and, thus, to poor mechanical strength, and the improved interfacial adhesion leads to higher mechanical strength..

**Table IV.6** The mechanical properties of recycled PS, rPS/SAN, and rPS/SAN/SEBS blend.

rPS/SAN	TensileStrength (MPa)	Tensile Modulus (MPa)	Elongation at break (%)	Impact Strength (kJ/m <sup>2</sup> )
rPS	25.6 ± 1.7	2930 ± 48	3.6 ± 0.3	8.2 ± 0.5
rPS <sub>30</sub>	44.6 ± 2	3100 ± 67	4.7 ± 0.3	7.1 ± 1.2
rPS <sub>50</sub>	30.6 ± 2	3080 ± 59	3.8 ± 0.1	6.6 ± 0.7
rPS <sub>70</sub>	28.7 ± 1.4	2990 ± 24	3.6 ± 0.5	7.8 ± 0.5
rPS <sub>30</sub> C5	28.9 ± 1.2	2680 ± 61	4.9 ± 0.4	7.6 ± 0.1
rPS <sub>50</sub> C5	23.7 ± 1	2680 ± 90	5.1 ± 0.4	7.9 ± 0.8
rPS <sub>70</sub> C5	23 ± 2.2	2700 ± 41	3.8 ± 0.5	8.5 ± 0.8
rPS <sub>30</sub> C10	27 ± 1	2330 ± 155	6.1 ± 0.3	10.8 ± 0.3
rPS <sub>50</sub> C10	21.3 ± 1.2	2190 ± 112	5.9 ± 0.5	10.4 ± 0.8
rPS <sub>70</sub> C10	17.4 ± 2.6	2230 ± 157	4.8 ± 0.2	9.5 ± 0.4
SAN	51 ± 4.7	3140 ± 55	3.4 ± 0.4	11 ± 1

The incorporation of SEBS can improve the compatibility of the rPS/SAN blends. Moreover, the impact strength, of the binary rPS/SAN blends increased with increasing SEBS content (which acts as an impact modifier that improves the toughening and ductility of the brittle rPS/SAN, thus increasing the energy absorption capacity of the blends. When highly dispersed, the SEBS rubbery phase acts as an effective stress concentrator, thus enhancing both crazing and shear yield in the blend. Because both processes can dissipate a large amount of energy, there is a significant increase in the toughness of the blends. This increase of impact strength is possible due to the fact that SEBS compatibilizer contains EB block segments chemically identical to rPS and with SAN, which have relatively high affinity with the SAN phase.

It can be concluded that SEBS acts as an efficient compatibilizer. <sup>[15-17]</sup>

#### IV.2.2.2 Tensile Strength

Generally, it has been long established that immiscible polymer blends have inferior mechanical properties because of the existence of weak interfacial adhesion and poor dispersion of the components. In this study, the mechanical properties before and after the compatibilization effect of rPS/SAN blends by the SEBS block copolymer were investigated.

Tensile parameters (strength, Modulus and Elongation at break) are summarized in Table IV.6. It can be seen that the mechanical properties of SAN are higher than those of rPS.

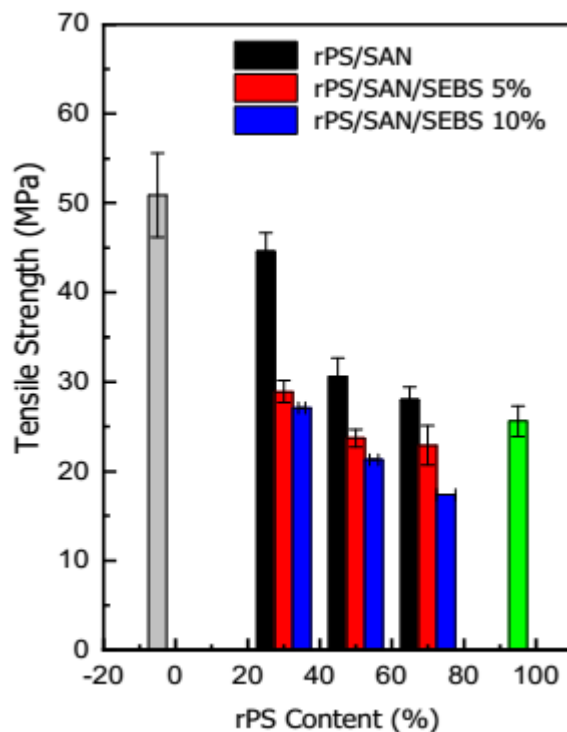


**Figure IV.19** Effect of SEBS compositions on tensile strength of rPS/SAN compositions

The trend for the tensile strength of the blends with SEBS (Figure IV.19) is different from the trend for notch impact strength. The addition of 5 and 10 wt% SEBS decreases slightly tensile strength of pure recycled PS, SAN and rPS/SAN blends. This may be attributed to the fact that SEBS is an elastomer with a lower tensile modulus and affects the rigidity of the blends.

As expected the reduction in tensile strength of the blends during the mechanical test implies a higher energy dissipation, also this associated with two hypotheses; the SEBS elastomeric character that leads to more flexible blends requiring lower tensile load for deforming; or due to interfacial saturation due to compatibilizer excess, this approach corroborates impact results, whereas the compatibilizer content increases the greater the Impact strength, i.e., with higher dissipation energy level for the blends, while reducing the tensile strength compared to neat SAN. It is common knowledge that the toughness will be increased, whereas the modulus will be decreased when elastomer is added [18].

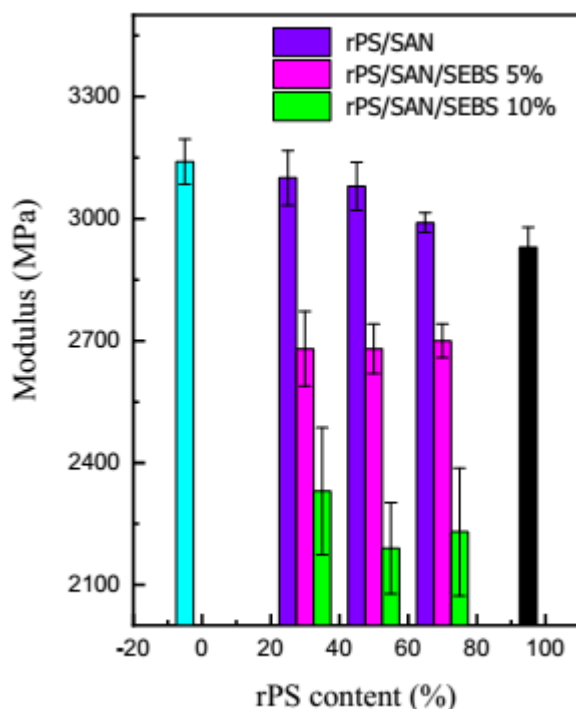


**Figure IV.20** Shows the evolution of elastic modulus test of rPS/SAN noncompatibilized and compatibilized blends.

Figure IV.20. Shows the evolution of elastic modulus of recycled PS, SAN and rPS/SAN blend as function of both rPS and SEBS content. It can be seen that SAN had the highest elastic modulus, with a typical brittle behavior of rPS/SAN blends. , Compatibilized blends had reduced elastic modulus in relation to pure SAN and rPS. The decrease in the modulus

with increasing elastomer content is expected and well reported for the rubber toughening of rigid polymers [19]. As revealed in literature by la Mantia et al. [20]. The SEBS is able reducing the brittleness of at least one of the two phases and locates selectively at the interface, it was also verified that SEBS decreased the elastic modulus of blends, this being attributed to the SEBS's elastomeric nature. However, these losses in the elastic modulus were accompanied by gains in impact strength, as shown in Figure IV.18.

The elongation at break of the binary rPS/SAN blends in comparison with neat rPS, SAN and ternary rPS/SAN/SEBS blends is shown in Fig IV.21. Addition of SEBS, the Softness and flexibility of this polymer will increased the elongation of the blend. All values are higher than that of the pure SAN.

As expected, it can be seen in Tab IV.6. That the most effective compatibilizer was a styrene-ethylene/butadiene-styrene triblock copolymer (SEBS). This substance caused a significant increase in the ductility of rPS/SAN. Even at as low as 5 wt% compatibilizer, the elongation- values

increased over all samples compatibilized. This is considerably higher than has previously been reported for PS/SAN blends compatibilized by SEBS. At least two explanations exist for this effect of the SEBS.

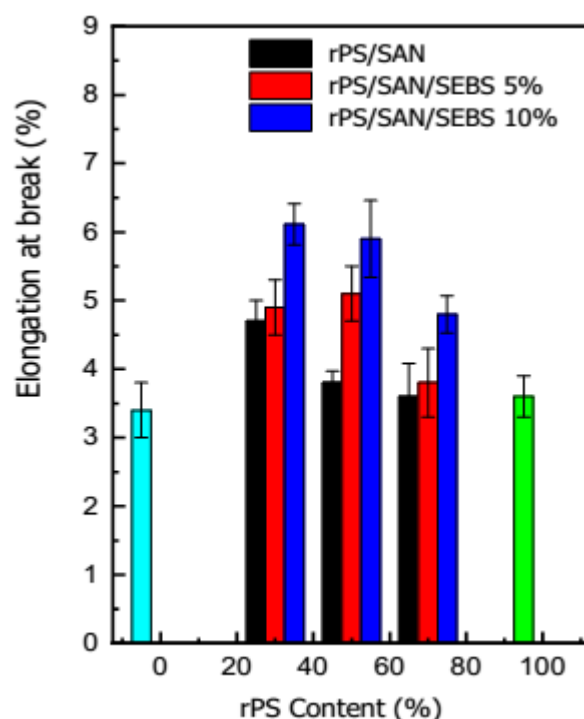


**Figure IV.21** Shows the evolution of elongation at break test of rPS/SAN noncompatibilized and compatibilized blends.

Firstly, the SEBS is a block copolymer with sections that are similar and, thus, compatible, to the two types of polymers (polystyrene and styrene-co-acrylonitrile) in the blend. It could act as a surface-active material, reducing the surface tension between the two phases during processing. This reduction in interfacial tension should result in a reduction of the domain size that is expected to improve the properties of the mixture. An alternative explanation offered by La Mantia is that the SEBS is not a true compatibilizer, instead it reduces the brittleness of at least one of the phases instead of accumulating at the interfaces <sup>[20]</sup>.

Figure IV.22 shows the tensile stress-strain curves of the pure recycled PS, SAN, and the rPS/SAN blends containing different amounts (5 and 10 wt%) of SEBS. It can be seen that rPS and SAN copolymer presents hard, brittle and fragile character with an ultimate elongation less than 4%. However, the blend of Recycled PS and SAN without addition of SEBS does not display any improvement in toughness. It is still brittle and fractured in a brittle mode. There is no yield point on its stress-strain curves and it broke at a strain of about 3.5%. In other hand the rPS/SAN blend combines the poorest properties of the components. However, after the addition of only 5 wt% of SEBS to the blend, a completely different

tensile behavior occurs (Fig IV.22, curve of rPS30C5), the blends display a ductile behavior as indicated by the presence of a yielding point. Its stress-strain curve exhibits the characteristics of a typical toughened plastic. Such as acrylonitrile-butadiene-styrene terpolymer and high impact PS. All rPS/SAN blends compatibilized by SEBS exhibited a similar behavior.

The tensile specimens of these blends show whitening but no obvious necking in the tensile process. Indicating its ductility and high stiffness while the fragile character was maintained, corroborating the results of impact strength, which were similar.

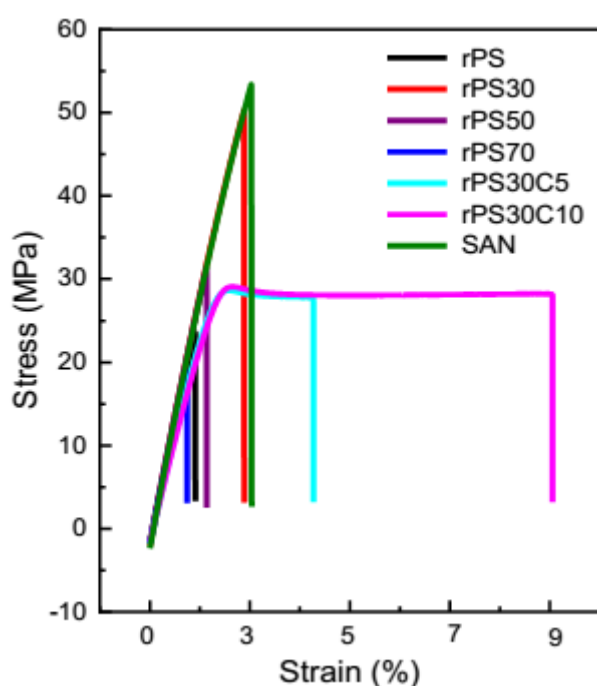


**Figure IV. 22** Stress versus strain plots of rPS, rPS/SAN blend and compatibilized ones as function of rPS content.

In contrast, the incorporation of the third component SEBS with 5 and 10 wt% produced a higher strain compared to SAN, rPS and rPS/SAN blends, and changed the brittle fracture to a ductile fracture, This increase in strain and absorption of more energy indicates an increase in flexibility of the compatibilized samples in comparison to samples rPS, SAN and rPS/SAN. It is noteworthy that the increase in flexibility in compatibilized samples compared to samples without SEBS is consistent with the results of impact strength already presented. It may be noted that the compatibility of blends was improved upon SEBS addition for all samples analysed, which resulted in a gradual increase of elongation at break. Similar results were reported in the literature. Diaz et al <sup>[19]</sup> reported that the increase in elongation at break due to the adhesion between matrix and dispersed phase. It is important to note that an increase in toughness is normally associated with a decrease in stiffness and strength, in our case the addition of the SEBS only caused a moderate decrease in these important mechanical properties.

### IV.2.3 DSC analysis and morphology observation

The glass transition behavior of rPS, SAN, and their blends, without and with SEBS as compatibilizer, at different concentrations was studied by DSC (Figure IV.23). The results obtained for samples with 30, 50, and 70 wt% rPS are summarized in Table IV.7

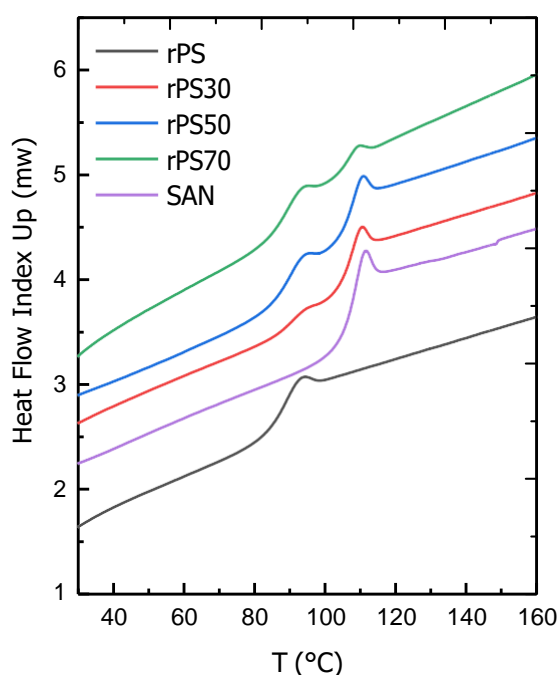


**Figure IV.23** DSC scans of rPS/SAN blends without compatibilizer SEBS

It can be seen that the  $T_g$  values of rPS and SAN determined were  $89.04^\circ\text{C}$  and  $110^\circ\text{C}$ , respectively. The range of testing temperature was from 0 to  $150^\circ\text{C}$ . The  $T_g$  of the EB part in SEBS was not included in this range, and the  $T_g$  of the styrene block in SEBS was probably overlapped by the  $T_g$  of rPS. However, as SEBS was added into rPS and SAN, their  $T_g$  changed to  $98.83^\circ\text{C}$  and  $107.53^\circ\text{C}$ , respectively. Two  $T_g$ 's occurred in the rPS/SAN alloy, namely, a  $T_{g2}$  of  $106.33^\circ\text{C}$  for SAN phase and the other  $T_{g1}$  of  $89.93^\circ\text{C}$  for rPS30 phase. There were also two  $T_g$ 's in rPS50 and rPS70 alloys. Moreover, all the blend compositions show two distinct  $T_g$ 's corresponding to neat rPS and SAN phases, suggesting the immiscible nature of the blend. Generally, the decrease in the difference of the glass transition temperatures of the two phases implies an improved compatibility in the polymer alloy.

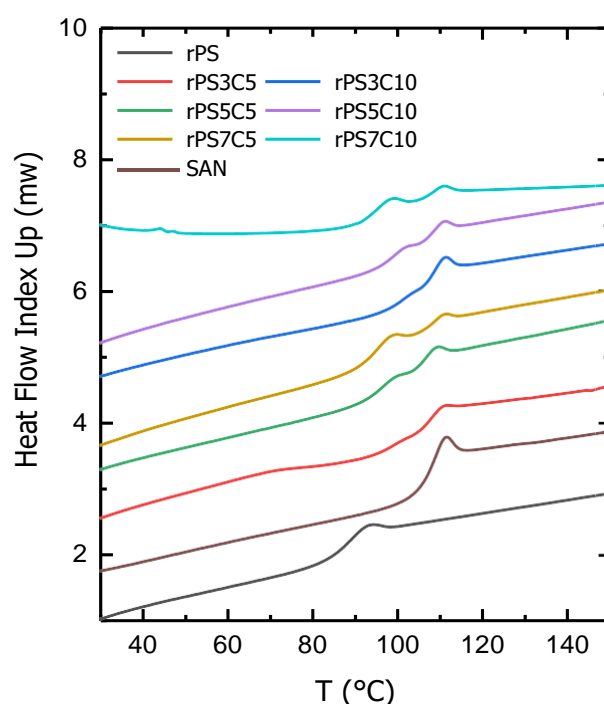


**Figure IV.24** DSC scans of rPS/SAN blends with SEBS.

**Table IV.7** Glass Transition Temperatures ( $T_g$ ) of rPS, SAN, and their blends.

Samples ( $^\circ\text{C}$ )	Ratio	$T_{g1}$ ( $^\circ\text{C}$ )	$T_{g2}$ ( $^\circ\text{C}$ )	$T_{g2} - T_{g1}$
rPS	-	<b>89.04</b>	-	
SAN	-	-	<b>110</b>	
rPS/SAN	<b>30/70</b>	<b>89.93</b>	<b>106.33</b>	<b>16.4</b>
	<b>50/50</b>	<b>89.96</b>	<b>107.23</b>	<b>17.27</b>
	<b>70/30</b>	<b>89.56</b>	<b>104.75</b>	<b>15.19</b>
rPS/SAN/SEBS	<b>30/70/5</b>	<b>98.83</b>	<b>107.53</b>	<b>8.7</b>
	<b>30/70/10</b>	<b>101.12</b>	<b>107.59</b>	<b>6.47</b>

The  $T_g$  difference ( $T_{g2} - T_{g1}$ ) in the rPS/SAN/SEBS blends is lower than that of the rPS/SAN blends, which confirms that the SEBS can enhance the compatibility of the rPS/SAN blends.. This could be proved by morphology observation as follows.

#### IV.2.4 Scanning electron microscopy (SEM)

The phase morphology of immiscible polymer blends depends on several factors including composition, processing conditions, interfacial tension, and rheological properties of the individual constituents. The micrographs of the cryogenically fractured surface of rPS/SAN and rPS/SAN/SEBS compounds are displayed in Fig. IV.25-26, with major content of SAN (rPS30) and major content con rPS (rPS70), respectively. By analyzing morphology of physical blends, it is possible to note that in both cases there are fragile-ductil fracture edges and wide distribution of domain sizes. The inspection of these micrographs indicates two phases with different domain size and shape, which reveal immiscible character of rPS/SAN, with voids presence and dispersed particles.

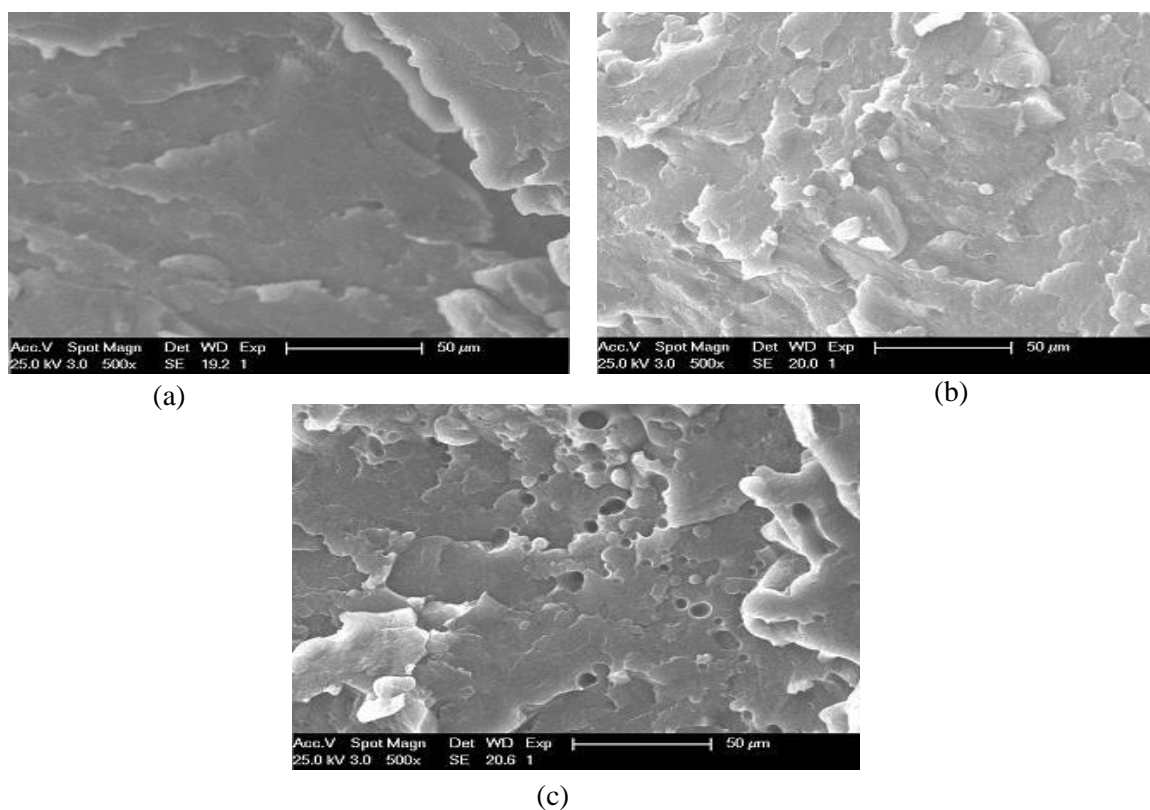


**Figure IV.25** SEM micrographs of cryo-fractured surfaces of rPS/SAN with SEBS : (a) rPS/SAN 30/70, (b) rPS/SAN/SEBS 30/70/5, (c) rPS/SAN/SEBS 30/70/10.



It is well known that the polymer present in the lower concentration usually forms a discontinuous phase whereas the polymer present in the higher concentration forms a continuous phase and such morphology of blends is usually named a particle-in-matrix type. In addition, low interaction is noted, which suggests poor adhesion between recycled PS and SAN, due to the weak interfacial interaction among the phases in the blends.

In general, high interfacial tension of the blends with poor compatibility will cause poor transference of load from matrix to the dispersed phase, leading to a smooth morphology. In compatibilized blends with 5 and 10% of SEBS it can be clearly observed a size reduction of dispersed particles in recycled PS matrix compared to the binary blend. This result agrees with literature [20,21]. This effect is related to the compatibilizer migration to the blend interfaces, promoting a reduction of interfacial energy and avoiding coalescence [16].

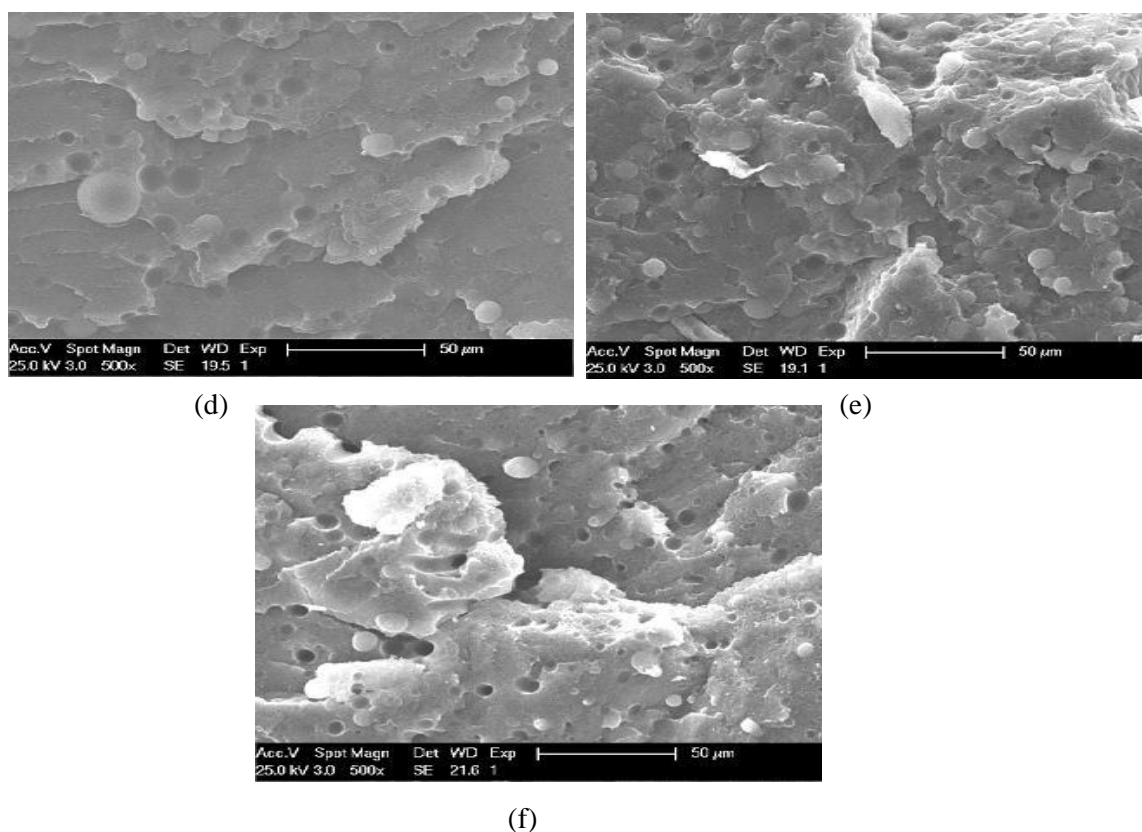


**Figure IV.26** SEM micrographs of cryo-fractured surfaces of rPS/SAN with SEBS : (d) rPS/SAN 70/30, (e) rPS/SAN/SEBS 70/30/5, (f) rPS/SAN/SEBS 70/30/10.

The compatibilizer diffusion to the interface is reinforced as observed in Figure 8, which indicates the prominent compatibilization of the SEBS. The possible reasons are that SEBS

facilitates the dispersion of the recycled PS dispersed phase and results in strong interfacial adhesion of the rPS/SAN blends.

In conclusion, compatibilizer play a key role to improve the interfacial adhesion between the components and to reduce the interfacial tension between the components. They exhibit interfacial activities in heterogeneous polymer blends. The interfacial activity of compatibilizers helps to stabilize the morphology by enhancing interfacial adhesion. Compatibilizers resist the coalescence of dispersed phases, thereby reducing the interfacial tension and the size of the dispersed domains which results in an increase of adhesion at the

Interface and improved properties of the final product. Commonly used compatibilizers are block, graft, or random copolymers consisting of dissimilar blocks <sup>[22]</sup>.

## CONCLUSION

In this part of research, the rheological, mechanical and morphological properties of the recycled PS, rPS/PSAN and rPS/SAN/SEBS blends were studied. The addition of SEBS copolymers increased the viscosity of all composition at low frequencies suggesting that the reactions between the copolymers and blend was achieved. The complex viscosity increased with the increase in the copolymers content. It was also observed that  $G'$  become higher than  $G''$  at low frequencies indicating that a refined morphology was obtained. A significant improvement in compatibilisation and toughness of recycled PS and SAN was achieved through the use of SEBS. The evidences of compatibilisation were obtained from the impact properties and the mechanical properties. The result shows that adding SEBS to rPS/SAN blends improved toughness and elongation but decreased strength and stiffness because of its rubbery character. The SEBS acts as an interfacial agent between the matrix and the dispersed phases. It lowers the interfacial tension and improves the interfacial adhesion. These results were confirmed by SEM observations which revealed that the incorporation of SEBS was effective in reducing the domain size of the recycled PS or SAN dispersed phases. The DSC analysis and the SEM photos confirmed that SEBS could greatly enhance the compatibility of the rPS/SAN blends, The overall variations in all properties suggest that the SEBS copolymer could be used as an effective compatibilizer for the rPS /SAN mixtures.

## REFERENCES

- [1] D. J. Kinning, E. L. Thomas, et L. J. Fetters, 1989 « Morphological studies of micelle formation in block copolymer/homopolymer blends », *J. Chem. Phys.*, vol. 90. 5806-5825.
- [2] R. Krache et I. Debah, 2011 « Some Mechanical and Thermal Properties of PC/ABS Blends », *Mater. Sci. Appl.*, vol. 02. 404-410
- [3] D. Escobar, E. Mendizabal, et R. González-Núñez, 2008 « Compatibilization of poly(vinyl chloride) and polystyrene blends with poly(styrene- co - n - methylolacrylamide) », *J. Appl. Polym. Sci.*, vol. 110. 297-303
- [4] L. Priya et J. P. Jog, 2003 « Intercalated poly (vinylidene fluoride)/clay nanocomposites: Structure and properties », *J. Polym. Sci. Part B Polym. Phys.*, vol. 41. 31-38.
- [5] B. C. Jang, S. Y. Huh, J. G. Jang, et Y. C. Bae, 2001 « Mechanical properties and morphology of the modified HDPE/starch reactive blend », *J. Appl. Polym. Sci.*, vol. 82. 3313-3320
- [6] S. Tostar, E. Stenvall, M. Foreman, et A. Boldizar, 2016 « The Influence of Compatibilizer Addition and Gamma Irradiation on Mechanical and Rheological Properties of a Recycled WEEE Plastics Blend », *Recycling*, vol. 1. 101-110.
- [7] A. M. Hameed et E. G. Daway, 2015 « Morphology and Mechanical Properties of (Epoxy/PVC) Blend », vol. 11. 7.
- [8] S. Benmesli et F. Riahi, 2014 « Dynamic mechanical and thermal properties of a chemically modified polypropylene/natural rubber thermoplastic elastomer blend », *Polym. Test.*, vol. 36. 54-61
- [9] Y. X. Pang, D. M. Jia, H. J. Hu, D. J. Hourston, et M. Song, 2000 « Effects of a compatibilizing agent on the morphology, interface and mechanical behaviour of polypropylene/poly(ethylene terephthalate) blends », *Polymer*, vol. 41. 357-365.
- [10] Nascimento, W. A. do, Agrawal, P. & Mélo, T. J. A (2019) Effect of copolymers containing glycidyl methacrylate functional groups on the rheological, mechanical, and morphological properties of poly (ethylene terephthalate). *Polymer Engineering & Science* 59, 683–693.
- [11] Wang, J., Li, Y., Song, J., He, M., Song, J. & Xia, K (2015) Recycling of acrylonitrile–butadiene–styrene (ABS) copolymers from waste electrical and electronic equipment (WEEE), through using an epoxy-based chain extender. *Polymer Degradation and Stability* 112, 167–174.
- [12] Da Costa, H. M., Ramos, V. D., da Silva, W. S. & Sirqueira, A. S (2010) Analysis and optimization of polypropylene (PP)/ethylene–propylene–diene monomer (EPDM)/scrap rubber tire (SRT) mixtures using RSM methodology. *Polymer Testing* 29, 572–578

- [13] Graebbling, D., Muller, R. & Palierne, J. F (2002) Linear viscoelastic behavior of some incompatible polymer blends in the melt. Interpretation of data with a model of emulsion of viscoelastic liquids. doi:10.1021/ma00054a011
- [14] Bousmina, M. & Muller, R (1993) Linear viscoelasticity in the melt of impact PMMA. Influence of concentration and aggregation of dispersed rubber particles. *Journal of Rheology* 37, 663–679.
- [15] Hwang IJ, Lee MH, Kim BK (1998) Preparation and properties of SAN/EPDM/CPE ternaryblends. *Eur Polym J* ;34:671–675
- [16] Mélo, T. J. A. de, Carvalho, L. H., Calumby, R. B., Brito, K. G. Q., D’Almeida, J. R. M. & Spieth, E (2000) Propriedades mecânicas e morfologia de uma blenda polimérica de PP/HIPS compatibilizada com SEBS. *Polímeros* 10, 82–89
- [17] Incarnato, L., Scarfato, P. & Acierno, D (1999) Rheological and mechanical properties of recycled polypropylene. *Polymer Engineering & Science* 39, 749–755.
- [18] Tostar, S., Stenvall, E., Foreman, M. R. S. J. & Boldizar, A (2016) The Influence of Compatibilizer Addition and Gamma Irradiation on Mechanical and Rheological Properties of a Recycled WEEE Plastics Blend. *Recycling* 1, 101–110
- [19] Díaz, M. F., Barbosa, S. E. & Capiati, N. J (2005) Improvement of mechanical properties for PP/PS blends by in situ compatibilization. *Polymer* 46, 6096–6101.
- [20] Lourenço, E. & Felisberti, M. I (2006) Photochemical aging of in situ polymerized blends of polystyrene and poly [acrylonitrile-g-(ethylene-co-propylene-co-diene)-g-styrene] (AES). *Polymer Degradation and Stability* 91, 2968–2978.
- [21] Araújo JP, Agrawal P and Mélo TJA (2015) Blendas PLA/PEgAA: Avaliação da reatividade entre os polímeros e da concentração de PEgAA nas propriedades e na morfologia. *Rev Elet Mat Proc*; 10: 118–127.
- [22] Cavanaugh, T. J., Buttle, K., Turner, J. N. & Bruce Nauman, E (1998) The study of various styrene-butadiene copolymers as compatibilisers in bulk blends of polystyrene/polybutadiene. *Polymer* 39, 4191–4197

***Chapter V GENERAL***  
***CONCLUSIONS AND***  
***RECOMMENDATIONS***

**Chapter V.** General conclusions and recommendations**V.1 General Conclusions**

In the present work, attempts were made to develop a polymer with desirable properties by mixing two hard and brittle polymers, PS and SAN, with a triblock SEBS thermoplastic elastomer. Mechanical, thermal and rheological studies, and electron microscopy of blends containing PS with SAN and SEBS, have been carried out in order to elucidate the morphology and characteristics of these blends.

From the result of these investigations, the following conclusions can be drawn:

- 1) PS/SAN blends without compatibilizer exhibit tensile properties and impact strength lower than pure polymers, due to the immiscibility and lack of interfacial adhesion between the two polymers.
- 2) Addition of SEBS as compatibiliser in the PS/SAN blends caused that the blends became compatible. It was found that the tensile modulus and strength of PS/SAN blends decreased with increasing the compatibiliser content because of the rubbery nature of SEBS. The presence of SEBS in the blends system enhanced the interfacial adhesion between PS and SAN phases.
- 3) The elongation at break of the PS/SAN increased very significantly by the addition of SEBS at all composition studied.
- 4) Impact strength showed a similar trend as compared to elongation at break. This indicates that SEBS compatibilizer enhanced the interfacial adhesion and improved the compatibility of the blends.
- 5) The DSC results for blend of PS/SAN confirm the miscibility by recording one glass-transition temperature located between the values of the pure polymers; its value decreases with increasing PS proportions.
- 6) The DSC results for blend system of PS/SAN/SEBS gave a good indications of improvement in state of partial miscibility.
- 7) The SEM results for blend system of PS/SAN at low proportions of PS or SAN show That the minor phase is dispersed in the continuous matrix phase, while for intermediate proportions show co-continuous phases.

- 8) The addition of SEBS copolymers increased the viscosity of all composition at low frequencies suggesting that the reactions between the copolymers and blend was achieved.
- 9) The complex viscosity increased with the increase in the copolymers content. It was also observed that  $G'$  become higher than  $G''$  at low frequencies indicating that a refined morphology was obtained.
- 10) An improvement in compatibilisation and toughness of PS and SAN was achieved through the use of SEBS
- 11) In general the morphological behaviors of polymer blends depend strongly on blend ratios and method of preparation. To satisfy the goal of blend formulation to achieve additive behavior, a machine of high mixing quality must be used.
- 12) The overall variations in all properties suggest that the SEBS copolymer could be used as an effective compatibilizer for the rPS /SAN mixture.

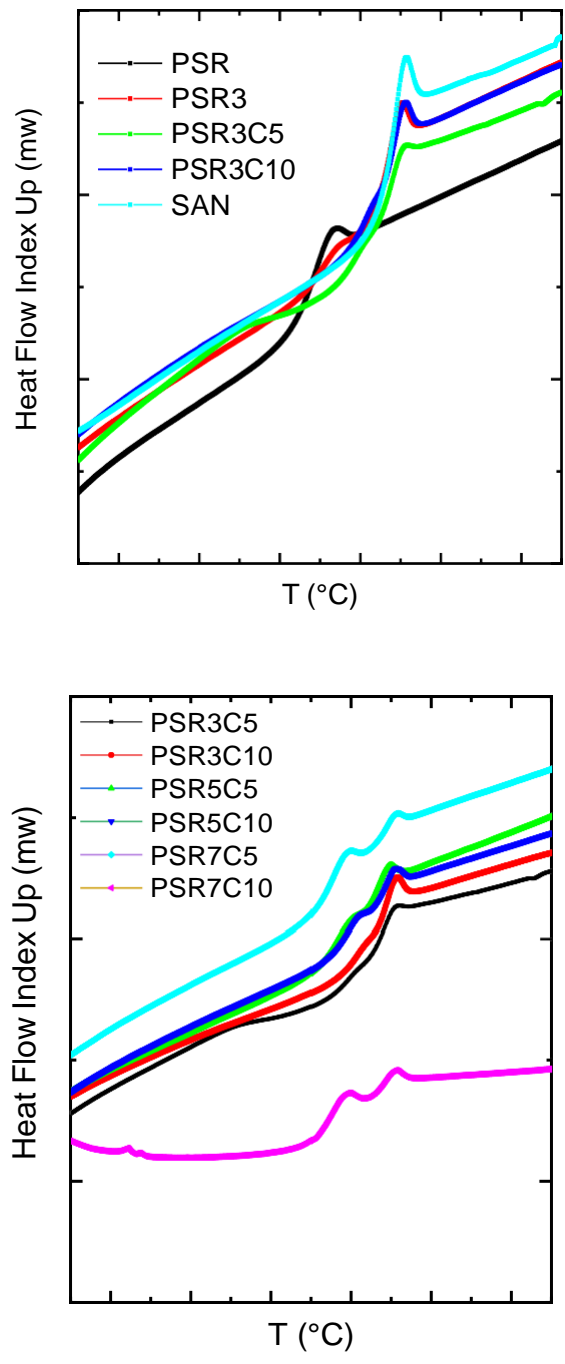


## **V.2 Suggestions for future work**

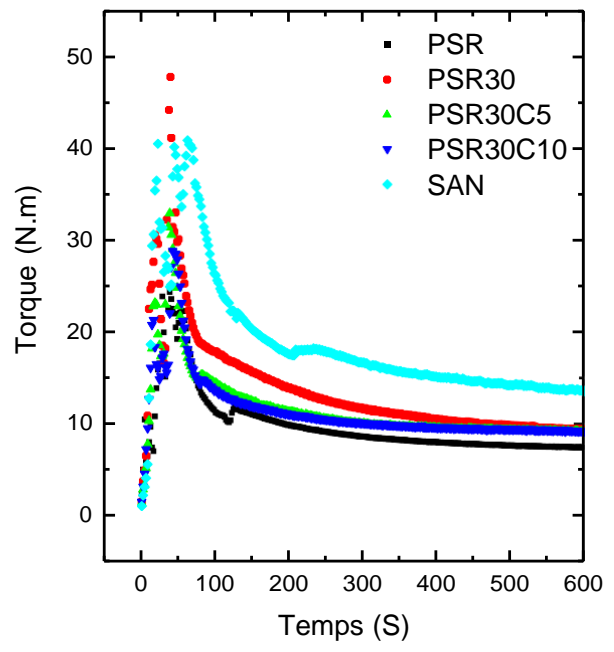
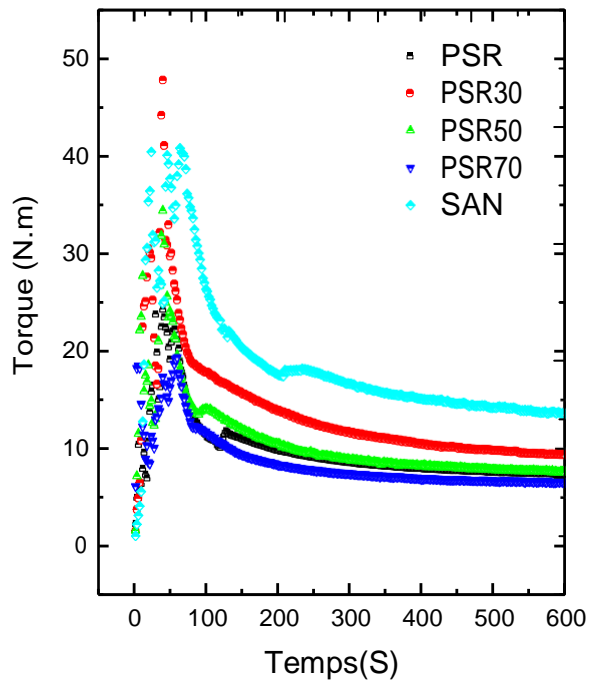
Based on the experience gained during this study, the following recommendations for future work can be made

1. In this thesis, the test result of pristine PS and recycled PS has been analyzed separately. So another possibility of improving the test could be adding raw material or pristine polystyrene with the recycled polystyrene during the recycling process in order to analyze how the mixing can change the properties of the material.
2. Extend the investigation of PS/SAN with different reactive compatibilizer method.
3. Extend the investigation of PS/SAN blend with casting method.
4. The possibilities and suggestions to improve this experiment for the future work has been discussed along with the limitations. First of all, one of the biggest limitation during the experiment was not having good amount of PS recycled as it was quite challenging to collect post-consumer cups. Since PS is a very brittle in characteristics, during the recycling process a fair amount of material has been lost as waste which was realized after starting the process. The number of recycling runs could have increased to at least 3-5times if there was enough material for the test. So in order to do the similar test, it is recommended to start recycling with good enough material considering the wastage fact.

# ANNEXES



**Figure 1.** DSC thermograms of recycled PS/ SAN without and with SEBS compatibilizer.



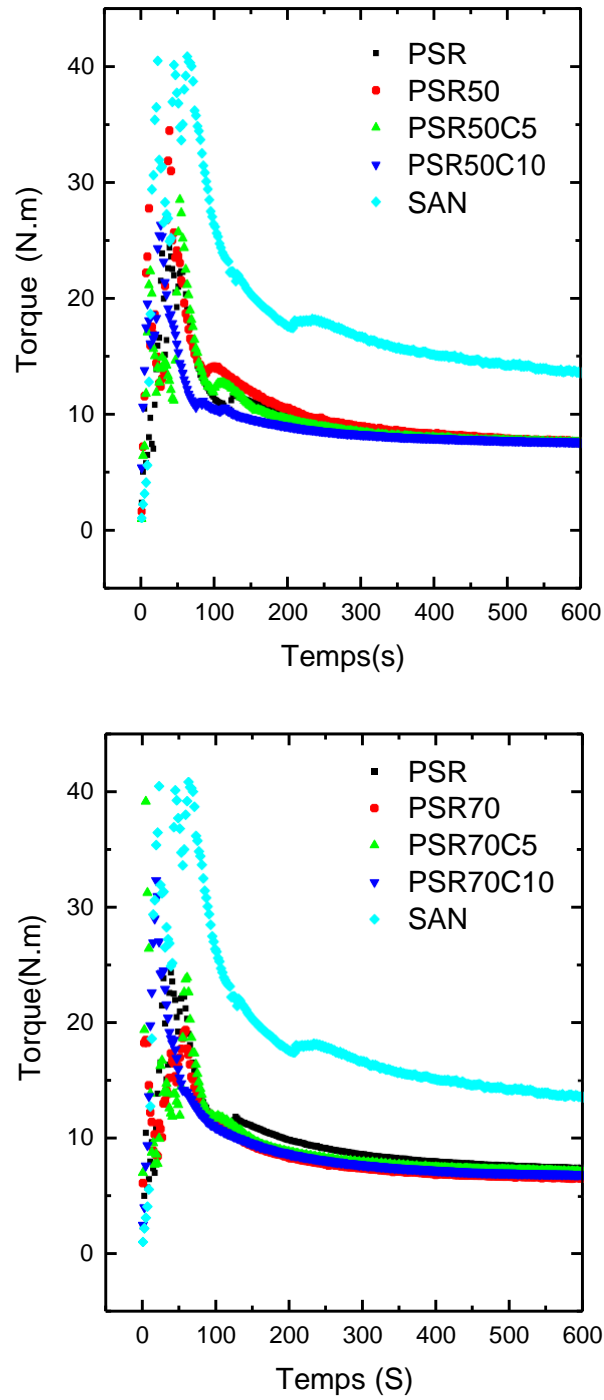


**Figure 2.** Torque vs time data of recycled PS, SAN and RPS/SAN blends without and with compatibilizer.

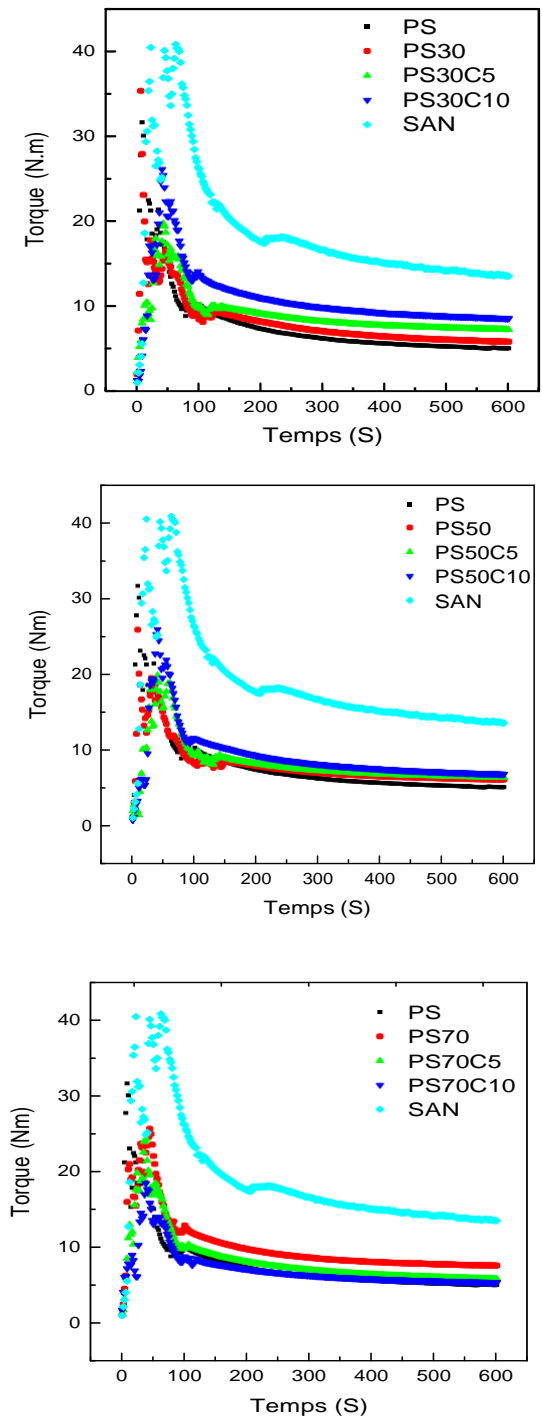


**Figure 3.** Torque vs time data of neat PS, SAN and PS/SAN blends without and with compatibilizer.

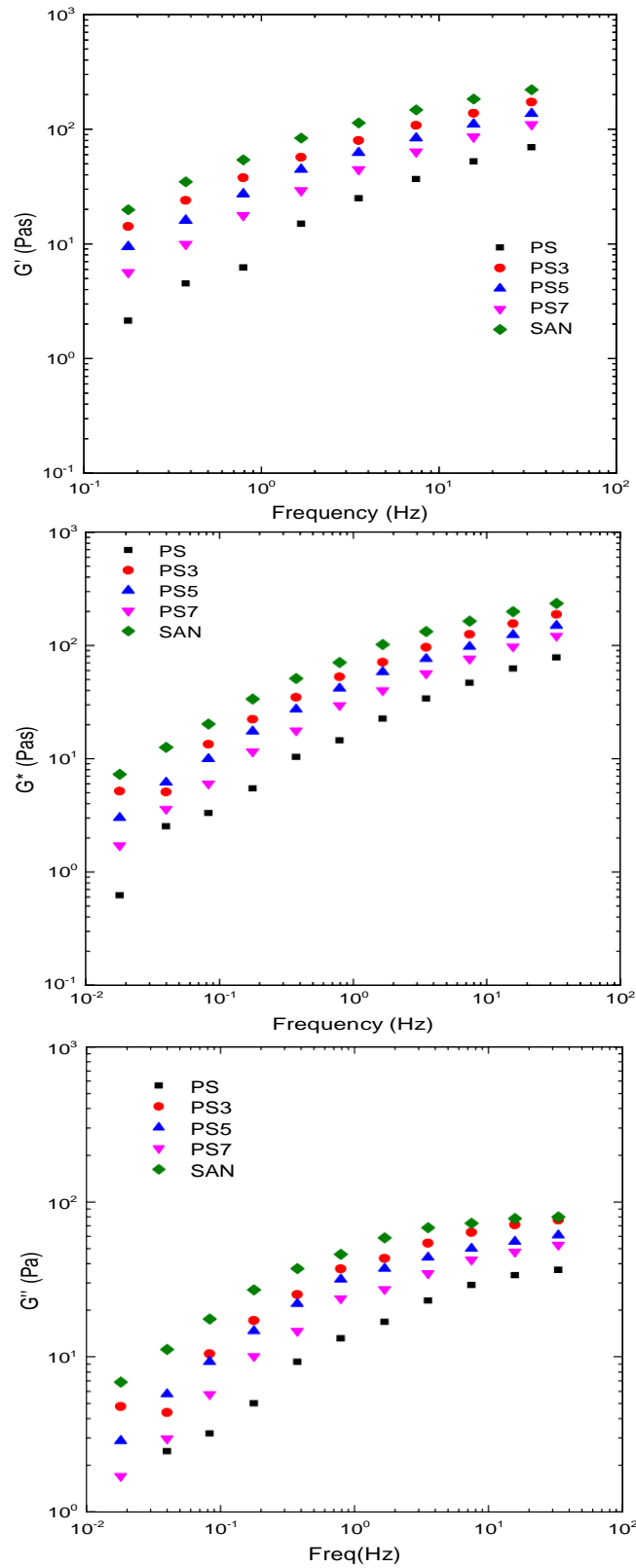


**Figure 4.** Rheological properties of PS, SAN and PS/SAN blends.

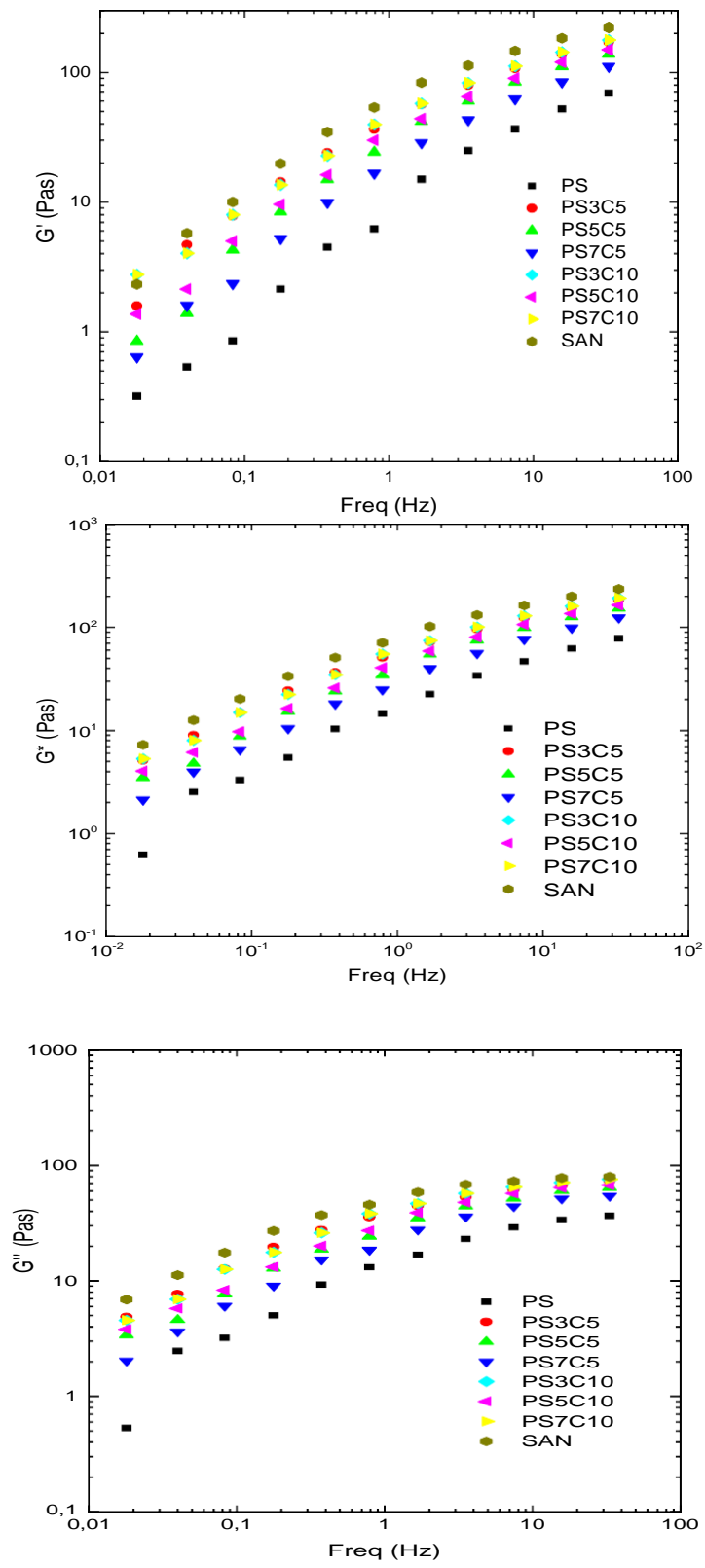


**Figure 5.** Rheological properties of PS, SAN and PS/SAN blends with compatibilizer.



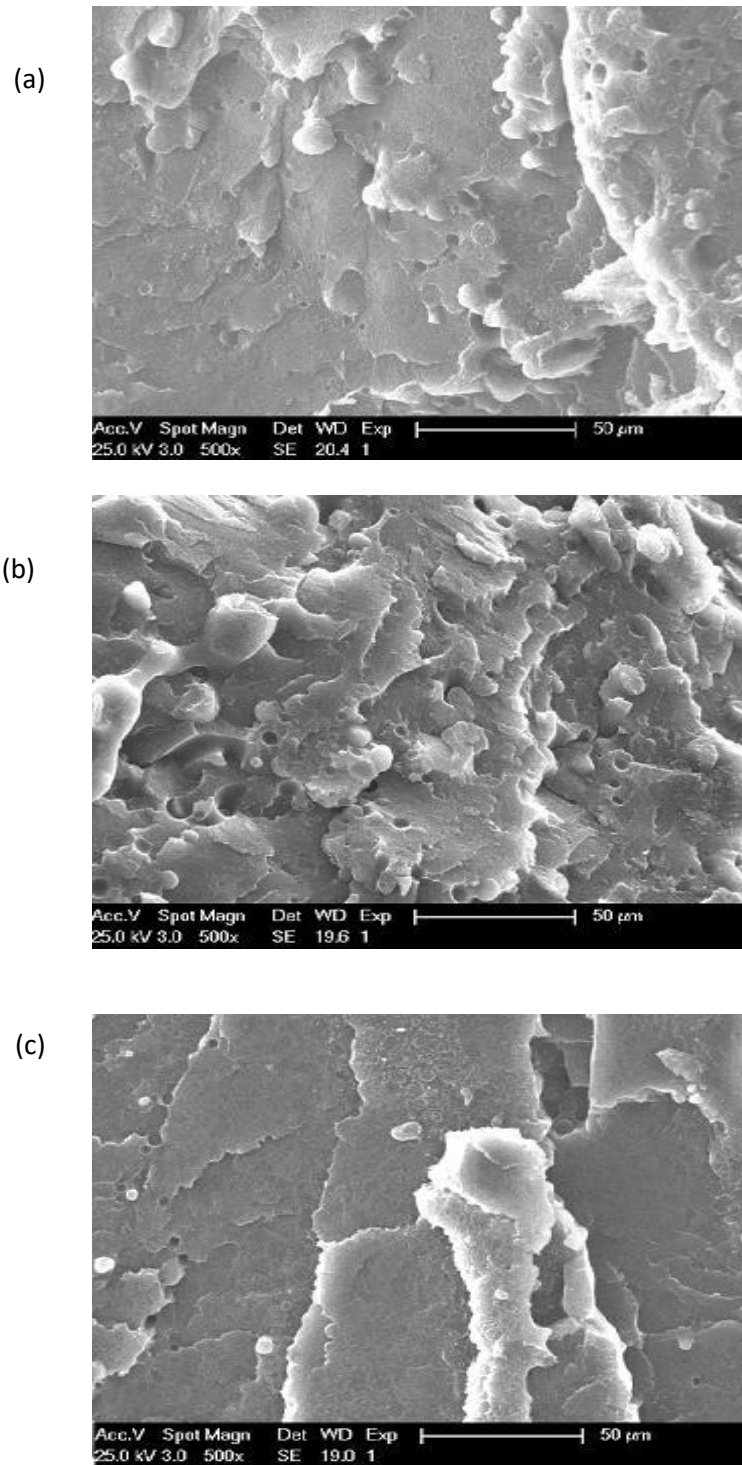


**Figure 6.** SEM micrographs of fractured surface of RPS/SAN5 for the Composition ; a) RPS50, b) RPS50C5, c) RPS50C10.

## Abstract

The thesis involved preparation of polymer blend as two systems, the first polystyrene with styrene acrylonitrile copolymer PS/SAN, rPS/SAN and the second PS/SAN/SEBS prepared by melt compounding in Haake extruder (Brabender). Different composition ratios were used with the aim of arriving at the best physical blending percentage, studied the effect of recycled PS and SEBS compatibilizer.

In order to study the influence of blending on the mechanical properties, rheological, thermal properties and morphology several tests are performed including (tensile, impact resistance, Differential scanning calorimetry and dynamique thermomechanique analysis (DSC, DMAT), optical microscopy and scanning electron microscopy (SEM). It was found that the addition of the compatibilizer increases the mechanical properties, complex viscosity, and thermal stability the results from this work show that properties for blend system PS/SAN at compositions 30/70, 50/50 and 70/30 have mechanical properties much better than the pure constituents. And the mechanical properties for the blend system of PS/SAN with compatibilizer SEBS are better than PS/SAN without SEBS, dependent on the amount of SEBS content, The thermal properties (DSC, DMTA), for blend system of PS/SAN gives good indication of improving state of miscibility for most blend ratios; there is only one glass transition temperature between the two values for pure polymers. The optical microscope and SEM results for both systems fully support the results obtained from the mechanical properties.

**Keywords:** Mechanical properties recycled Polystyrene, PS/SAN, DSC, Compatibilization.

## Résumé

Ce travail porte essentiellement à la préparation d'un mélange de polymères sous forme de deux systèmes, l'un est le polystyrène avec un copolymère de styrène acrylonitrile (PS/SAN, rPS/SAN) sans compatibilisant et l'autre avec l'ajout du SEBS. Ont été préparé par malaxage à l'état fondu à l'aide d'un mélangeur interne (Brabender), l'effet de la composition des mélanges du PS/SAN sans et avec agent compatibilisant SEBS a été suivi par des tests dont (traction, résistance aux chocs, calorimétrie différentielle à balayage et analyse thermomécanique dynamique (DSC, DMAT), microscopie optique et microscopie électronique à balayage (SEM). Il a été trouvé que l'ajout de SEBS augmente les propriétés mécaniques, la viscosité complexe et la stabilité thermique, les résultats de ce travail montrent que les propriétés du système de mélange PS/SAN avec les compositions 30/70, 50/50 et 70/30 ont des propriétés supérieures par rapport aux polymères purs. Les propriétés thermiques (DSC, DMTA), pour le mélange PS/SAN, donnent une bonne indication de l'amélioration de l'état de miscibilité des compositions de mélange; il n'y a qu'une seule température de transition vitreuse entre les valeurs des deux polymères. Les résultats de (SEM) propriétés pour les deux systèmes confirment les résultats des propriétés mécaniques obtenus.

**Mots-clés:** propriétés mécaniques, polystyrène recyclé, PS/SAN, DSC, compatibilisation.

## ملخص

حضرت ج انسابت حوضهش فرض ح خيطت نايونيت اويوش بهيت ظهري ، اوطب الوه اوي من خياش او اوتل PS ع وده امشور خال ج سخايش (SAN) اوي بيوسيت بيوطب اشب فق حوضه خيط وده اوي من خياش او اوتل PS (او RPS) ع وده SAN) بيصنيت عي انخبس SEBS. حوضهش فرض ح بلسطت هميت Haake extruder (Brabender). ح الخيط بهسرب وحشام فرض خيتت يشع الحطيه عي افصرو سرب خيط نيفسايوت. ومزول دسارت حلتش ابي من هوش ٠ اوعيد حذوش (rPS) وعي انخبس SEBS ن ايفس ح (PS/SAN).

والخو دسارت حلتش افصرا ن اخباص اناونب ٠ ن اخباص الحساسيت و اوبوت و الشينيت اخش ج عده نحى طبت ش ووج) قوريت انظوت - اشذ - اشعش اشعش انقبضيت - افحص اندهشي انضيت - و اندهش النخشو اشعش .

اظهشيت ٠ خيواح فحوض اويويك اناونب ٠ ن بيوطب الوه ا سرب الخيط (00/00, 00/00, 00/00) خيول خيطيئ نيفسايوت (اويوضوت والس خيول اوحساسيت) افصرو ٠ اوتاد الطيوت ويو اويخيط. مزول بي ج خيواح فحوض اويويك اناونب ٠ ن بيوطب اوتد ٠ اوتد اويوضوت بيخلاق SEBS حلت ا اصبنت هزا الخيوش اوي فرض ح اويوشات سوح بيخس ٠ ٠ خيول اويخيطنض ومزول الخيواح بي انخط Mixture. ٠ خاله خيواح افحص) بيوسعش الحساسيت اويخيطي٠ (اظهشيت ٠ خيواح هزا افحص حوق ال خيواح بيوسيت بيوطب اوتد ٠ اوتد اصبنت عي انخبس SEBS خيولت بيوسيت بيوطب فرض ح) SAN 70/ PS00) وريول ع طشق مسدي و دسخت اخبه مبخخيت واحده حو حيت و سرت

فيسوت ع دسخت ال اخبه الضبخه نزال اويديع ٠. مزول اظهشيت ٠ خيواح هزا افحص حطيه ظهشة ال خيواح اندهش بيونيوت خيوط اوطب اوتد ٠.

اوي خيواح افحص بيخعنه اندهش اويوش و اويدهش الينخشو ٠ اشعش نفا دع ج وبطسة مبهشة ٠ خيواح ايفحص اناونب ٠ ن نزال اويخيطي٠. **كلمات مفتاحية:** اويخيطيئ اناونب ٠ ن ابي من هوش ٠ اوعيد حذوش ٠ فرض ح PS/SAN, DSC, اويخلاق.

PAPER

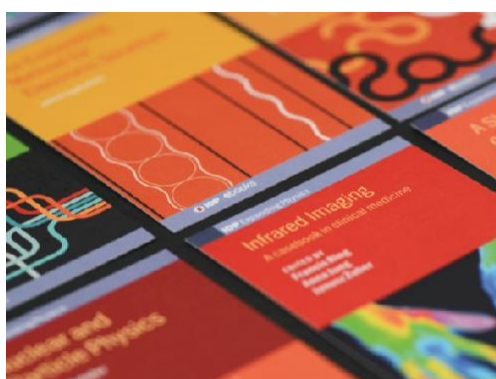
# The effect of compatibilizer SEBS on the mechanical, morphological and thermal properties of the polystyrene/poly (styrene-co-acrylonitrile) copolymer blends

## Recent citations

- [From Disposal to Technological Potential: Reuse of Polypropylene Waste from Industrial Containers as a Polystyrene Impact Modifier](#)  
Carlos Bruno Barreto Luna *et al*

To cite this article: Khaled Bedjaoui *et al* 2019 *Mater. Res. Express* **6** 105334

View the [article online](#) for updates and enhancements.



**IOP ebooks™**

Bringing together innovative digital publishing with leading authors from the global scientific community.

Start exploring the collection—download the first chapter of every title for free.



## PAPER

# The effect of compatibilizer SEBS on the mechanical, morphological and thermal properties of the polystyrene/poly (styrene-co-acrylonitrile) copolymer blends

RECEIVED

14 June 2019

REVISED

27 July 2019

ACCEPTED FOR PUBLICATION

6 August 2019

PUBLISHED

23 August 2019

Khaled Bedjaoui<sup>1</sup>, Rachida Krache<sup>1</sup>, Angel Marcos-Fernández<sup>2</sup> and Melia Guessoum<sup>3</sup><sup>1</sup> Process Engineering Department, Laboratory of Multiphase Polymeric Materials (LMPMP), Faculty of Technology, University Ferhat Abbas Sétif-1, Algeria<sup>2</sup> Institute of Polymer Science and Technology, CSIC, C/Juan de la Cierva 3, 28006 Madrid, Spain<sup>3</sup> Process Engineering Department, Laboratoire de Physico-chimie des hauts Polymères (LPCHP), Faculty of Technology, University Ferhat Abbas Sétif-1, Algeria

E-mail:

[khaledbedjaoui@gmail.com](mailto:khaledbedjaoui@gmail.com)

Keywords: PS/SAN blend, compatibilization, SEBS, mechanical properties, thermal stability,

morphology

## Abstract

In this study, the effect of styrene-*b*-(ethylene-co-butylene)-*b*-styrene (SEBS) as compatibilizer on polystyrene/poly(styrene-co-acrylonitrile) copolymer (PS/SAN) blends was investigated. For this purpose, blends of various compositions with different content of compatibilizer were prepared by melt blending using a co-rotating twin-screw extruder, and their physical properties, namely the mechanical properties including tensile and impact tests, thermal properties by differential scanning calorimetric (DSC) and thermal stability by thermogravimetric analysis (TGA), studied. Morphological observations using scanning electron microscope (SEM) and viscoelastic properties using dynamic mechanical thermal analysis (DMTA) were also carried out. The results revealed that the mechanical properties were highly improved due to the addition of SEBS which allowed the increase of the blend ductility by enhancing the elongation at break and impact strength. SEM micrographs revealed that the droplet-matrix microstructure was notably refined and the droplets size decreased from 6.7  $\mu\text{m}$  to 2.37  $\mu\text{m}$  in the presence of the compatibilizer. DSC results showed a single glass transition temperature ( $T_g$ ) for the composition PS/SAN (30/70) compatibilized with 5 and 10% wt of SEBS which confirms the compatibilization of the blend for these compositions.

## 1. Introduction

Blending of polymers provides an efficient way to achieve useful combinations of the individual attributes of the neat components, thus avoiding the need to synthesize new polymers [1, 2]. One of the most important commercial plastic nowadays is polystyrene (PS). This polymer is actually widely used in automobile industry, household and electrical/electronic appliances [3] as

well as in the manufacture of packing containers [4, 5]. In order to improve PS properties, particularly its impact resistance,

the polymer has been compounded with several other materials. In this context, Buthaina and Karrer [6] investigated the tensile and thermal properties of the blend formed from PS and acrylonitrile/butadiene/styrene (ABS) copolymer that they prepared by melt blending in a single screw-extruder with various compositions. The results revealed better mechanical properties for the blend system than those of the neat polymer. The thermal study also showed a single glass transition temperature thereby confirming the complete miscibility of the blend. Furthermore, Nina *et al* [7] observed improvements in the impact strength of compatibilized PS/polybutadiene (PB) blends prepared by solvent casting technique. Similarly, Joseph and Thomas [8] studied the influence of PS/PB blend ratio on their morphology and mechanical properties.

The blend formed from polystyrene (PS) and SAN (styrene-acrylonitrile) is an important material because it combines the desirable properties of PS such as good processability, rigidity and low cost [9] with the high

thermal stability and good mechanical properties of SAN [7, 10, 11]. However, most polymers are immiscible and the PS/SAN blend is not an exception [12]. PS/SAN blend exhibits a poor interfacial adhesion which causes heterogeneous morphology, weak dispersion, phase separation and weak mechanical properties (low tensile strength, modulus and ductility) [13, 14]. Therefore, in order to improve the PS/SAN blend miscibility and achieve better properties, the compatibilization process is usually necessary [15, 16]. Yang *et al* [3] studied the compatibility of PS/SAN blend and the results indicated an upper critical solution temperature (UCST) behavior for PS/SAN (49/51) blend containing 20% of acrylonitrile with a 171.8 °C of UCST temperature.

Fowler *et al* [17] studied the effect of mixing technique and sequence on the distribution of core-shell impact modifier particles, methacrylated butadiene-styrene (MBS) type, in a two-phase PS/SAN blend and found that the MBS particles are located exclusively in the SAN phase or lined up at the interface. Hyun *et al* [18] investigated the properties of the blend consisting of syndiotactic PS and polystyrene-block-poly(ethylene-co-butylene)-block-polystyrene (SEBS) triblock copolymer. This study revealed that the morphology and impact and tensile properties were greatly affected by SPS block ratios and the molecular weight of SEBS.

SEBS has also been used as an effective compatibilizer for many polymers blends including PS or SAN. This copolymer acts at the interface between the polymeric phases, reduces the interfacial tension and stabilizes the morphology by diminishing the coalescence phenomena which results in a finer dispersion of the dispersed phase into the matrix [17, 19–25]. Xu *et al* [26, 27] used SEBS as compatibilizer for PS and low density polyethylene (LDPE) blend. They reported that the mechanical properties melt rheological behavior, deformation, and toughening of PS/LDPE have been extensively affected by the SEBS ratio into the blend.

Correspondingly, Taha and Frerejean [27] compatibilized the PS/LDPE blend using SEBS and styrene/ethylene-butylene (SEB). They reported that the finest and more stable dispersion are obtained with diblock copolymer. Li *et al* [28] observed also that both SEB and SEBS copolymers efficiently reduce the PS domain size. Schwarz *et al* [29] used SEBS to compatibilize the immiscible blend of high density polyethylene (HDPE) and a copolymer of PS and polyether. Yin *et al* [30] investigated the effect of SEBS on PC/SAN blends and concluded that the addition of SEBS increases the Izod notched impact strength and the elongation at break however it decreases the tensile and flexural strengths.

Regarding the high effectiveness of SEBS triblock copolymer in increasing the respective PS and SAN mixtures mechanical properties and also in refining their morphologies, it seems that, it should be also an efficient component for compatibilizing the binary mixture of both polymers. So, this work proposes to investigate the effect of the addition of SEBS triblock copolymer as compatibilizer for PS/SAN blends. The motivation is the existence of a similar structure between the blend matrix and SEBS which contains segments chemically identical to those of PS and SAN phases. The improvement in the interaction between both phases would lead to an improvement in the mechanical properties of the blends that would allow the recycling of PS and SAN, the two most common polymers found in electronic plastic waste.

There is not research work in the literature that reports on the study of the effect of SEBS as compatibilizer on the morphological, mechanical and thermal properties of PS/SAN blends. Hence, in this study, the compatibilizer SEBS will be added at different concentrations. The microstructure will be investigated by analyzing the SEM images to determine the SEBS distribution into the PS and SAN phases and its effect on the blend morphology. Also, to verify if the mechanical properties have been improved, tensile and impact tests will be performed.

Finally, to determine the impact of the addition of SEBS on the two phases (PS and SAN), their glass transition regions will be characterized by both viscoelastic and thermal analyses.

## 2. Experimental

### 2.1. Materials

The used polystyrene has the trade name GPPS 1540 and was obtained from Total petrochemical, Belgium. PS has the following characteristics: density:  $1.05 \text{ g cm}^{-3}$ ,  $M_w = 300,000$ ,  $M_n = 87,000$ ;  $M_w/M_n = 3.4$ ). The poly(styrene-co-acrylonitrile) (SAN) has the trade name Luran 368 R and contains 22 wt% of acrylonitrile (AN). It was supplied by BASF, Germany, has a density of  $1.08 \text{ g cm}^{-3}$  and a melt flow rate (MFI) of 11 g/10 min). The SEBS triblock copolymer is a Kraton G 1651 product supplied by Kraton Polymer (USA). It has a molecular weight of  $20,000 \text{ g mol}^{-1}$  and a styrene content of 28 wt%.

### 2.2. Melt blending

Prior to processing, the neat polymers PS, SAN were dried at  $80 \text{ }^\circ\text{C}$  and  $100 \text{ }^\circ\text{C}$ , respectively, overnight in a vacuum oven. Uncompatibilized and compatibilized PS/SAN blends of various compositions were prepared. The uncompatibilized mixtures contain 0, 30, 50, 70 and 100 wt% of SAN and are denoted respectively as PS, PS30, PS50, PS70, and SAN. The compatibilized blends consist of the same contents of PS and SAN with 5 and 10 wt% SEBS and are denoted according to the same designation but with C5 or C10 termination, respectively.



Table 1. Compositions of blends

Samples	Composition (wt%)		
	PS	SAN	SEB
	S		
PS <sub>30</sub>	30	70	—
PS <sub>50</sub>	50	50	—
PS <sub>70</sub>	70	30	—
PS <sub>30</sub> C5	30	70	5
PS <sub>50</sub> C5	50	50	5
PS <sub>70</sub> C5	70	30	5
PS <sub>30</sub> C10	30	70	10
PS <sub>50</sub> C10	50	50	10
PS <sub>70</sub> C10	70	30	10

The melt-blending was performed in a Brabender® (GmbH & Co. KG, Duisburg, Germany) internal mixer, allowing the monitoring of the torque versus temperature curves for each formulation. The mixing was operated at 210 °C during 10 min and at a rotor speed of 50 rpm. At the start, PS and SAN were allowed to soften for 2 min then SEBS was added thereafter. At the end of the mixing process, the molten mixtures were removed from the chamber, cooled then pelletized. Samples for the mechanical and viscoelastic characterizations were compression-molded at 200 °C for 8 min in a preheated hydraulic press. The blends compositions are summarized in table 1.

### 2.3. Characterization

#### 2.3.1. Scanning electron microscopy (SEM)

Cryogenically fractured surfaces of PS/SAN blends specimens were observed, after gold-coating, by scanning electron microscopy using a Hitachi S-27100 (Japan) electron microscope operated at 15 kV. The average diameter and volume  $R_n$  and  $R_w$ , respectively, of the cross-section particles were evaluated by measuring and counting at least 100 particles from the PS/SAN and PS/SAN/SEBS blends micrographs. The calculation of the particles average number and volume diameter values was performed using the following equations (1) and (2) [31]:

$$R_n = \sum n_i * R_i / \sum n_i \quad (1)$$

$$R_w = \sum n_i * R_i^3 / \sum n_i * R_i^2 \quad (2)$$

Where  $n_i$  is the number of droplets 'i' of diameter  $R_i$ .

#### 2.3.2. Thermal properties

Differential scanning calorimetry (DSC) measurements were carried out in a Perkin Elmer DSC 8500 instrument connected to a liquid nitrogen cooling accessory with a nitrogen purge. For the DSC scans, roughly 10 mg of each sample were used under the following conditions: temperature range: 40 °C–150 °C; heating rate: 20 °C min<sup>-1</sup>.

Dynamic mechanical analysis (DMA) was carried out in a TA Q800 Instrument. The scans were carried out from -100 °C to 140 °C at a constant heating rate of 4 °C min<sup>-1</sup> and at a frequency of 1 Hz.

Thermogravimetric analysis (TGA) was performed on TA Q500 apparatus under nitrogen



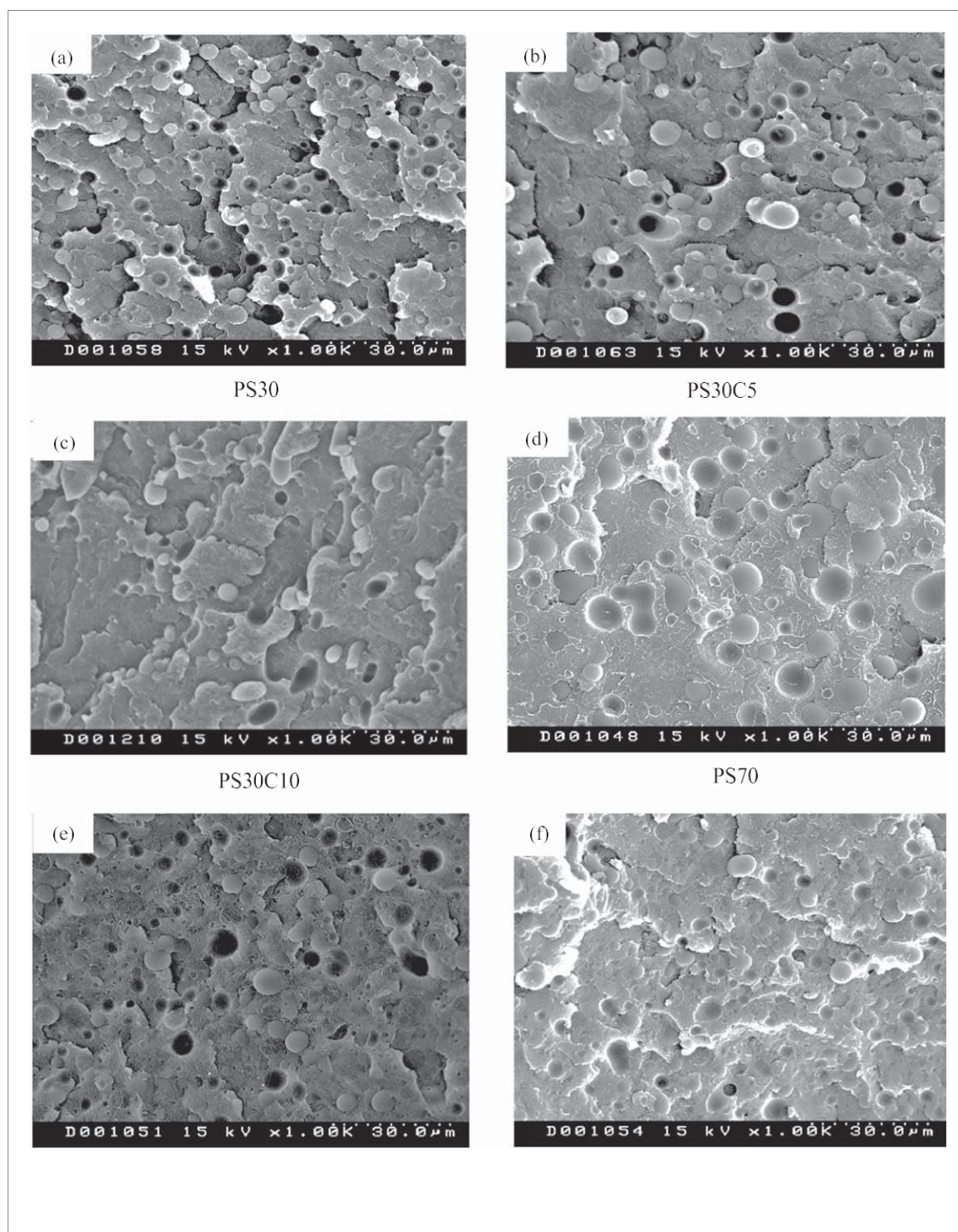
atmosphere. Samples of 5–9 mg weight were heated from 25 °C up to 600 °C in Hi-Resolution mode with an initial heating rate of 10 °C min<sup>-1</sup>.

### 2.3.3. Mechanical

*testing*

The tensile behavior of the samples was evaluated using a Universal Testing Instron 4301 (USA) machine. At least seven specimens for each formulation were tested at a cross-head speed of 10 mm min<sup>-1</sup>. Young's modulus, tensile strength and elongation at break were determined, and the average values were calculated then reported.

Notched Izod impact test was performed at room temperature using a resil impactor (Ceast 6548). Five replicates of each composition were tested and the average values were recorded to check the good reproductibility of the experiment.



### 3. Results and discussion

#### 3.1. Microstructure

analysis

Morphology of polymer blends depends on several factors such as the composition, the mixing conditions and the interfacial tension between the mixed polymers. Figure 1 exhibits the microstructure of PS30 and PS70 blends prepared without and with 5 and 10 wt% of SEBS as compatibilizer. Also, table 2 reports the values of  $R_{nd}$  and  $R_w$  as determined for uncompatibilized and compatibilized PS30 and PS70 blends using Image J analyzer.

The micrographs of figures 1(a)–(f) showed a droplet/matrix two-phase morphology typical of immiscible polymer blends. The PS phase in PS30 blends was dispersed as spherical domains

with a droplet size of  $1.70\ \mu\text{m}$  which seems to be the result of the interplay between the mixture composition, the mixing conditions, the existing interfacial tension and finally the system rheology [32]. After adding 5 and 10 wt% of SEBS, the PS droplet size decreased significantly to attain  $5.52$  and  $2.37\ \mu\text{m}$ , whereas  $R_w$  presented values of  $13.86$  and

Table 2. Average size of holes in SEM morphology of the blend analysed with ImageJ software.

Composition	R <sub>n</sub> ( $\mu\text{m}$ )	R <sub>w</sub> ( $\mu\text{m}$ )
PS <sub>30</sub>	3.70	10.69
PS <sub>30</sub> C5	5.52	13.86
PS <sub>30</sub> C10	2.37	10.57
PS <sub>70</sub>	7.58	13.14
PS <sub>70</sub> C5	4.50	9.71
PS <sub>70</sub> C10	3.43	8.57

Table 3. Mechanical properties of the uncompatibilized and compatibilized PS/SAN blends.

Samples	Tensile strength (MPa)	Tensile modulus (MPa)	Elongation at break (%)	Impact strength (kJ m <sup>-2</sup> )
SAN	51 ± 4	3140 ± 50	2 ± 0.2	11 ± 1
PS <sub>30</sub>	28 ± 3	3010 ± 80	1.1 ± 0.04	3.2 ± 0.7
PS <sub>50</sub>	30 ± 4	3150 ± 90	1.06 ± 0.06	3.1 ± 0.1
PS <sub>70</sub>	22 ± 2	3040 ± 70	0.8 ± 0.01	2.6 ± 0.9
PS	30 ± 1	2920 ± 40	1.2 ± 0.03	2.9 ± 1.3
PS <sub>30</sub> C5	29.4 ± 0.7	2800 ± 90	3.0 ± 0.2	4.1 ± 0.9
PS <sub>50</sub> C5	23.5 ± 0.6	2720 ± 60	2.1 ± 0.04	3.4 ± 0.5
PS <sub>70</sub> C5	27 ± 6	2690 ± 90	1.2 ± 0.1	3.1 ± 0.7
PS <sub>30</sub> C10	27 ± 4	2400 ± 60	4.7 ± 0.9	5.2 ± 0.4
PS <sub>50</sub> C10	21 ± 0.8	2180 ± 80	4.2 ± 0.8	3.8 ± 0.7
PS <sub>70</sub> C10	21. ± 1	2320 ± 70	1.7 ± 0.5	3.5 ± 0.8

10.57  $\mu\text{m}$ , respectively. Similarly, the PS70 blends showed a considerable morphology refinement as the SEBS concentration increases. The SAN droplet size decreased from 7.58 for the uncompatibilized blend to 4.50 and 3.43  $\mu\text{m}$  for the blends compatibilized, respectively by 5 and 10 wt% of SEBS. At the same time, R<sub>w</sub> declined from 13.14 for the blend without SEBS to 9.71 and 8.57  $\mu\text{m}$  for the blends with 5 and 10 wt% of the compatibilizer. The evident reduction in the droplet size of PS and SAN with increasing the SEBS concentration resulted from the decrease in the interfacial tension which is expected to be caused by the localization of the SEBS molecules at the interface between the droplets and the matrix.

### 3.2. Mechanical properties

#### 3.2.1. Tensile properties of PS/SAN blends

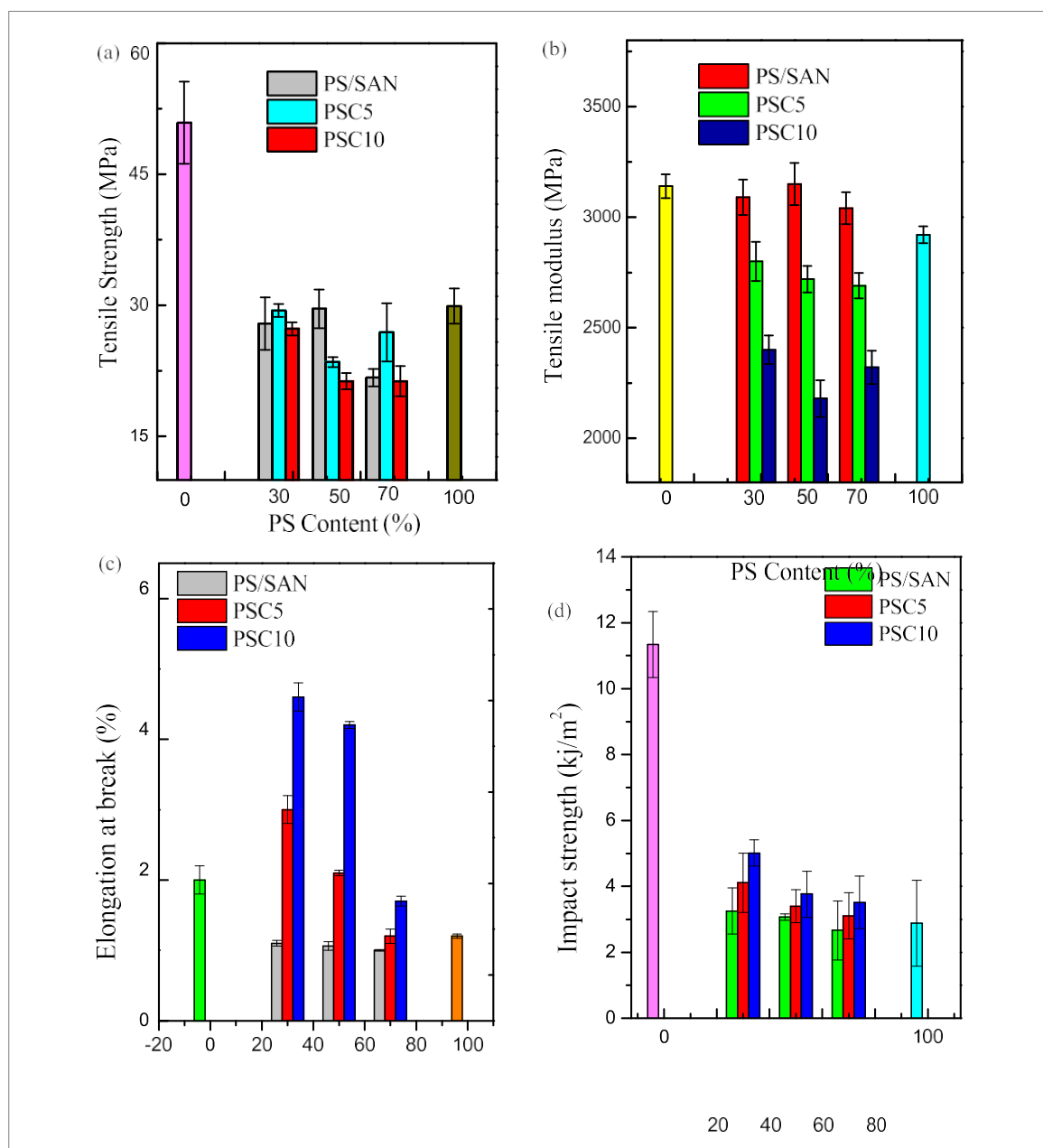
The assessment of the mechanical behavior of blends is considered as the more crucial parameter to conclude about the compatibilizing effect. Generally, immiscible blends show poor mechanical properties due to the weak interfacial adhesion between the components [33]. The results of tensile test including tensile strength, tensile modulus, and elongation at break and those of impact strength for PS/SAN blends are summarized in table 3. It can be seen that the mechanical properties of SAN are higher than those of PS.

Figures 2(a)–(c), shows the variation of PS/SAN blends tensile properties as a function of both blend ratio and compatibilizer content. As expected, PS and SAN are immiscible and did not show any improvement in the mechanical properties for the whole studied compositions. This may be due to the weak interfacial adhesion between the PS and SAN phases [34], which induces a poor

stress transfer between the two phases of the blends [35].

From figure 2(a), it can be seen that the tensile strength of PS/SAN blends As seen in the table 3 the values of tensile strength of the uncompatibilized blends is higher than compatibilized ones. After the addition of 5 wt% of SEBS, the tensile strength of the PS/SAN blend exhibits a slight increase, especially, for the PS30, PS50 and PS70 mixtures. This result is attributed to the favorable intermolecular interactions between PS/SAN, which is originated from their structural similarity and expected compatibility between the PS and SAN matrix phases and the compatibilizer segments [36]. However, the addition of 10 wt% of compatibilizer produces a lower tensile strength compared to the sample with 5 wt% of SEBS. This could be explained by the eventual effect of SEBS micelles in the blend when was added with higher concentration

The evolution of the PS/SAN blends tensile modulus as a function of both the PS and SEBS contents is displayed in figure 2(b). The tensile modulus of the pure PS and SAN are 2920 MPa and 3140 MPa, respectively. The tensile modulus of uncompatibilized mixtures show higher values than that of the PS due to the contribution of the SAN phase and to the fact that the tensile modulus is closely related to the harder domain of the material [37]. After adding SEBS, the tensile modulus shows a sharp decrease and it is observed that the



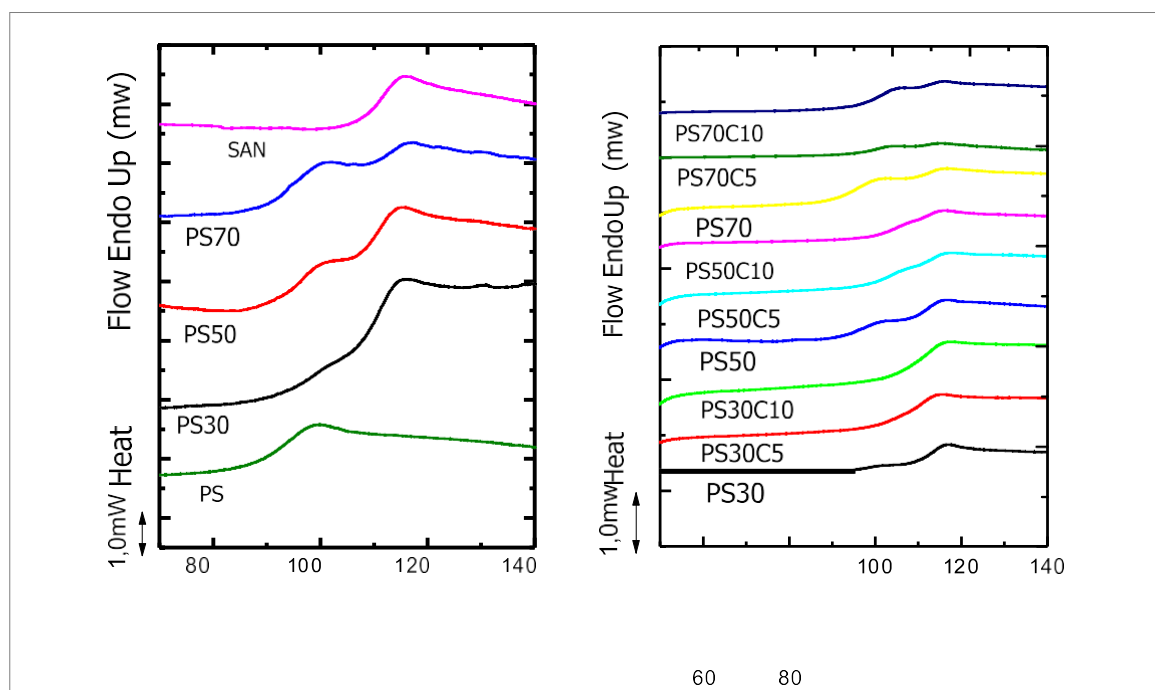
higher the SEBS content, the lower are the blends moduli. The tensile strength and tensile modulus of the PS/ SAN blends are found to be negatively affected by the addition of SEBS due to the elastomeric nature of the later. Thus, the incorporation of soft moléculés belonging to an elastomer compatibilizer as it is the case of SEBS triblock copolymer which plays a major role in improving the blend ductility by inducing a transition from a brittle behavior of the incompatible mixture to a more ductile one. This is due to better interphase adhesion and the rubbery nature of the compatibilizer. As revealed in literature by la Mantia *et al* [38], the SEBS is able of reducing the brittleness of at least one of the two phases and locates selectively at the interface.

Figure 2(c) shows the variations of the elongation at break as a function of both the blend ratio and SEBS content. It can be observed that the elongation at break of uncompatibilized blends shows lower values compared to the pure components and it increases as the SAN contribution in the mixture increases. As SEBS is added, the blends ductility is favored and an enhancement of the elongation at break is registered, particularly for 10 wt% of the compatibilizer as shown in table 3. These results confirm the effectiveness of SEBS as a compatibilizer for PS/SAN blends and fit well with those found by other researchers [39] who have reported that the elongation at break shows a positive deviation for the composition 25/75, thus indicating some favorable

interactions between the component of blend .

### 3.2.2. *Impact strength of PS/SAN blends*

The notched Izod impact strength is used to evaluate the toughness of the samples. The variations of the impact strength for PS/SAN blends before and after the incorporation of SEBS are shown in figure 2(d). Like for tensile



properties, the impact strength of SAN is higher than that of PS and as expected, the uncompatibilized blends reveal lower impact strength values than those of the neat polymers, due to the mixtures immiscibility. After the blend compatibilizing, the impact strength increases for both 5 to 10 wt% of SEBS. The increase is more prominent for the composition PS30 containing 10 wt% of SEBS and more SAN. This demonstrates that the adhesion between the PS dispersed phase and the SAN matrix phase has been notably increased and that the stress is actually more efficiently transferred from one phase to the other. Also, this confirms that SEBS triblock copolymer is very effective for overcoming the brittleness of the uncompatibilized PS/SAN blend and for inducing a more energy dissipative process which is reflected in a more ductile behavior of the blends, as also concluded from the tensile test.

### 3.3. Thermal behavior of the blends

To ascertain the immiscibility and study the thermal properties of PS/SAN blends, DSC and DMA analyses have been performed (figures 3 and 4, respectively) and the glass transition temperatures of PS and SAN in both uncompatibilized and compatibilized have been determined (table 4). A miscible system blend normally exhibits a single  $T_g$  characteristic of a unique phase system, whereas, a two phase-separated blend exhibits two glass transitions. As determined from DSC, neat PS and SAN exhibit  $T_g$  values around 93 °C and 111 °C, respectively, while from the variations of the loss modulus or damping factor ( $Tan \delta$ ), higher values are obtained and they are about 102 and 118 °C for PS and SAN, respectively. This difference may be attributed to the different nature of the response of the sample toward DSC and DMA analysis conditions [40].

After melt blending without compatibilizer, the DSC thermograms showed that all the blends compositions PS30, PS50 and PS70 exhibited two distinct  $T_g$  values slightly different from those of the neat PS and SAN phases, thus suggesting the immiscible nature of the blend. Indeed, the  $T_g$  values of PS and SAN phases, particularly for PS50 and PS70, have changed probably due to the occurrence of interactions between the PS and SAN phases. However when the SEBS was added to blend with 5 and 10 wt %, a slight shift toward higher and lower temperature for both PS and SAN respectively. The same trend is observed for the DMA analysis, which pointed out that the closeness of the PS and SAN  $T_g$  values caused the merging of the glass transition peaks as an indication of a



somewhat blend compatibility.

SEM photographs demonstrate the existence of a two phase morphology and therefore, the existence of a single Tg can be only explained by the impossibility to detect the Tg of the PS phase, due probably to the sum of the facts that the low content of PS makes the change in calorific capacity small (as seen for PS30) and that the improvement on the interfacial adhesion produced by the compatibilizer increases slightly the Tg value for PS phase and probably makes it wider which makes it difficult to distinguish the transition.

#### 3.4. Thermal stability of PS/SAN blends

Thermogravimetry (TG) was performed to estimate the effects of the compatibilizer on the thermal stability and thermal decomposition behavior of PS/SAN blends. The TG and DTG curves giving, respectively, the weight variations with temperature and its derivative, versus time for PS, SAN and their uncompatibilized and compatibilized PS/SAN blends are shown in figure 5. The thermal decomposition values are listed in table 5. It

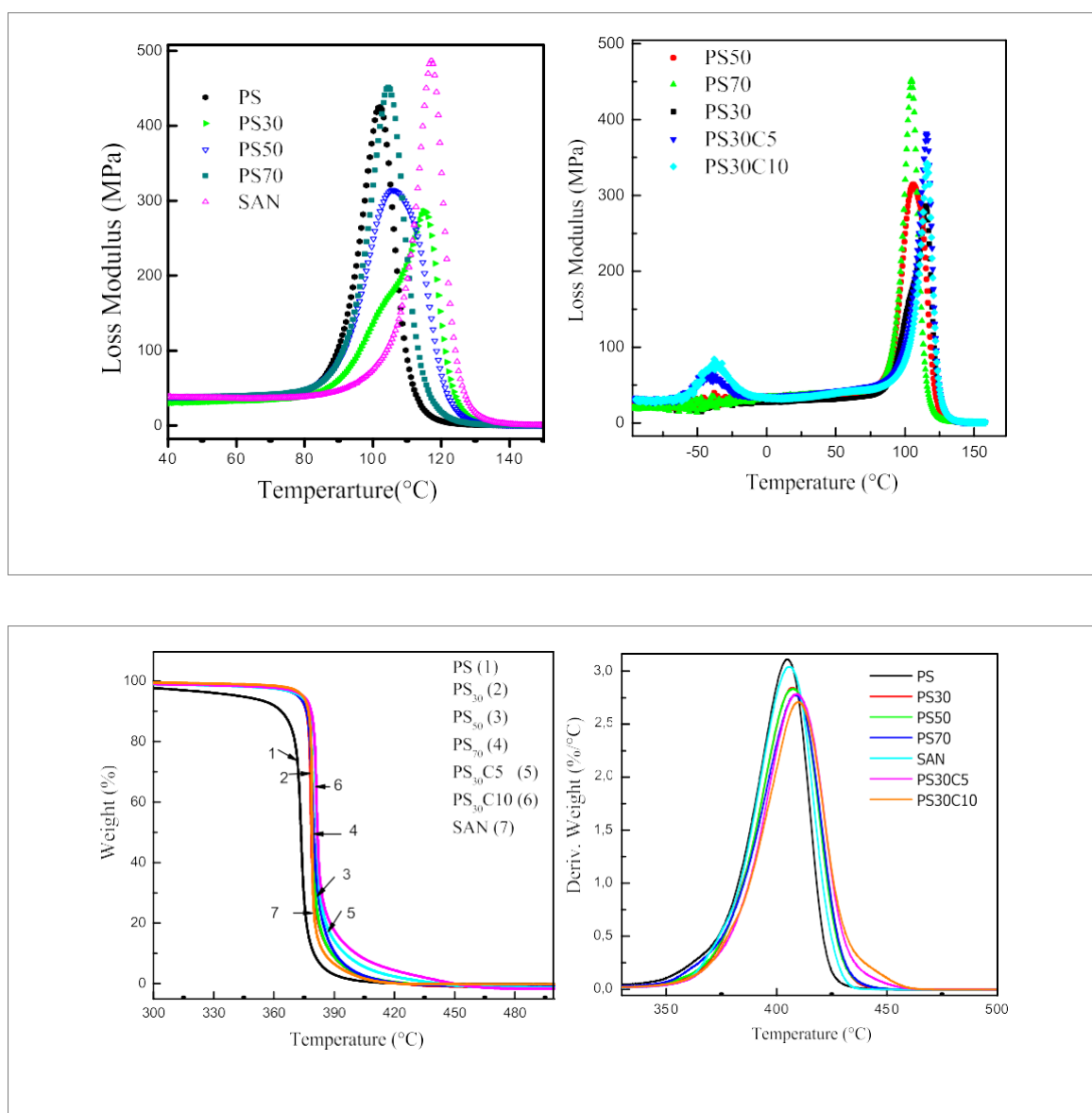


Table 4. Glass transition temperatures as measured from DMTA and DSC analyses for PS and SAN phases into uncompatibilized and

compatibilized PS/SAN blends.

Composition	Measured from DMA		Measured from DSC	
	Tg	Tg	Tg (PS)	Tg
	PS /°C	SAN /°C	(SAN)	
SAN	—	118	—	111
PS30	102.3	114.8	105	109
PS50	95.6	105.7	94.1	110.6
PS70	95	104.5	94.2	112.6
PS	102	—	93	—
PS <sub>30</sub> C5	115.5	109.3		
PS <sub>50</sub> C5	101.2	113.3	101.7	113.8
PS <sub>70</sub> C5	97	107.2	99.7	112
PS <sub>30</sub> C10	116	110.8		
PS <sub>50</sub> C10	101.	112.4	104.5	112.2

	8			
PS <sub>70</sub> C <sub>10</sub>	102.4	113	105.3	114.5

---

can be seen that pure PS presents a slightly lower thermal stability than SAN, they start to lose weight (Tonset) at about 353 and 363 °C and they end at Tend of 416 and 418 °C and reveal a T50 where half of the sample has beendecomposed at around 400 and 402 °C, respectively. The neat PS/SAN blends exhibit a relatively better thermal

Table 5. Thermal stability parameters as determined from TG and DTG thermograms for PS, SAN and their blends with and without compatibilizer.

Samples	$T_{\text{Onset}}$ (°C)	$T_{50\%}$ (°C)	$T_{\text{End}}$ (°C)	$T_{\text{max}}$ (° C)	Residue <sub>475 °C</sub> (%)
SAN	363	402	418	405	0.25
PS <sub>30</sub>	362	404	421	407	0.19
PS <sub>50</sub>	361	403	420	407	0.25
PS <sub>70</sub>	360	404	421	408	0.17
PS	353	400	416	405	0.01
PS <sub>30</sub> C5	363	409	423	409	0.2
PS <sub>50</sub> C5	364	407	425	411	0.25
PS <sub>70</sub> C5	359	410	424	411	0.11
PS <sub>30</sub> C1 0	362	407	423	409	0.36
PS <sub>50</sub> C1 0	364	407	424	410	0.17
PS <sub>70</sub> C1 0	361	407	424	410	0.46

stability as witnessed by the notable increase observed on the values  $T_{\text{onset}}$ ,  $T_{\text{end}}$  and  $T_{50}$ , thus pointing out the benefits of incorporating the SAN copolymer to the PS. After the incorporation of SEBS, the PS<sub>30</sub> thermal behavior is further improved due to the better dispersion and size refinement of the PS phase and to the localization of the compatibilizer at the interface between the two phases thus favoring a barrier effect. The localization of SEBS molecule at the interface contributes in delaying the SAN phase degradation that could be induced by the decomposed PS phase.

#### 4. Conclusions

In this work, the effect of SEBS compatibilizer on the properties of PS/SAN blends was studied. It was found that the addition of 5 wt% of SEBS has a beneficial effect on the morphology, mechanical and thermal properties of the blends. The PS/SAN blend without SEBS did not improve its mechanical properties due to the weak interfacial adhesion between PS and SAN phases. However, materials with improved mechanical properties have been obtained when the adhesion between the PS and SAN phases has been enhanced by the presence of SEBS. These results were confirmed by SEM observations which revealed that the incorporation of SEBS was effective in reducing the domain size of the PS or SAN dispersed phases. The DSC results revealed that the compatibility of blend is improved with addition of compatibilizer SEBS. A single  $T_g$  was observed only for PS<sub>30</sub> blend with 5 and 10 wt% of SEBS, thus confirming a better adhesion between the two phases. The TGA analysis indicated that the thermal stability of PS/SAN blends increased with increasing SEBS content. The overall variations in all properties suggest that the SEBS copolymer could be used as an effective compatibilizer for the PS/SAN mixtures.

#### Acknowledgments

'K Bedjaoui would like to acknowledge Dr Nora Aramburu, Dr Jon Maiz, Prof Gonzalo Gerrika and Prof Alejandro J Müller for hosting him as a PhD intern to perform calorimetric and mechanical properties at POLYMAT and the Department of Polymer Science and Technology from the Faculty of Chemistry, University of the Basque Country UPV/EHU in San Sebastián, Spain'.

## ORCID iDs

Khaled Bedjaoui  <https://orcid.org/0000-0002-5935-9929>

## References

- [1] Wang D, Li Y, Xie X-M and Guo B-H 2011 Compatibilization and morphology development of immiscible ternary polymer blends *Polymer* **52** 191–200
- [2] Chirawithayaboon A and Kiatkamjornwong S 2004 Compatibilization of high-impact polystyrene/high-density polyethylene blends by styrene/ethylene-butylene/styrene block copolymer *J. Appl. Polym. Sci.* **91** 742–55
- [3] Yang Q, Mao Y, Li G, Huang Y, Tang P and Lei C 2004 Study on the UCST behavior of polystyrene/poly(styrene-co-acrylonitrile) blend, *Mater. Lett.* **58** 3939–44
- [4] Michaeli W, Grefenstein A and Frings W 1993 Synthesis of polystyrene and styrene copolymers by reactive extrusion *Adv. Polym. Technol.* **12** 25–33
- [5] Khan Z and Baloch M K 2013 Investigating the miscibility of polystyrene/poly(styrene-co-acrylonitrile) blend in tetrahydrofuran by simple physical techniques at various temperatures *Polym. Bull.* **70** 2015–33

- [6] Ibrahim B A and Kadum K M 2012 Morphology studies and mechanical properties for PS/SBS blends *Int. J. Eng.* 12 9
- [7] Marwat Z K and Baloch M K 2015 Investigating miscibility of polymers and its impact on the morphology, thermal, and mechanical properties of polymer blends *Int. J. Thermophys.* 36 2755–68
- [8] Mizutani T, Arai K, Miyamoto M and Kimura Y 2006 Preparation of spherical nanocomposites consisting of silica core and polyacrylate shell by emulsion polymerization *J. Appl. Polym. Sci.* 99 659–69
- [9] Khan Z and Baloch M K 2014 Effect of solvent on the miscibility of polystyrene/poly(styrene-Co-Acrylonitrile) blends at different temperatures *J. Macromol. Sci. Part B* 53 1027–49
- [10] Du B, Handge U A, Majeed S and Abetz V 2012 Localization of functionalized MWCNT in SAN/PPE blends and their influence on rheological properties *Polymer* 53 5491–501
- [11] Stadler F J, Piel C, Kaminsky W and Münstedt H 2006 Rheological characterization of long-chain branched polyethylenes and comparison with classical analytical methods *Macromol. Symp.* 236 209–18
- [12] Hachiya H, Takayama S and Takeda K 1998 Properties of immiscible polymer alloys without compatibilizer *J. Appl. Polym. Sci.* 70 2515–20
- [13] Li T, Topolkaraev V A, Hiltner A, Baer E, Ji X Z and Quirk R P 1995 Block copolymers as compatibilizers for blends of linear low density polyethylene and polystyrene *J. Polym. Sci., Part B: Polym. Phys.* 33 667–83
- [14] Wu J, Guo B, Chan C-M, Li J and Tang H-S 2001 Synergistic toughening effect of SBS and HDPE on the fracture of the PS/HDPE/SBS blends *Polymer* 42 8857–65
- [15] Aranburu N and Eguiazábal J I 2015 Improved mechanical properties of compatibilized polypropylene/polyamide-12 blends *Int. J. Polym. Sci.*, 2015 1–8
- [16] Jiang G, Wu H and Guo S 2010 Reinforcement of adhesion and development of morphology at polymer-polymer interface via reactive compatibilization: a review *Polym. Eng. Sci.* 50 2273–86
- [17] Sundararajs U and Macosko C W 1995 *Drop Breakup and Coalescence in Polymer Blends: The Effects of Concentration and Compatibilization* 28 11
- [18] Scaffaro R, La Mantia F P, Canfora L, Polacco G, Filippi S and Magagnini P 2003 Reactive compatibilization of PA6/LDPE blends with an ethylene-acrylic acid copolymer and a low molar mass bis-oxazoline *Polymer* 44 6951–7
- [19] Mathew M and Thomas S 2003 Compatibilisation of heterogeneous acrylonitrile-butadiene rubber/polystyrene blends by the addition of styrene-acrylonitrile copolymer: effect on morphology and mechanical properties *Polymer* 44 1295–307
- [20] Krache R, Benachour D, Cagiao M E, Calleja F J B, Bayer R K and Tschöpe F 2003 Micromechanical studies on binary and ternary blends of polyethylene, polypropylene, and polyamide 66: influence of the compatibilizer *Int. J. Polym. Mater. Polym. Biomater.*, 52 939–56
- [21] Pang Y X, Jia D M, Hu H J, Hourston D J and Song M 2000 Effects of a compatibilizing agent on the morphology, interface and mechanical behaviour of polypropylene/poly(ethylene terephthalate) blends *Polymer* 41 357–65
- [22] Kim J H and Kim C K 2003 Changes in the interfacial properties of PC/SAN blends with compatibilizer *J. Appl. Polym. Sci.* 89 2649–56
- [23] Guo T, Ding X, Han H, Zhang L, Zhang Y and Zhou K 2012 Wide-angle x-ray diffraction investigation on crystallization behavior of PA6/PS/SEBS-g-MA blends *J. Polym. Res.* 19 3
- [24] Guo F, Packirisamy S, Mani R S, Aronson C L, Gvozdic N V and Meier D J 1998 Compatibilizing effects of block copolymers in low-density polyethylene/polystyrene blends *Polymer* 39 2495–505
- [25] Debbah I, Krache R, Aranburu N, Fernández M and Etxeberria A 2018 Effect of SEBS-g-MAH addition on the mechanical, rheological, and morphological properties of polycarbonate/acrylonitrile-butadiene-styrene blends *J. Elastomers Plast.* 50 611–33
- [26] Xu S-A, Zhu L, Xie J-W and Jiang M 1999 Melt rheology of compatibilized polystyrene/low density polyethylene blends, *Polym. Int.* 48 1113–20
- [27] Shi-Ai Xu 1998 Polystyrene/high density polyethylene blends compatibilized by a tri-block copolymer: I. Properties and morphology *Polym. J.* 30 552–8
- [28] Chen B, Tang T, Li X, Xu S, Zhang X and Huang B 2004 Morphology, tensile strength and thermal behavior of isotactic polypropylene/syndiotactic polystyrene blends compatibilized by SEBS copolymers *Polym. J.* 36 284–93
- [29] Schwarz M C, Barlow J W and Paul D R 1988 Mechanical properties of HDPE/(PEC/PS)/SEBS blends *J. Appl. Polym. Sci.* 35 2053–67
- [30] Yin N, Zhang Y, Zhang Y, Zhang X and Zhou W 2007 Preparation and properties of PC/SAN alloy modified with styrene-ethylene-butylene-styrene block copolymer *J. Appl. Polym. Sci.* 106 637–43
- [31] Kroeze E 1997 Compatibilization of low-density polyethylene/polystyrene blends by segmented EBOPS-block-EB) n block copolymers <https://doi.org/10.1007/s002890050039>
- [32] Pang Y X, Jia D M, Hu H J, Hourston D J and Song M 2000 Effects of a compatibilizing agent on the morphology, interface and mechanical behaviour of polypropylene/poly(ethylene terephthalate) blends, *Polymer* 41 357–65
- [33] Kinning D J, Thomas E L and Fetters L J 1989 Morphological studies of micelle formation in block copolymer/homopolymer blends

- J. Chem. Phys.* **90** 5806–25
- [34] Krache R and Debah I 2011 Some mechanical and thermal properties of PC/ABS blends *Mater. Sci. Appl.* **02** 404–10
- [35] Escobar D, Mendizabal E and González-Núñez R 2008 Compatibilization of poly(vinyl chloride) and polystyrene blends with poly (styrene-co-n-methylolacrylamide) *J. Appl. Polym. Sci.* **110** 297–303
- [36] Priya L and Jog J P 2003 Intercalated poly(vinylidene fluoride)/clay nanocomposites: structure and properties *J. Polym. Sci., Part B: Polym. Phys.*, **41** 31–8
- [37] Jang B C, Huh S Y, Jang J G and Bae Y C 2001 Mechanical properties and morphology of the modified HDPE/starch reactive blend *J. Appl. Polym. Sci.* **82** 3313–20
- [38] Tostar S, Stenvall E, Foreman M and Boldizar A 2016 The influence of compatibilizer addition and gamma irradiation on mechanical and rheological properties of a recycled WEEE plastics blend *Recycling* **1** 101–10
- [39] Hameed A M and Daway E G 2015 *Morphology and Mechanical Properties of (Epoxy/PVC) Blend* 11 7
- [40] Benmesli S and Riahi F 2014 Dynamic mechanical and thermal properties of a chemically modified polypropylene/natural rubber thermoplastic elastomer blend *Polym. Test.* **36** 54–61